Transverse Momentum Distributions

Draft of June 5, 2012

Lectures

Alessandro Bacchetta

Contents

Notations and conventions

The conventions will mainly follow the book of Peskin and Schroeder [102]. We use the metric tensor

$$g^{\mu\nu} = \begin{pmatrix} 1 & 0 & 0 & 0 \\ 0 & -1 & 0 & 0 \\ 0 & 0 & -1 & 0 \\ 0 & 0 & 0 & -1 \end{pmatrix}, \tag{1}$$

with Greek indices running over 0,1,2,3. We define the antisymmetric tensor so that

$$\epsilon^{0123} = +1, \qquad \epsilon_{0123} = -1. \tag{2}$$

Ambiguities in this definition are a notorious source of sign errors. Repeated indices are summed in all cases.

Light-cone vectors

Light-cone vectors will be indicated as

$$a^\mu = [a^-,\ a^+,\ \boldsymbol{a}_T]\,. \tag{3}$$

The dot-product in light-cone components is

$$a \cdot b = a^+ b^- + a^- b^+ - \boldsymbol{a}_T \cdot \boldsymbol{b}_T \tag{4}$$

The light-cone decomposition of a vector can be written in a Lorentz covariant fashion using two light-like vectors n_+ and n_- satisfying $n_\pm^2 = 0$ and $n_+ \cdot n_- = 1$ and promoting $\boldsymbol{a}_T$ to a four-vector $a_T^\mu = [0, 0, \boldsymbol{a}_T]$ so that

$$a^\mu = a^+ n_+^\mu + a^- n_-^\mu + a_T^\mu, \tag{5}$$

where

$$\begin{aligned} a^+ &= a \cdot n_-, \\ a^- &= a \cdot n_+, \\ a_T \cdot n_+ &= a_T \cdot n_- = 0. \end{aligned} \tag{6}$$

Note that

$$a_T \cdot b_T = -\boldsymbol{a}_T \cdot \boldsymbol{b}_T \tag{7}$$

We introduce the projector on the transverse subspace

$$g_T^{\mu\nu} = g^{\alpha\beta} - n_+^\alpha n_-^\beta - n_-^\alpha n_+^\beta = \begin{pmatrix} 0 & 0 & 0 & 0 \\ 0 & -1 & 0 & 0 \\ 0 & 0 & -1 & 0 \\ 0 & 0 & 0 & 1 \end{pmatrix}. \tag{8}$$

We can define the transverse antisymmetric tensor

$$\epsilon_T^{\alpha\beta} = \epsilon^{\alpha\beta\rho\sigma} n_{+\rho} n_{-\sigma} \tag{9}$$

Note that $\epsilon_T^{12} = -\epsilon_T^{21} = 1$.

Dirac matrices

Dirac matrices will be often expressed in the following representations (which is almost the same as the chiral or Weyl representation)

$$\gamma^0 = \begin{pmatrix} 0 & \mathbf{1} \\ \mathbf{1} & 0 \end{pmatrix}, \qquad \gamma^i = \begin{pmatrix} 0 & \boldsymbol{\sigma}^i \\ -\boldsymbol{\sigma}^i & 0 \end{pmatrix}, \qquad \gamma_5 = \begin{pmatrix} -\mathbf{1} & 0 \\ 0 & \mathbf{1} \end{pmatrix}. \tag{10}$$

The above representation is almost precisely the chiral or Weyl representation (see, e.g., Eqs. 3.25 and 3.72 of Peskin and Schroeder [102]. In any case, valid representations can be obtained by applying a unitary transformation to the matrices of any other representation. In certain sections of these notes I will use a representation obtained from the chiral representation through the application of the orthogonal matrix

$$U = \begin{pmatrix} 0 & 0 & 1 & 0 \\ 0 & 1 & 0 & 0 \\ 1 & 0 & 0 & 0 \\ 0 & 0 & 0 & 0 \end{pmatrix}. \tag{11}$$

The resulting representation is, explicitly,

$$\gamma^0 = \begin{pmatrix} 0 & 0 & 1 & 0 \\ 0 & 0 & 0 & 1 \\ 1 & 0 & 0 & 0 \\ 0 & 1 & 0 & 0 \end{pmatrix}, \qquad \gamma^3 = \begin{pmatrix} 0 & 0 & -1 & 0 \\ 0 & 0 & 0 & -1 \\ 1 & 0 & 0 & 0 \\ 0 & 1 & 0 & 0 \end{pmatrix},$$

$$\gamma^1 = \begin{pmatrix} 0 & -1 & 0 & 0 \\ 1 & 0 & 0 & 0 \\ 0 & 0 & 0 & 1 \\ 0 & 0 & -1 & 0 \end{pmatrix}, \qquad \gamma^2 = \begin{pmatrix} 0 & \mathrm{i} & 0 & 0 \\ \mathrm{i} & 0 & 0 & 0 \\ 0 & 0 & 0 & -\mathrm{i} \\ 0 & 0 & -\mathrm{i} & 0 \end{pmatrix},$$

$$\gamma_5 = \begin{pmatrix} 1 & 0 & 0 & 0 \\ 0 & -1 & 0 & 0 \\ 0 & 0 & -1 & 0 \\ 0 & 0 & 0 & 1 \end{pmatrix}$$

The reason to choose this representation is to have a nice form of the projectors

$$\mathcal{P}_+ = \frac{1}{2}\,\gamma^-\gamma^+, \qquad\qquad \mathcal{P}_- = \frac{1}{2}\,\gamma^+\gamma^-. \tag{12}$$

In fact, together with

$$\mathcal{P}_R = (1+\gamma_5)/2, \qquad\qquad \mathcal{P}_L = (1-\gamma_5)/2$$

we obtain, explicitly

$$\mathcal{P}_R\mathcal{P}^+ = \begin{pmatrix} 1 & 0 & 0 & 0 \\ 0 & 0 & 0 & 0 \\ 0 & 0 & 0 & 0 \\ 0 & 0 & 0 & 0 \end{pmatrix}, \qquad \mathcal{P}_L\mathcal{P}^+ = \begin{pmatrix} 0 & 0 & 0 & 0 \\ 0 & 1 & 0 & 0 \\ 0 & 0 & 0 & 0 \\ 0 & 0 & 0 & 0 \end{pmatrix},$$

$$\mathcal{P}_R\mathcal{P}^- = \begin{pmatrix} 0 & 0 & 0 & 0 \\ 0 & 0 & 0 & 0 \\ 0 & 0 & 0 & 0 \\ 0 & 0 & 0 & 1 \end{pmatrix}, \qquad \mathcal{P}_L\mathcal{P}^- = \begin{pmatrix} 0 & 0 & 0 & 0 \\ 0 & 0 & 0 & 0 \\ 0 & 0 & 1 & 0 \\ 0 & 0 & 0 & 0 \end{pmatrix}$$

We will make use of the Dirac structure

$$\sigma^{\mu\nu} \equiv \frac{\mathrm{i}}{2}\,[\gamma^\mu, \gamma^\nu]\,. \tag{13}$$

Transverse momenta

These notes are written using the so-called "Amsterdam notation," as done in Piet Mulders's lectures. In the recent paper [35] a slightly different notation was adopted. Notation differences are a common source of headaches, but it would be too difficult in these lecture notes to abandon the Amsterdam notation. Here, however, a correspondence table is provided:

Amsterdam	[35]	Description
p	k	momentum of parton in distribution function
$\boldsymbol{p}_T$	$\boldsymbol{k}_\perp$	parton transverse momentum in distribution function
k	p	momentum of fragmenting parton
$\boldsymbol{k}_T$	$\boldsymbol{p}_\perp$	trans. momentum of fragmenting parton w.r.t. final hadron
$\boldsymbol{K}_T$	$\boldsymbol{P}_\perp$	trans. momentum of final hadron w.r.t. fragmenting parton
$\boldsymbol{P}_{h\perp}$	$\boldsymbol{P}_{hT}$	transverse momentum of final hadron w.r.t. virtual photon

1

Introduction

This first part is partially based on Ref. [17].

We are still profoundly far from fully understanding QCD and nucleons. If we take a look at the list of nucleons properties in the Particle Data Group tables, we can read what is the nucleons mass, spin, quark content, charge, magnetic moment, charge radius... It is fair to say that, with the partial exception of the mass, we cannot explain any single one of these quantities from first principles. The fundamental reason is that we are unable to explain confinement (see, e.g., [111]).

One of the ways we can follow to better understand QCD and confinement is to study the inner structure of the nucleon in higher and higher details. In these years, thanks to the contributions of HERMES, COMPASS and the JLab experiments, we are reaching the opportunity to reconstruct multi-dimensional pictures of the nucleon. The knowledge of the multi-dimensional structure allows the analysis of properties otherwise inaccessible: quark-gluon correlations, effects of final-state interactions, spin-orbit and spin-spin correlations, and much more. The situation may be compared to protein studies: our present knowledge of the proton structure is limited to one dimension and can be compared to knowing the sequence of amino acids of proteins. It is an extremely important piece of information, but insufficient to understand them. Starting from the 1960s, it has become possible to reconstruct their 3D structure. These advances literally revolutionized our understanding of protein chemistry. Hopefully, we can expect to do the same in hadronic physics: we are opening the era of "stereo femtophysics."

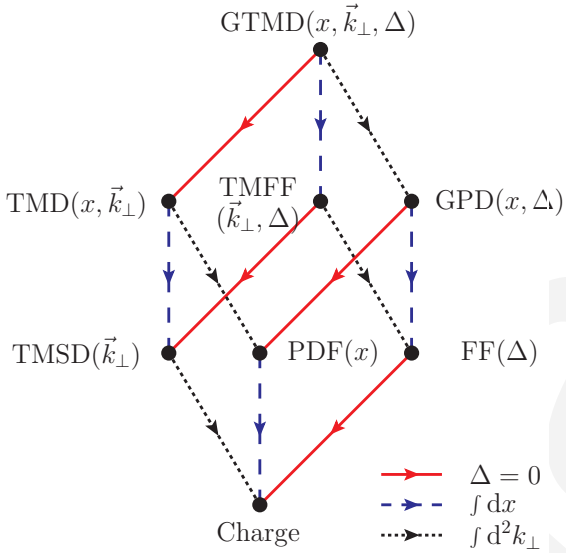

Figure 1.1: Representation of the projections of the GTMDs into parton distributions and form factors (picture from ref. [89])

1.1 Two words on Wigner distributions

Partons inside the proton can have a specific momentum and a specific position (with respect to some definition of the center of the proton). Their state can be described by Wigner distributions in six-dimensions (three position and three momentum coordinates) [27,76]. Wigner distributions are the quantum-mechanical constructions that are closest to a classical probability density in phase-space. Strictly speaking, due to the Heisenberg uncertainty principle, they cannot be considered as probability densities and are not positive definite. For this reason, they are often defined as quasi-probability distributions. However, they can be used to compute the expectation value of any physical observable. In this sense, they represent the maximal knowledge of the partonic structure. They are equivalent to knowing the complete wavefunction of partons inside the nucleon.

Projections of Wigner distributions on some of the available dimensions do have a probabilistic interpretation (see Fig. 1.1). Of these, we will take into consideration in these lectures only Transverse-Momentum-dependent parton Distribution functions (TMDs). In order to be able to define them, we need to distinguish a longitudinal direction from two transverse directions. To observe the internal structure of the proton we need a hard probe (i.e., with high four-momentum). This requirement allows us to define a longitudinal direction: it could be defined as the direction of the probe in the rest-frame of the nucleon, or the direction of the nucleon in the center-of-mass frame of nucleon and probe (or in any other frame where proton and probe are collinear). The transverse plane is the one orthogonal to the longitudinal direction.

If we integrate over all coordinates and the two transverse components of momentum we obtain a projection of the Wigner distributions on the longitudinal momentum only. These projections are well studied and have a name: they correspond to the standard Parton Distribution Functions (PDFs). They represent the probability of finding a parton inside a nucleon with a given fraction of

the nucleons longitudinal momentum. In this sense, they are pictures of the partonic structure of the nucleon in only one dimension in momentum space. At this point, it is worthwhile remarking that this interpretation is valid at the parton-model level, i.e., when the nucleon constituents can be treated approximately as free for the purpose of calculating the interaction with the probe. In the formal QCD treatment, this interpretation is modified and corresponds to the parton-model concept only in the lowest order of perturbation theory [49, 53]. In this sense, we can say that parton distributions are approximate images of the partonic structure.

1.2 Transverse-momentum distributions

If we integrate Wigner distributions over all coordinates, we obtain the so-called transverse-momentum distributions (TMDs). They represent pictures of three-dimensional densities in momentum space.

Historically, partonic transverse momentum has been discussed as early as in the Seventies (see, e.g., [47, 114]), few years after the birth of the parton model [30, 63]. Transverse momentum can be generated also by the radiation of gluons: the first analysis of this contribution was done in 1979 [101], few years after the birth of QCD. The first study that put together the nonperturbative and perturbative components of TMDs in a formally solid way was an article of Collins and Soper in 1981 [56]: we could probably identify the birth of TMDs in this work. We started using the name TMDs only very recently. For a while we have been talking about transverse-momentum-dependent parton distribution functions (TMD PDFs), then simplified it to TMDs (see, e.g., Ref. [18]). Especially in the field of low-x physics, the name "unintegrated parton distribution functions" is also commonly used (see, e.g., [81]).

In spite of this relatively long history, TMDs represent still a largely unexplored field. There are many nontrivial questions that do not have an answer yet. For instance, we still do not have a clear understanding of the detailed shape of the proton (in momentum space). At present, we know that experimental data are consistent with a Gaussian distribution with a width (i.e., an average transverse momentum) of about 0.6 GeV at an energy scale of 2 GeV. Roughly speaking, half of it is coming from the primordial transverse momentum of the quark and half is acquired through perturbative gluon radiation. There are indications that the transverse-momentum distribution becomes larger at lower longitudinal momentum. We also dont know if there is a difference in the distribution of partons with different flavors: is one flavor more concentrated in the center and the other in the sides? Or are the flavors uniformly mixed? There are first feeble indications from experimental measurements and from lattice-QCD computations that the down quark distribution is larger than the up [96, 98].

The above considerations apply when we average over the nucleons spin direction. There is even more fun when spin is taken into account. For instance, suppose the spin of the nucleon is moving toward us and its spin is pointing upwards: it turns out that we see up quarks moving preferentially to the right and down quarks to the left. In terms of images in momentum space, the distributions are not cylindrically symmetric anymore, but distorted in opposite ways for up and down quarks (see Fig. 1.2).

It is worthwhile describing the progress made in understanding this kind of effect. It was first

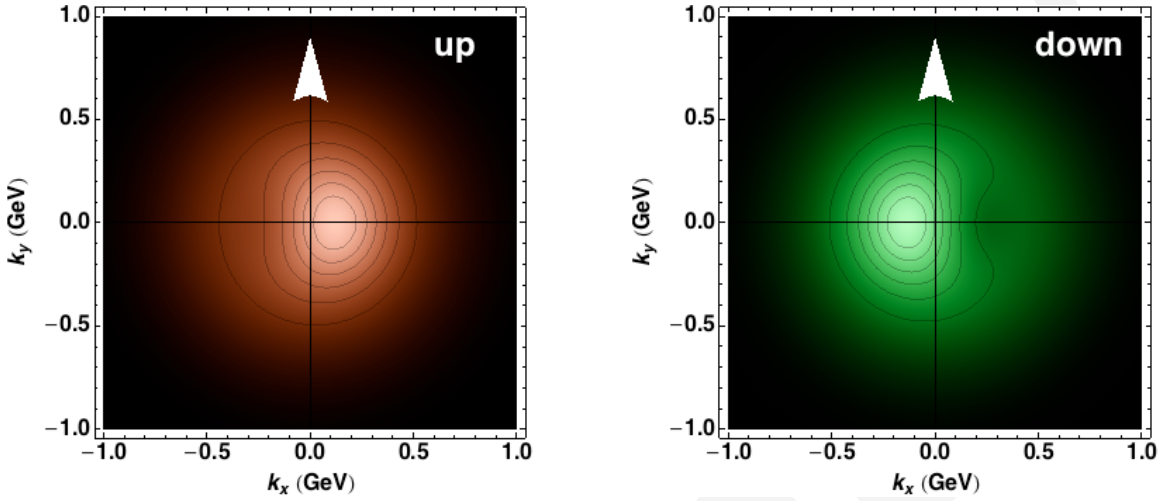

Figure 1.2: The up and down quark density distortion in transverse-momentum space, obtained by studies of the Sivers function [22].

proposed by D. Sivers in 1990 as a way to explain large left-right asymmetries observed in pion-nucleus collisions [112]. For this reason we nowadays normally speak about the Sivers effect, and the Sivers function describes the left-right distortion in the distribution of partons. For more than a decade, this effect was thought to vanish due to time-reversal symmetry. Starting from a model calculation in 2002, theory studies made clear that the Sivers function could be nonzero [44]. In 2004, the first experimental evidence of a nonzero Sivers effect was reported by the HERMES collaboration [2], recently confirmed by the COMPASS collaboration [4]. These break-throughs forced a profound revision of the QCD treatment of transverse momentum distributions, still partially underway [49]. For instance, one of the consequences is that the Sivers function in deep inelastic scattering (where an electron strikes a quark inside the nucleon) has an opposite sign compared to the Sivers function in DrellYan processes (where an antiquark annihilates a quark inside the nucleon). In other words, an antiquark probe should see a distortion exactly opposite to Fig. 5. This striking prediction, due to John Collins [52], should be confirmed (of falsified!) in the next few years by planned experiments (e.g., COMPASS at CERN, AnDY at Brookhaven National Lab).

1.3 Impact-parameter distributions

If we integrate the Wigner distributions over transverse momenta and the longitudinal coordinate, we obtain the so-called impact-parameter distributions [45]. They reveal the distribution of partons as a function of their longitudinal momentum and their transverse position with respect to the center of momentum of the nucleon (i.e., the relevant transverse coordinates). If we integrate even over the longitudinal momentum, we obtain pictures of the partonic structure in transverse coordinate space, as seen from the point of view of a hard probe hitting the nucleon. As far as we know today, this is probably as close as we can get to the everyday concept of a photo of the nucleon. These

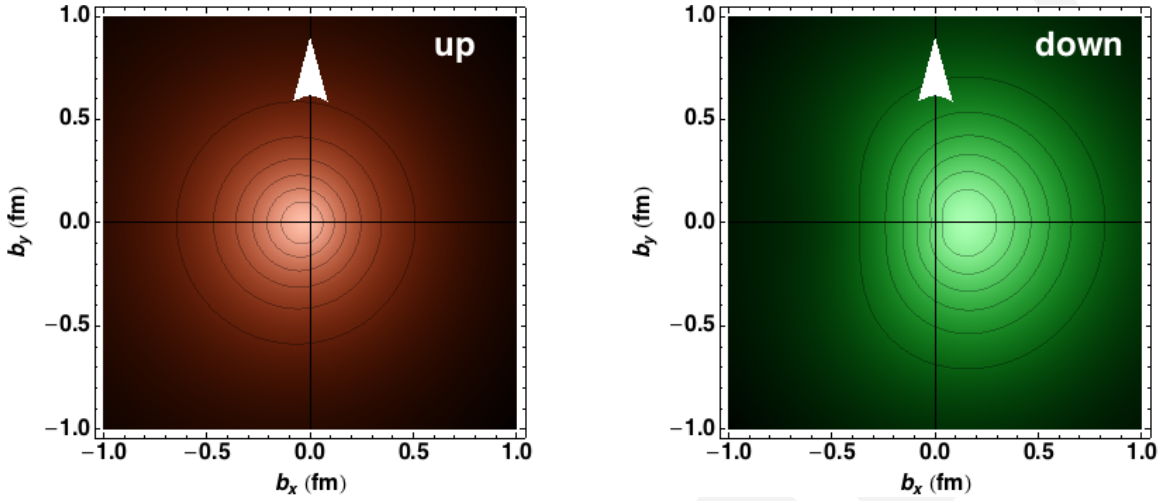

Figure 1.3: The up and down quark density distortion in impact parameter space space, obtained by studies of the Pauli form factor.

distributions can be computed using models or lattice QCD techniques. But the good news is that they can also be reconstructed from experimental data. In fact, they are directly related to two-dimensional Fourier transforms of the nucleon form factors. Historically, nucleon form factors provided the first indications that protons and neutrons are not elementary particles. For instance, when in 1933 the first SternGerlach experiment on the proton was performed, most physicists expected the magnetic moment of the proton (i.e., the value of the magnetic form factor $G_M(t)$ at $t = 0$) to be one nuclear magneton. Shockingly, it turned out to be 2.5 magnetons. Form-factor measurements started in the 1950s led to the first estimates of the proton radius (to be precise, one if its possible definitions), fixing it at around 0.8 femtometers. After fifty years of studies, we have made some steps forward, but we have also unearthed many mysteries. For instance, the proton seems to shrink in a muonium atom (made by a proton and a muon): the radius of the proton in a muonium atom is 0.84184(67) fm, which differs by five standard deviations from the hydrogen value of 0.8768(69) fm [103]. These estimates are inferred from Lamb-shift measurements, not from direct measurement of form factors. From the point of view of nucleon imaging, we can measure the transverse densities of partons, as seen from a hard probe, and their associated radius. We cannot reach the precision quoted above, but the information we obtain is much richer. For instance, measuring the Dirac and Pauli form factors of protons and neutrons and performing a two-dimensional Fourier transform [94], we can obtain the images of the quark density in impact parameter space. As for momentum distributions, we can first take a look at the average over nucleon polarization. From the information we have on the proton and neutron form factors and using some assumptions, we can conclude that the up distribution is narrower than the down. When the orientation of the nucleon spin is fixed, we discover that the up and down distributions are distorted in opposite ways. The distortion of the down quarks seems to be much larger than the up.

When looking at the distributions in impact parameter space, we are tempted to compare them with the momentum distributions. First of all, it must be stressed that the two distributions are not

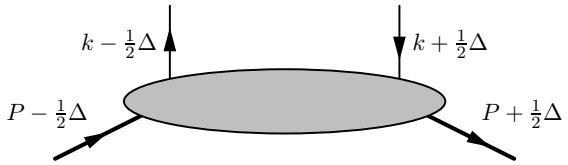

Figure 1.4: Kinematics for the fully unintegrated generalized quark-quark correlator

connected by a Fourier transform. Secondly, it must be kept in mind that the impact-parameter distributions obtained from the form factors refer to the valence quark combinations (i.e., quark minus antiquarks). Finally, the impact-parameter distributions obtained from form factors are integrated over the longitudinal momentum fraction x.

In order to overcome these limitations, we have to turn our attention to a generalization of the form factors that embodies also the dependence on x. Such quantities are called generalized parton distributions (GPDs) (see, e.g., [60, 74]). They are hybrids between a parton distribution function and a form factor. They effectively are like tomographic slices of the form factors at a fixed value of the momentum fraction x. The x dependence of GPDs is extremely important, in particular it is essential to quantify partonic angular momentum, which can be related to an x-weighted integral of the GPDs corresponding to the Pauli and Dirac form factors [75].

In order to study all these interesting issues, we need first of all to get acquinted with the underlying formalism.

1.4 More formally...

This part is based on Refs. [89, 93]. In order to formally define the objects of interest, we may start from the generalized fully-unintegrated quark-quark correlator for a spin-1/2 hadron, which can be defined as

$$W(P,k,\Delta,S) = \frac{1}{2}\int \frac{d^4\zeta}{(2\pi)^4}\, e^{ik\cdot\zeta}\, \langle P+\Delta/2,S|\,\bar{\psi}(-\zeta/2)\,\psi(\zeta/2)\,|P-\Delta/2,S\rangle\,. \tag{1.1}$$

The correlator W depends on the spin S, the average momentum P of the initial and final hadron, the momentum transfer Δ to the hadron, and the average quark momentum k. (For the kinematics we also refer to figure 1.4.) For the moment, we did not introduce in the definition the gauge links which are necessary to render the object gauge invariant. The above object can be parametrized in terms of fully-unintegrated generalized parton distribution functions, also called generalized parton correlation functions (GPCFs).

In all "parton distributions" we will take into account we start with integrating the above correlator over k^-. This means that the quark fields inside the definition are taken at $\zeta^- = 0$ (same "light-cone time"):

$$W(P,x,k_\perp,\Delta,S) = \int dk^-\, W(P,k,\Delta,S) = \frac{1}{2}\int \frac{d\zeta^- d^2\zeta_T}{(2\pi)^3}\, e^{ik\cdot\zeta}\, \langle P+\Delta/2,S|\,\bar{\psi}(-\zeta/2)\,\psi(\zeta/2)\,|P-\Delta/2,S\rangle\Big|_{\zeta^+=0}\,. \tag{1.2}$$

This object can be parametrized in terms of generalized transverse-momentum-dependent parton distribution functions (GTMDs). There are in total 64 of them (complex-valued). For reference, 16 of them are "leading-twist" (see later). Sometimes, these functions are called also the "mother distributions."

Setting $\Delta^+ \to 0$ and taking a two-dimensional Fourier transform with respect to Δ_T of the above correlator we obtain

$$W(P, x, \boldsymbol{k}_\perp, \boldsymbol{b}_\perp, S) = \frac{1}{(2\pi)^2} \int d^2\Delta_\perp e^{-i\boldsymbol{b}_\perp \boldsymbol{\Delta}_\perp} W(P, x, k_\perp, \Delta_\perp, S)\Big|_{\Delta^+=0}. \tag{1.3}$$

This correlator can be parametrized in terms of Wigner distributions. At the moment, there is no idea on how to actually measure all the quantities defined so far. Although in the introduction we described Wigner distributions as depending on six variables (three positions and three momenta), here in reality we see that they depend on three momenta and only two positions. This is due to the peculiarity of the component Δ^+: even if we perform a Fourier transform with respect to Δ^+ we do not obtain a probabilistic interpretation of the result.

Setting $\Delta \to 0$ in Eq. 1.2, we obtain the transverse-momentum-dependent correlation function

$$\Phi(P, x, k_\perp, S) = W(P, x, k_\perp, 0, S) = \frac{1}{2} \int \frac{d\zeta^- d^2\zeta_T}{(2\pi)^3} e^{ik\cdot\zeta} \langle P, S | \bar{\psi}(-\zeta/2)\, \psi(\zeta/2) | P, S \rangle \Big|_{\zeta^+=0}. \tag{1.4}$$

which can be parametrized in terms of Transverse-Momentum Distributions (TMDs), in total 32 of them (of which 8 are leading-twist). As all parton distributions, they can be "measured" in a broad sense. To be precise, we should say that they are extracted from experimental measurements through well-defined prescriptions that have however a certain degree of arbitrariness (for instance, at NLO in the $\overline{\text{MS}}$ scheme).

Integrating Eq. (1.2) over transverse momentum (i.e., the quark fields are now are taken at $\zeta^- = \zeta_T = 0$), we obtain

$$F(P, x, \Delta, S) = \int dk^- W(P, k, \Delta, S) = \frac{1}{2} \int \frac{d\zeta^-}{2\pi} e^{ik\cdot\zeta} \langle P{+}\Delta/2, S | \bar{\psi}(-\zeta/2)\, \psi(\zeta/2) | P{-}\Delta/2, S \rangle \Big|_{\zeta^+=0, \zeta_T=0}. \tag{1.5}$$

This correlator can be parametrized in terms of Generalized Parton Distribution functions (GPDs), in total 32 of them (8 leading-twist). Setting $\Delta^+ \to 0$

Integrating Eq. (1.4) over transverse momentum or equivalently setting $\Delta \to 0$ in Eq. (1.5), we obtain

$$\Phi(P, x, S) = F(P, x, 0, S) = \int d^2k_\perp \Phi(P, x, k_\perp, S) \tag{1.6}$$

The procedure of integrating over transverse momentum is actually delicate and in principle it is possible only at "parton-model" level, i.e., when neglecting higher-order QCD corrections. The above correlator can be parametrized in terms of Parton Distribution Functions (PDFs). In total there are 9 of them (3 leading-twist).

If we integrate Eq. **??** over x the quark field are taken at $\zeta = 0$. We obtain

$$F(P, \Delta) = \frac{1}{P^+} \langle P + \Delta/2, S | \bar{\psi}(0)\, \psi(0) | P - \Delta/2, S \rangle. \tag{1.7}$$

The correlator can be parametrized in terms of 22 Form Factors (FF) (7 leading twist).

Finally, if we integrate Eq. (1.6) over x or alternatively set Δ to zero in Eq. (1.7), we obtained the fully-integrated quark-quark correlator

$$F(P) = \frac{1}{P^+}\langle P, S\,|\,\bar{\psi}(0)\,\psi(0)\,|P, S\,\rangle\,. \tag{1.8}$$

which can be parametrized in terms of hadronic charges. There are in total 4 of them (3 leading twist). They are the scalar, vector, axial, tensor charges of the nucleon.

2

Inclusive DIS

I will not repeat here all the details of the analysis of inclusive DIS but summarize only some of the relevant results that will be useful for later.

We consider the process

$$\ell(l) + N(P) \to \ell(l') + X, \tag{2.1}$$

where ℓ denotes the beam lepton, N the nucleon target, and where four-momenta are given in parentheses. We neglect the lepton mass. We denote by M the mass of the nucleon. As usual we define $q = l - l'$ and $Q^2 = -q^2$ and introduce the variables

$$x_B = \frac{Q^2}{2\,P\cdot q}, \qquad\qquad y = \frac{P\cdot q}{P\cdot l} = \frac{Q^2}{x_B s}. \tag{2.2}$$

In this lectures, we will systematically neglect all correction of order M/Q, unless otherwise specified.

The spin vector of the target is denoted by S. Our definition of the azimuthal angle ϕ_S of the outgoing hadron and the target spin is shown in Fig. 3.1 and consistent with the Trento conventions [19]. The helicity of the lepton beam is denoted by λ_e. $S_\perp$ is the transverse parts of S with respect to the photon momentum. $S_\parallel$ is the component of S in the negative z-direction in Fig. 3.1, i.e. positive $S_\parallel$ corresponds to the target spin pointing against the virtual photon.

The cross section for polarized electron-nucleon scattering can be written in a general way as the contraction between a leptonic and a hadronic tensor

$$\frac{\mathrm{d}^3\sigma}{\mathrm{d}x_B\,\mathrm{d}y\,\mathrm{d}\phi_S} = \frac{\alpha^2}{2\,s\,x_B\,Q^2}\,L_{\mu\nu}(l,l',\lambda_e)\;2MW^{\mu\nu}(q,P,S), \tag{2.3}$$

where $\alpha = e^2/4\pi$. The formula above is valid in the so-called "single-photon exchange approximation." Some QED radiative corrections can be included without modifying this formula [3], but effects such as double-photon exchange are left out [109].

Considering the lepton to be longitudinally polarized, in the massless limit the leptonic tensor is given by

$$\begin{aligned} L_{\mu\nu} &= \sum_{\lambda'_e} \Big(\bar{u}(l',\lambda'_e)\,\gamma_\mu\,u(l,\lambda_e)\Big)^* \Big(\bar{u}(l',\lambda'_e)\,\gamma_\nu\,u(l,\lambda_e)\Big) \\ &= -Q^2 g_{\mu\nu} + 2\left(l_\mu l'_\nu + l'_\mu l_\nu\right) + 2\mathrm{i}\,\lambda_e\,\epsilon_{\mu\nu\rho\sigma}\,l^\rho l'^\sigma. \end{aligned} \tag{2.4}$$

Ex. 1
Compute the leptonic tensor using Mathematica and the FeynCalc package (www.feyncalc.org). The most important instructions are

```
<< HighEnergyPhysics`FeynCalc`

ScalarProduct[l, lp] = Q^2/2;

Amp0 = Contract[
  Spinor[l].(-I e GA[\[Mu]]).((1 + GA[5] \[Lambda])/2).Spinor[lp]]

Amp0bar = ComplexConjugate[Amp0] /. \[Mu] -> \[Nu]

FermionSpinSum[Amp0 Amp0bar]

Lept = FermionSpinSum[Amp0 Amp0bar]
       /. {DiracTrace -> Tr} /. {\[Lambda]^2 -> 1}
```

It may be convenient (for reasons that will be clear when considering the structure of the hadronic tensor) to write the formulas in a more different way, by introducing the normalized vectors

$$\hat{q}^\mu = \frac{q^\mu}{Q}, \tag{2.5}$$

$$\hat{t}^\mu = \frac{2x_B}{Q\sqrt{1+\gamma^2}}\left(P^\mu - \frac{P\cdot q}{q^2}q^\mu\right), \tag{2.6}$$

$$\hat{l}^\mu = -\frac{g_\perp^{\mu\nu} l_\nu}{|g_\perp^{\mu\nu} l_\nu|} \tag{2.7}$$

with the projectors on the transverse space is defined as

$$g_\perp^{\mu\nu} = g^{\mu\nu} + \hat{q}^\mu\hat{q}^\nu - \hat{t}^\mu\hat{t}^\nu, \tag{2.8}$$

$$\epsilon_\perp^{\mu\nu} = \epsilon^{\mu\nu\rho\sigma}\hat{t}_\rho\hat{q}_\sigma. \tag{2.9}$$

It turns out that

$$l^\mu = \frac{Q}{2}\hat{q}^\mu + \frac{(2-y)}{2y}\hat{t}^\mu + \frac{Q\sqrt{1-y}}{y}\hat{l}^\mu \tag{2.10}$$

from which we can obtain

$$\begin{aligned} L^{sym}_{\mu\nu} = \frac{2Q^2}{y^2}\Big[&-\Big(1-y+\frac{y^2}{2}\Big)g_{\perp\mu\nu} + 2(1-y)\,\hat{t}_\mu\hat{t}_\nu \\ &+ 2(1-y)\Big(\hat{l}_{\perp\mu}\hat{l}_{\perp\nu} + \frac{1}{2}g_{\perp\mu\nu}\Big) + 2(2-y)\sqrt{1-y}(\hat{t}_\mu\hat{l}_\nu + \hat{t}_\nu\hat{l}_\mu)\Big] \end{aligned} \tag{2.11}$$

The leptonic tensor contains all the information on the leptonic probe, which can be described by means of perturbative QED, while the information on the hadronic target is contained in the hadronic tensor

$$2MW^{\mu\nu}(q,P,S) = \frac{1}{2\pi}\sum_X \int \frac{\mathrm{d}^3\boldsymbol{P}_X}{(2\pi)^3\,2P^0_X}\,(2\pi)^4\,\delta^{(4)}\Big(q+P-P_X\Big)\,H^{\mu\nu}(P,S,P_X), \tag{2.12}$$

$$H^{\mu\nu}(P,S,P_X) = \langle P,S\,|\,J^\mu(0)\,|X\rangle\langle X|\,J^\nu(0)\,|P,S\,\rangle. \tag{2.13}$$

The state X symbolizes any final state, with total momentum P_X. It is integrated over since in inclusive processes the final state goes undetected.

In general, the structure of the hadronic tensor can be parametrized in terms of *structure functions*.

Let us start from unpolarized DIS. We can use the vectors q^μ and P^μ. Let me define the parity-reversal transformation

$$L^\rho_\sigma = \begin{pmatrix} 1 & 0 & 0 & 0 \\ 0 & -1 & 0 & 0 \\ 0 & 0 & -1 & 0 \\ 0 & 0 & 0 & -1 \end{pmatrix} \tag{2.14}$$

The following conditions must be fulfilled:

Hermiticity: $$W^*_{\mu\nu}(q,P,S) = W_{\nu\mu}(q,P,S), \tag{2.15a}$$

parity: $$L^\rho_\mu L^\sigma_\nu W_{\rho\sigma}(q,P,S) = W_{\mu\nu}(\tilde{q},\tilde{P},-\tilde{S}), \tag{2.15b}$$

time-reversal: $$L^\rho_\mu L^\sigma_\nu W^*_{\rho\sigma}(q,P,S) = W_{\mu\nu}(\tilde{q},\tilde{P},\tilde{S}) \tag{2.15c}$$

where $\tilde{q}^\nu = L^\nu_\rho q^\rho$ and so forth for the other vectors (i.e., change sign to the spatial components of the vectors).

We could build the combinations

$$2MW^{\mu\nu} = 2M\left[A\,g^{\mu\nu} + B\,q^\mu q^\nu + C\,\frac{P^\mu P^\nu}{M^2} + D\,\frac{P^\mu q^\nu + q^\mu P^\nu}{M^2}\right], \tag{2.16}$$

where each of the terms can depend on the scalar products Q^2 and $P\cdot q$, or more conveniently on Q^2 and x_B. A combination such as $\mathrm{i}\epsilon^{\mu\nu\rho\sigma}P_\rho q_\sigma$ is excluded only by parity invariance and should be taken

into account when considering, e.g., neutrino scattering. A combination such as $P^{\{\mu}\epsilon^{\nu\}\alpha\rho\sigma}P_\rho q_\sigma S_\alpha$ is forbidden by time-reversal invariance.

Finally, electromagnetic gauge invariance requires that

$$q_\mu W^{\mu\nu} = q_\nu W^{\mu\nu} = 0. \tag{2.17}$$

From this condition, it follows that

$$D = -\frac{P\cdot q}{q^2}B, \qquad C = \left(\frac{P\cdot q}{q^2}\right)B + \frac{M^2}{q^2}A. \tag{2.18}$$

Therefore, there are only two independent structure functions.

In terms of our normalized vectors and projectors we can write

$$2MW^{\mu\nu}(q,P,S) = \frac{1}{x_B}[-g_\perp^{\mu\nu}F_T(x_B,Q^2) + \hat{t}^\mu\hat{t}^\nu F_L(x_B,Q^2)]. \tag{2.19}$$

In the case of polarized inclusive DIS, given the constraints, we can introduce four structure functions. There are multiple definitions of the structure functions. A possible one is

$$\begin{aligned} 2MW^{\mu\nu}(q,P,S) = \frac{1}{x_B}\Big[& -g_\perp^{\mu\nu}F_T(x_B,Q^2) + \hat{t}^\mu\hat{t}^\nu F_L(x_B,Q^2) \\ & + \mathrm{i}S_L\epsilon_\perp^{\mu\nu}2x_B\,(g_1(x_B,Q^2) - \gamma^2 g_2(x_B,Q^2)) \\ & + \mathrm{i}\hat{t}^{[\mu}\epsilon_\perp^{\nu]\rho}S_\rho 2x_B\gamma\,(g_1(x_B,Q^2) + g_2(x_B,Q^2))\Big] \end{aligned} \tag{2.20}$$

where the involved vectors and tensors are defined in the same way as in Piet Mulders's notes. The connection with the standard unpolarized structure functions is

$$F_T(x_B,Q^2) = 2x_B F_1(x_B,Q^2), \tag{2.21}$$

$$F_L(x_B,Q^2) = (1+\gamma^2)F_2(x_B,Q^2) - 2x_B F_1(x_B,Q^2). \tag{2.22}$$

The contraction of the leptonic and hadronic tensors leads to the following expression for the inclusive DIS cross-section

$$\begin{aligned} \frac{d\sigma}{dx_B\,dy\,d\phi_S} = \frac{2\alpha^2}{x_B y Q^2}\,\frac{y^2}{2\,(1-\varepsilon)}\Big\{ & F_T + \varepsilon F_L + S_\parallel\lambda_e\,\sqrt{1-\varepsilon^2}\,2x_B\,(g_1 - \gamma^2 g_2) \\ & - |\boldsymbol{S}_\perp|\lambda_e\,\sqrt{2\,\varepsilon(1-\varepsilon)}\,\cos\phi_S\,2x_B\gamma\,(g_1+g_2)\Big\}, \end{aligned} \tag{2.23}$$

where the structure functions on the r.h.s. depend on x_B and Q^2 (i.e. $P\cdot Q$ and q^2). We also introduced the ratio ε of longitudinal and transverse photon flux in

$$\varepsilon = \frac{1-y}{1-y+\frac{1}{2}y^2}, \qquad \text{and} \qquad \gamma = \frac{2Mx_B}{Q} \tag{2.24}$$

It is often necessary, especially for experimental reasons, to distinguish also the component of S parallel or orthogonal to the lepton beam instead of the virtual photon. However, the difference

between the two quantities is M/Q suppressed. A thorough discussion about this point has been presented, e.g., in Ref. [61].

Ex. 2
Eq. (2.23) does not yet look as the standard results in the literature, e.g., Eq. (2.7) in [86]. Check the correspondence by expressing the results with respect to the lepton beam direction, making use of the following relations

$$S^{\gamma}_{\parallel} = \cos\theta\, S^{e}_{\parallel} + \sin\theta\, |\boldsymbol{S}^{e}_{\perp}| \cos\psi,$$
$$|\boldsymbol{S}^{\gamma}_{\perp}| \cos\phi_S = \cos\theta\, |\boldsymbol{S}^{e}_{\perp}| \cos\psi - \sin\theta\, S^{e}_{\parallel}$$

and

$$\cos\theta = \frac{1+\gamma^2 y/2}{\sqrt{1+\gamma^2}} = \frac{1-(1-y)\varepsilon}{\sqrt{1-\varepsilon^2}},$$
$$\sin\theta = \gamma \sqrt{\frac{1-y-\gamma^2 y^2/4}{1+\gamma^2}} = \frac{\varepsilon y}{\sqrt{2\,\varepsilon(1-\varepsilon)}}$$

2.1 DIS in the parton model

For the treatment of inclusive DIS, it is convenient to choose a frame where the proton and photon momenta have no transverse components. In terms of light-cone vectors, it means

$$P^{\mu} = P^{+} n^{\mu}_{+} + \frac{M^2}{2P^{+}}\, n^{\mu}_{-}\,, \tag{2.25}$$
$$q^{\mu} = -x_B P^{+} n^{\mu}_{+} + \frac{Q^2}{2x_B P^{+}}\, n^{\mu}_{-}\,. \tag{2.26}$$

The spin vector of the target can then be decomposed as

$$S^{\mu} = S_L\, \frac{(P\cdot n_-)\, n^{\mu}_{+} - (P\cdot n_+)\, n^{\mu}_{-}}{M} + S^{\mu}_{T}\,. \tag{2.27}$$

It is particularly convenient to work in a reference frame where

$$xP^{+} = Q/\sqrt{2}. \tag{2.28}$$

Ex. 3
Derive the following expressions of the involved momenta in the frame we are using

$$P^\mu = \left[\frac{x_B M^2}{Q\sqrt{2}},\ \frac{Q}{x_B\sqrt{2}},\ \mathbf{0}\right] \tag{2.29a}$$

$$q^\mu = \left[\frac{Q}{\sqrt{2}},\ -\frac{Q}{\sqrt{2}},\ \mathbf{0}_T\right] \tag{2.29b}$$

$$l^\mu = \left[\frac{Q}{y\sqrt{2}},\ \frac{(1-y)Q}{y\sqrt{2}},\ \frac{Q\sqrt{1-y}}{y},\ 0\right], \tag{2.29c}$$

$$l'^\mu = \left[\frac{(1-y)Q}{y\sqrt{2}},\ \frac{Q}{y\sqrt{2}},\ \frac{Q\sqrt{1-y}}{y},\ 0\right]. \tag{2.29d}$$

The phenomenology of DIS taught us that at sufficiently high Q^2 we can assume that the scattering of the electron takes place off a quark of mass m inside the nucleon. The final state $\mathcal{X}$ can be split in a quark with momentum k plus a state X with momentum P_X. Considering the electron-quark interaction at tree level only, the hadronic tensor can be written as

$$\begin{aligned} 2MW^{\mu\nu}(q,P,S) = \frac{1}{2\pi}\sum_q e_q^2 \sum_X \int \frac{\mathrm{d}^3\boldsymbol{P}_X}{(2\pi)^3\,2P_X^0} \int \frac{\mathrm{d}^3\boldsymbol{k}}{(2\pi)^3\,2k^0}\,(2\pi)^4\,\delta^{(4)}\Big(P+q-k-P_X\Big) \\ \times \langle P,S\,|\,\bar\psi_i(0)\,|X\rangle\langle X|\,\psi_j(0)\,|P,S\,\rangle\,\gamma^\mu_{ik}\,(\not k + m)_{kl}\,\gamma^\nu_{lj}, \end{aligned} \tag{2.30}$$

where k is the momentum of the struck quark, the index q denotes the quark flavor and e_q is the fractional charge of the quark. Note that, for simplicity, we omitted the flavor indices on the quark fields. The integration over the phase space of the final-state quark can be replaced by a four-dimensional integral with an on-shell condition,

$$\int \frac{\mathrm{d}^3\boldsymbol{k}}{2k^0} \longrightarrow \int \mathrm{d}^4k\ \delta\left(k^2-m^2\right)\,\theta\left(k^0-m\right), \tag{2.31}$$

so that the hadronic tensor can be rewritten as

$$\begin{aligned} 2MW^{\mu\nu}(q,P,S) = \sum_q e_q^2 \sum_X \int \frac{\mathrm{d}^3\boldsymbol{P}_X}{(2\pi)^3\,2P_X^0} \int \mathrm{d}^4k\ \delta\left(k^2-m^2\right)\,\theta\left(k^0-m\right) \\ \times \delta^{(4)}\Big(P+q-k-P_X\Big)\,\langle P,S\,|\,\bar\psi_i(0)\,|X\rangle\langle X|\,\psi_j(0)\,|P,S\,\rangle\,\gamma^\mu_{ik}\,(\not k + m)_{kl}\,\gamma^\nu_{lj}. \end{aligned} \tag{2.32}$$

Next, we Fourier transform the Dirac delta function according to

$$\delta^{(4)}\Big(P+q-k-P_X\Big) \longrightarrow \int \frac{\mathrm{d}^4\xi}{(2\pi)^4}\,\mathrm{e}^{\mathrm{i}\,(P+q-k-P_X)\cdot\xi} \tag{2.33}$$

and we introduce the momentum $p = k - q$ to obtain

$$\begin{aligned} 2MW^{\mu\nu}(q,P,S) = \sum_q e_q^2 \sum_X \int \frac{\mathrm{d}^3\boldsymbol{P}_X}{(2\pi)^3\,2P_X^0} \int \mathrm{d}^4p\ \delta\left((p+q)^2-m^2\right)\,\theta\left(p^0+q^0-m\right) \\ \times \int \frac{\mathrm{d}^4\xi}{(2\pi)^4}\,\mathrm{e}^{\mathrm{i}\,(P-p-P_X)\cdot\xi}\,\langle P,S\,|\,\bar\psi_i(0)\,|X\rangle\langle X|\,\psi_j(0)\,|P,S\,\rangle\,\gamma^\mu_{ik}\,(\not p + \not q + m)_{kl}\,\gamma^\nu_{lj}. \end{aligned} \tag{2.34}$$

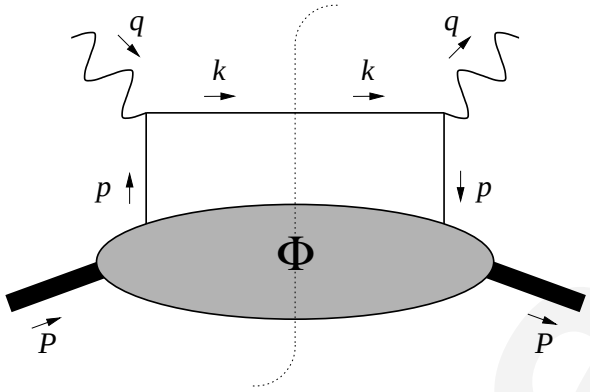

Figure 2.1: The handbag diagram, describing the hadronic tensor for inclusive DIS at Born level.

Finally, we use part of the exponential to perform a translation of the field operators and we use completeness to eliminate the unobserved X states, so that

$$\begin{aligned} 2MW^{\mu\nu}(q,P,S) = \sum_q e_q^2 \int \mathrm{d}^4p\, \delta\Big((p+q)^2 - m^2\Big)\, \theta\Big(p^0+q^0-m\Big) \int \frac{\mathrm{d}^4\xi}{(2\pi)^4}\, \mathrm{e}^{-\mathrm{i}p\cdot\xi} \\ \times \Big(\langle P,S\,|\,\bar\psi_i(\xi)\,\psi_j(0)\,|P,S\rangle\, \gamma^\mu_{ik}\,(\not p + \not q + m)_{kl}\,\gamma^\nu_{lj}\Big). \end{aligned} \tag{2.35}$$

The hadronic tensor can be written in a more compact way by introducing the quark-quark correlation function Φ

$$\begin{aligned} 2MW^{\mu\nu}(q,P,S) = \sum_q e_q^2 \int \mathrm{d}^4p\, \delta\Big((p+q)^2 - m^2\Big)\, \theta\Big(p^0+q^0-m\Big) \\ \times \mathrm{Tr}\left[\Phi(p,P,S)\gamma^\mu\,(\not p + \not q + m)\,\gamma^\nu\right] \end{aligned} \tag{2.36}$$

where

$$\begin{aligned} \Phi_{ji}(p,P,S) &= \frac{1}{(2\pi)^4}\int \mathrm{d}^4\xi\, \mathrm{e}^{-\mathrm{i}p\cdot\xi}\langle P,S\,|\,\bar\psi_i(\xi)\,\psi_j(0)\,|P,S\rangle \\ &= \sum_X \int \frac{\mathrm{d}^3\boldsymbol{P}_X}{(2\pi)^3\,2P_X^0}\,\langle P,S\,|\,\bar\psi_i(0)\,|X\rangle\langle X|\,\psi_j(0)\,|P,S\rangle\,\delta^{(4)}\Big(P-p-P_X\Big), \end{aligned} \tag{2.37}$$

As the quark fields should carry a flavor index that we omitted, also the correlation functions are flavor dependent and they should be indicated more appropriately as Φ^q. A graphical representation of the hadronic tensor at tree level in the parton model is given by the so-called *handbag diagram*, depicted in Fig. 2.1.

We parametrize the quark momentum p in the following way

$$p^\mu = \left[\frac{p^2+|\boldsymbol{p}_T|^2}{2xP^+},\ xP^+,\ \boldsymbol{p}_T\right]. \tag{2.38}$$

In our approach, we assume that neither the virtuality of the quark, p^2, nor its transverse momentum squared, $|\boldsymbol{p}_T|^2$, can be large in comparison with the hard scale Q^2. Under these conditions, the

quark momentum is soft with respect to the hadron momentum and its relevant component is xP^+. In Eq. (2.36), neglecting terms which are $1/Q$ suppressed, we can use an approximate expression for the delta function

$$\delta\left((p+q)^2 - m^2\right) \approx \delta(p^+ + q^+) \approx P^+\,\delta(x - x_B) \tag{2.39}$$

and replace

$$\mathrm{d}^4 p = \mathrm{d}^2\boldsymbol{p}_T\;\mathrm{d}p^-\;P^+\;\mathrm{d}x \tag{2.40}$$

and obtain

$$\begin{aligned} 2MW^{\mu\nu}(q,P,S) &\approx \sum_q e_q^2 \int \mathrm{d}^2\boldsymbol{p}_T\,\mathrm{d}p^-\,\mathrm{d}x\;\frac{P^+}{2P\cdot q}\;\delta\,(x - x_B) \\ &\quad \times \mathrm{Tr}\left[\Phi^q(p,P,S)\,\gamma^\mu\,(\not{p} + \not{q} + m)\,\gamma^\nu\right] \\ &= \sum_q e_q^2\;\frac{1}{2}\mathrm{Tr}\left[\Phi^q(x_B,S)\,\gamma^\mu\frac{P^+}{P\cdot q}\,(\not{p} + \not{q} + m)\,\gamma^\nu\right] \end{aligned} \tag{2.41}$$

where we introduced the integrated correlation function

$$\begin{aligned} \Phi^q_{ji}(x,S) &= \int \mathrm{d}^2\boldsymbol{p}_T\,\mathrm{d}p^-\;\Phi^q_{ji}(p,P,S)\Big|_{p^+ = xP^+} \\ &= \int \frac{\mathrm{d}\xi^-}{2\pi}\;\mathrm{e}^{-\mathrm{i}p\cdot\xi}\langle P,S\,|\,\bar\psi^q_i(\xi)\;\psi^q_j(0)\,|\,P,S\rangle\Big|_{\xi^+ = \boldsymbol{\xi}_T = 0}. \end{aligned} \tag{2.42}$$

Here, the subscript and superscript q stands for the quark flavor.

Finally, from the outgoing quark momentum, $p + q$, we can select only the minus component and obtain the final form for the hadronic tensor at leading twist

$$2MW^{\mu\nu}(q,P,S) \approx \sum_q e_q^2\;\frac{1}{2}\mathrm{Tr}\left[\Phi^q(x_B,S)\,\gamma^\mu\gamma^+\gamma^\nu\right]. \tag{2.43}$$

A few words to justify the last approximation are in order. The dominance of the minus component is most easily seen in the infinite momentum frame, where $p^- + q^-$ is of the order of Q, while $p^+ + q^+ = 0$, and $\boldsymbol{p}_T$ and m are of the order of 1. However, if we perform a $1/Q$ expansion of the full expression, including the correlation function Φ^q [starting from Eq. (2.50)], we would be able to check that in any collinear frame the dominant terms arise only from the combination of plus component in the correlation function and minus components in the outgoing quark momentum.

2.2 The integrated correlation function

At this point, we need to analyze the structure of the correlation function Φ^q (in the following, we will omit the flavor superscript q).

To get more insight into the information contained in the correlation function, which is a Dirac matrix, we can decompose it in a general way on a basis of Dirac structures. Each term of the

decomposition can be a combination of the Lorentz vectors p and P, the Lorentz pseudovector S (in case of spin-half hadrons) and the Dirac structures

$$\mathbf{1},\ \gamma_5,\ \gamma^\mu,\ \gamma^\mu\gamma_5,\ \mathrm{i}\sigma^{\mu\nu}\gamma_5,$$

where $\sigma^{\mu\nu} = \mathrm{i}[\gamma^\mu, \gamma^\nu]/2$. The spin vector can only appear linearly in the decomposition. Moreover, each term of the full expression has to satisfy the conditions of Hermiticity and parity invariance

$$\text{Hermiticity:} \qquad \Phi(p, P, S) = \gamma^0\, \Phi^\dagger(p, P, S)\, \gamma^0, \tag{2.44a}$$

$$\text{parity:} \qquad \Phi(p, P, S) = \gamma^0\, \Phi(\tilde{p}, \tilde{P}, -\tilde{S})\, \gamma^0. \tag{2.44b}$$

To simplify the discussion, let's first consider an unpolarized target. The most general decomposition is

$$\Phi(p, P) = M\, A_1\, \mathbf{1} + A_2\, \not{P} + A_3\, \not{p} + \frac{A_4}{M}\, \sigma_{\mu\nu} P^\mu p^\nu, \tag{2.45}$$

where the amplitudes A_i are real scalar functions $A_i = A_i(p \cdot P, p^2)$ with dimension $1/[m]^4$. The above expression is what we could call the "doubly unintegrated correlation function" (see, e.g., Ref. [48]).

In reality, the above expression is incomplete, because on top of the vectors p, P we should also take into account the vector n_- which is related to the direction of the gauge link (see Sec. 3.8). Because of this, new structures appear in the decomposition of Eq. (2.50) [65]. The full decomposition for a nucleon target has been studied in Ref. [66]. For an unpolarized target we obtain [21]

$$\begin{aligned}\Phi(p, P|n_-) = {} & M\, A_1\, \mathbf{1} + A_2\, \not{P} + A_3\, \not{p} + \frac{A_4}{M}\, \sigma_{\mu\nu} P^\mu p^\nu \\ & + \frac{M^2}{P \cdot n_-} \not{n}_-\, B_1 + \frac{iM}{2P \cdot n_-} [\not{P}, \not{n}_-]\, B_2 + \frac{iM}{2P \cdot n_-} [\not{p}, \not{n}_-]\, B_3 \\ & + \frac{1}{P \cdot n_-} \varepsilon^{\mu\nu\rho\sigma} \gamma_\mu \gamma_5 P_\nu p_\rho n_{-\sigma}\, B_4.\end{aligned} \tag{2.46}$$

If we keep only the leading terms in $1/P^+$ (which in the end will turn out to appear in the cross section with a leading power in $1/Q$, i.e. leading twist), we obtain

$$\Phi(p, P) \approx P^+ (A_2 + xA_3)\, \not{n}_+ + P^+ \frac{\mathrm{i}}{2M} [\not{n}_+, \not{p}_T] A_4. \tag{2.47}$$

For our purposes, we are interested in the calculation of the object entering the expression of the hadronic tensor, what we called the integrated correlation function, Eq. (2.42). In the unpolarized case it is very simple (now reintroducing also the flavor index q):

$$\Phi^q(x) = f_1^q(x) \not{n}_+/2 \tag{2.48}$$

where we introduced the integrated parton distribution function

$$f_1^q(x) = \int \mathrm{d}^2\boldsymbol{p}_T\, \mathrm{d}p^2\, \mathrm{d}(2p \cdot P)\, \delta\left(\boldsymbol{p}_T^2 + x^2 M^2 + p^2 - 2xp \cdot P\right) \left[A_2^q + xA_3^q\right], \tag{2.49}$$

The function $f_1^q(x)$ is usually referred to as the unpolarized parton distribution, and it is often denoted also as simply $q(x)$ (where q stands for the quark flavor).

If we now extend the analysis to the polarized case, the most general decomposition of the correlation function Φ imposing Hermiticity and parity invariance is [97, 107]

$$\begin{aligned}\Phi(p,P,S) = {} & M A_1 \mathbf{1} + A_2 \not{P} + A_3 \not{p} + \frac{A_4}{M}\sigma_{\mu\nu}P^\mu p^\nu + \mathrm{i}A_5\, p\cdot S\,\gamma_5 \\ & + M A_6 \not{S}\gamma_5 + A_7 \frac{p\cdot S}{M}\not{P}\gamma_5 + A_8 \frac{p\cdot S}{M}\not{p}\gamma_5 + \mathrm{i}A_9\,\sigma_{\mu\nu}\gamma_5 S^\mu P^\nu \\ & + \mathrm{i}A_{10}\,\sigma_{\mu\nu}\gamma_5 S^\mu p^\nu + \mathrm{i}A_{11}\frac{p\cdot S}{M^2}\sigma_{\mu\nu}\gamma_5 P^\mu p^\nu + A_{12}\frac{\epsilon_{\mu\nu\rho\sigma}\gamma^\mu P^\nu p^\rho S^\sigma}{M},\end{aligned} \tag{2.50}$$

where the amplitudes A_i real scalar functions $A_i = A_i(p\cdot P, p^2)$ with dimension $1/[m]^4$. We don't give here the full expression when considering also the vector n_-, which can be found in Ref. [66].

The general expression of the integrated correlation function becomes

$$\Phi(x,S) = \frac{1}{2}\left\{f_1 \not{n}_+ + S_L\, g_{1L}\gamma_5 \not{n}_+ + h_1 \frac{[\not{S}_T, \not{n}_+]\gamma_5}{2}\right\}, \tag{2.51}$$

where we introduced the integrated parton distribution functions

$$f_1(x) = \int \mathrm{d}^2\boldsymbol{p}_T\,\mathrm{d}p^2\,\mathrm{d}(2p\cdot P)\,\delta\left(\boldsymbol{p}_T^2 + x^2M^2 + p^2 - 2xp\cdot P\right)[A_2 + xA_3]\,, \tag{2.52a}$$

$$\begin{aligned}g_{1L}(x) = {} & \int \mathrm{d}^2\boldsymbol{p}_T\,\mathrm{d}p^2\,\mathrm{d}(2p\cdot P)\,\delta\left(\boldsymbol{p}_T^2 + x^2M^2 + p^2 - 2xp\cdot P\right) \\ & \times\left[-A_6 - \left(\frac{p\cdot P}{M^2} - x\right)(A_7 + xA_8)\right],\end{aligned} \tag{2.52b}$$

$$\begin{aligned}h_1(x) = {} & \int \mathrm{d}^2\boldsymbol{p}_T\,\mathrm{d}p^2\,\mathrm{d}(2p\cdot P)\,\delta\left(\boldsymbol{p}_T^2 + x^2M^2 + p^2 - 2xp\cdot P\right) \\ & \times\left[-A_9 - xA_{10} + \frac{\boldsymbol{p}_T^2}{2M^2}A_{11}\right].\end{aligned} \tag{2.52c}$$

The function g_{1L}^q (after reinserting the quark flavor superscript) is the helicity distribution of parton q and it can be denoted also as Δq.[1] The function h_1 is known as the parton transversity distribution; in the literature it is sometimes denoted as δq, $\Delta_T q$, although in the original paper of Ralston and Soper [107] it was called h_T.

The individual distribution functions can be isolated by means of the projection

$$\Phi^{[\Gamma]} \equiv \frac{1}{2}\mathrm{Tr}\left(\Phi\Gamma\right), \tag{2.53}$$

where Γ stands for a specific Dirac structure. In particular, we see that

$$f_1(x) = \Phi^{[\gamma^+]}(x), \tag{2.54a}$$

$$g_{1L}(x) = \Phi^{[\gamma^+\gamma^5]}(x), \tag{2.54b}$$

$$h_1(x) = \Phi^{[\mathrm{i}\sigma^{i+}\gamma^5]}(x). \tag{2.54c}$$

[1] In the Amsterdam literature this function is usually denote as g_1. Here, however, we prefer to name it g_{1L} to clearly distinguish it from the structure function defined in Eq. (2.20)

The leading-twist part of the correlator Φ can be projected out using the projector

$$\mathcal{P}_+ = \frac{1}{2}\,\gamma^-\gamma^+, \tag{2.55}$$

Before the interaction with the virtual photon, the relevant components of the quark fields are the plus components, $\psi_+ = \mathcal{P}_+\,\psi$. They are usually referred to as the *good components*.

Finally, it is useful to define the matrix $F = \left(\mathcal{P}_+\,\Phi\gamma^+\right)^T$, i.e. the Dirac transpose of the leading-twist part of the correlation function, and observe that

$$\begin{aligned} F(x,\boldsymbol{p}_T)_{ij} &= \int \frac{\mathrm{d}\xi^-}{2\pi\sqrt{2}}\,\mathrm{e}^{-\mathrm{i}p\cdot\xi}\langle P|\,(\psi_+)_i^\dagger(\xi)\;(\psi_+)_j(0)\,|P\rangle\Big|_{\xi^+=0} \\ &= \frac{1}{\sqrt{2}}\sum_X \int \frac{\mathrm{d}^3\boldsymbol{P}_X}{(2\pi)^3\,2P_X^0}\langle X|\,(\psi_+)_i(0)\,|P\rangle^*\langle X|\,(\psi_+)_j(0)\,|P\rangle \\ &\quad\times\delta\Big((1-x)P^+ - P_X^+\Big) \end{aligned} \tag{2.56}$$

This matrix describes a probability to find a (good projection of a) quark with a certain chirality inside the target. For any Dirac spinor $|a\rangle$, the expectation value $\langle a|\,F\,|a\rangle$ must be positive (it a modulus squared). In mathematical terms, this means that the matrix is *positive semidefinite*, i.e. the determinant of all the principal minors of the matrix has to be positive or zero. This property will prove to be essential in deriving bounds on the components of the correlation function, i.e. the parton distribution functions.

The correlation function is a matrix in the parton chirality space and depends on the target spin. By introducing the helicity density matrix of the target

$$\rho(S)_{\Lambda_1\Lambda_1'} = \frac{1}{2}\,(1+\boldsymbol{S}\cdot\boldsymbol{\sigma})_{\Lambda_1\Lambda_1'} = \frac{1}{2}\begin{pmatrix} 1+S_L & S_x-\mathrm{i}S_y \\ S_x+\mathrm{i}S_y & 1-S_L \end{pmatrix}, \tag{2.57}$$

we can obtain the correlation function from the trace of the helicity density matrix and a new matrix in the quark chirality space $\otimes$ the target spin space:

$$\left(\mathcal{P}_+\,\Phi(x,S)\gamma^+\right)_{\chi_1'\chi_1} = \rho(S)_{\Lambda_1\Lambda_1'}\left(\mathcal{P}_+\,\Phi(x)\gamma^+\right)^{\Lambda_1'\Lambda_1}_{\chi_1'\chi_1}. \tag{2.58}$$

We will refer to the last term of this relation as the matrix representation of the correlation function or, more simply, as the correlation matrix. Fig. 3.6 shows pictorially the position of the spin indices.

Starting from Eq. (2.51) and using the relation

$$\Psi_U + S_L\Psi_L + S_x\Psi_x + S_y\Psi_y = \rho(S)_{\Lambda_1\Lambda_1'}\begin{pmatrix} \Psi_U+\Psi_L & \Psi_x-\mathrm{i}\Psi_y \\ \Psi_x+\mathrm{i}\Psi_y & \Psi_U-\Psi_L \end{pmatrix}^{\Lambda_1'\Lambda_1} \tag{2.59}$$

we can cast the correlation function in the matrix form

$$\left(\mathcal{P}_+\,\Phi(x)\gamma^+\right)^{\Lambda_1'\Lambda_1} = \begin{pmatrix} (f_1(x)+g_1(x)\,\gamma_5)\,\mathcal{P}_+ & h_1(x)\,(\gamma_x-\mathrm{i}\gamma_y)\,\gamma_5\mathcal{P}_+ \\ h_1(x)\,(\gamma_x+\mathrm{i}\gamma_y)\,\gamma_5\mathcal{P}_+ & (f_1(x)-g_1(x)\,\gamma_5)\,\mathcal{P}_+ \end{pmatrix}. \tag{2.60}$$

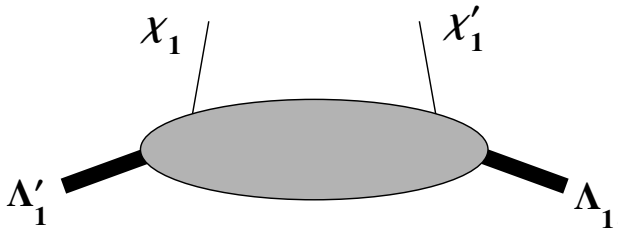

Figure 2.2: Illustration of the position of the indices of the correlation matrix.

The correlation function is a 4×4 Dirac matrix. However, due to the presence of the projector on the good components of the quark fields, the leading-twist part spans only a 2×2 Dirac subspace. This is evident if we express the Dirac structures of Eq. (3.37) in the chiral or Weyl representation (see also the discussion around Eq. (3.41)).

The resulting matrix is [13, 14]

$$F(x)^{\Lambda_1'\Lambda_1}_{\chi_1\chi_1'} = \left(\begin{array}{cc|cc} f_1(x)+g_{1L}(x) & 0 & 0 & 2h_1(x) \\ 0 & f_1(x)-g_{1L}(x) & 0 & 0 \\ \hline 0 & 0 & f_1(x)-g_{1L}(x) & 0 \\ 2h_1(x) & 0 & 0 & f_1(x)+g_{1L}(x) \end{array}\right). \tag{2.61}$$

where the inner blocks are in the hadron helicity space (indices $\Lambda_1'\Lambda_1$), while the outer matrix is in the quark chirality space (indices $\chi_1'\chi_1$). Note that because of the inversion of the quark indices, the lower left block has $\chi_1' = R, \chi_1 = L$ and vice versa for the upper right block. Since this matrix must be positive semidefinite, we can readily obtain the positivity conditions

$$f_1(x) \geq 0, \tag{2.62a}$$
$$|g_{1L}(x)| \leq f_1(x), \tag{2.62b}$$
$$|h_1(x)| \leq \tfrac{1}{2}(f_1(x) + g_{1L}(x)). \tag{2.62c}$$

The last relation is known as the *Soffer bound* [113].

The probabilistic interpretation of the functions f_1 and g_{1L} is manifest, since they occupy the diagonal elements of the matrix and they are therefore connected to squares of probability amplitudes

$$f_1(x) = \frac{1}{2}\left(F(x)^{\frac{1}{2}\frac{1}{2}}_{RR} + F(x)^{\frac{1}{2}\frac{1}{2}}_{LL}\right) \qquad g_{1L}(x) = \frac{1}{2}\left(F(x)^{\frac{1}{2}\frac{1}{2}}_{RR} - F(x)^{\frac{1}{2}\frac{1}{2}}_{LL}\right) \tag{2.63}$$

On the other hand, the transversity distribution is off-diagonal in the chirality basis. This should make clear that it is *chiral odd* and that it does not describe the square of a probability amplitude, but rather the interference between two different amplitudes

$$h_1(x) = \tfrac{1}{2}F(x)^{\frac{1}{2}-\frac{1}{2}}_{RL} \tag{2.64}$$

The transversity distribution recovers a probability interpretation if we choose the so-called *transversity basis*, instead of the helicity basis, for both quark and hadron [71,72]. The transversity

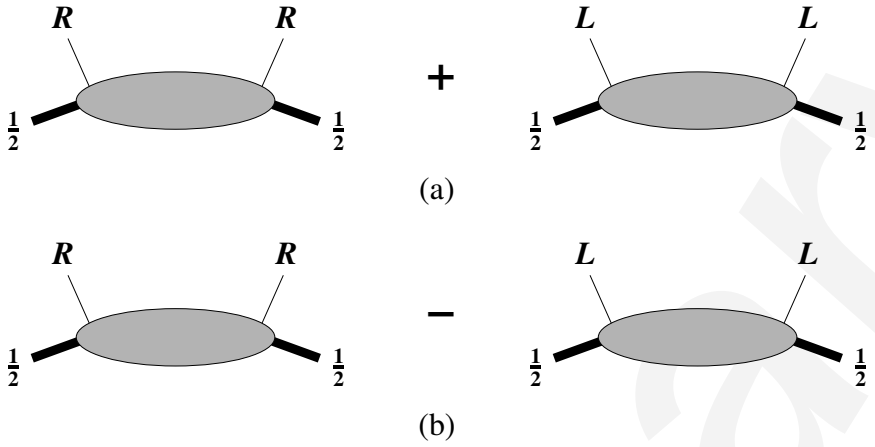

Figure 2.3: Probabilistic interpretation of the unpolarized distribution function f_1 (a), and of the helicity distribution function g_{1L} (b).

basis is formed by the "transversity up" and "transversity down" states. They can be expressed in terms of chirality eigenstates

$$u_\uparrow = \tfrac{1}{\sqrt{2}}\,(u_R + u_L)\,, \qquad\qquad u_\downarrow = \tfrac{1}{\sqrt{2}}\,(u_R - u_L)\,. \tag{2.65}$$

The same relation holds between the hadron transversity and helicity states.

In the new basis, the scattering matrix takes the form

$$F(x)^{\Lambda_1'\Lambda_1}_{\chi_1\chi_1'} = \left(\begin{array}{cc|cc} f_1(x)+h_1(x) & 0 & 0 & g_{1L}(x)+h_1(x) \\ 0 & f_1(x)-h_1(x) & g_{1L}(x)-h_1(x) & 0 \\ \hline 0 & g_{1L}(x)-h_1(x) & f_1(x)-h_1(x) & 0 \\ g_{1L}(x)+h_1(x) & 0 & 0 & f_1(x)+h_1(x) \end{array}\right), \tag{2.66}$$

and clearly the transversity distribution function can be defined as

$$h_1(x) = \frac{1}{2}\left(F(x)^{\uparrow\uparrow}_{\uparrow\uparrow} - F(x)^{\uparrow\uparrow}_{\downarrow\downarrow}\right). \tag{2.67}$$

2.3 DIS structure functions in the parton model

Once we have determined the general decomposition of the correlation function, we can compute the cross section using Eqs. (2.43) and (2.3).

Ex. 4

Using the leptonic tensor calculated in Ex. 1, compute the cross-section for polarized inclusive DIS in the parton model with Mathematica. The relevant instructions are

```
GAp = GS[Momentum[nm]];
GAm = GS[Momentum[np]];
GA5 = DiracGamma[5];

ScalarProduct[nm, np] = 1;
ScalarProduct[l, np] = 1/Sqrt[2] (((2 - y) Q)/(2 y) - Q/2);
ScalarProduct[l, nm] = 1/Sqrt[2] (((2 - y) Q)/(2 y) + Q/2);
ScalarProduct[lp, np] = 1/Sqrt[2] (((2 - y) Q)/(2 y) + Q/2);
ScalarProduct[lp, nm] = 1/Sqrt[2] (((2 - y) Q)/(2 y) - Q/2);

Phi = (f1 + Sl g1 GA5 + h1  GA5 .GS[Momentum[St]]).(GAm/2)

MW = 1/2 1/2 (Tr[Phi.GA[\[Mu]].GAp .GA[\[Nu]]]) //
  Collect[#, {f1 D1, h1perp H1perp}, Simplify] &

(\[Alpha]^2 y)/(2 Q^4) Contract[Lept 2 MW] // Simplify
```

The final result of the cross section can be obtained from the expressions of the structure functions, which is summarized in the following relations:

$$F_1 = \frac{1}{2} \sum_q e_q^2 \, f_1^q(x_B), \tag{2.68}$$

$$F_L = 0, \tag{2.69}$$

$$g_1 = \frac{1}{2} \sum_q e_q^2 \, g_{1L}^q(x_B), \tag{2.70}$$

$$g_1 + g_2 = 0. \tag{2.71}$$

A few remarks about the above results. First of all, we see that the transversity distribution does not occurr in any of the above structure functions. This is due to the specific Dirac structure of the transversity term in the correlation function, Eq. (2.51): that term contains two Dirac matrices, and it enters a trace with three more Dirac matrices in Eq. (2.43). Therefore, the term disappears. Another interesting observation is that the structure-function combination $g_1 + g_2$ vanishes. We mention that the function becomes nonzero when going to the subleading-twist level in the analysis of the correlation function. Finally, the longitudinal structure function F_L vanishes, and it remains zero also at the next-to-leading-twist (NLT) level. To obtain a nonzero function we have to consider QCD corrections of order α_S (set to zero at the parton-model level) or go to the NNLT level.

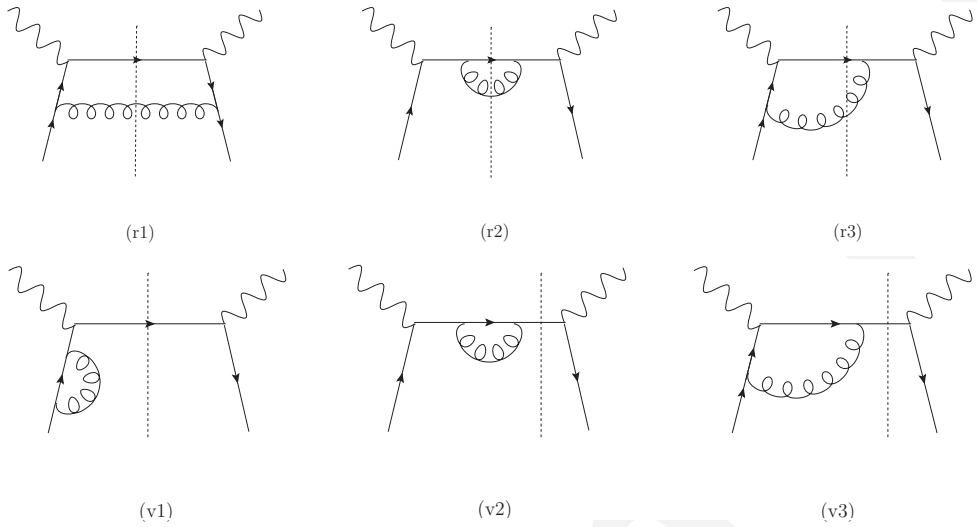

Figure 2.4: Cut diagrams representing real and virtual corrections to the $\gamma^* q \to q$ process. Some Hermitean conjugate diagrams are not shown.

2.4 DIS beyond the parton model

In these short lectures, we did not have time to study much of the QCD corrections to the parton-model picture. For what concerns inclusive DIS and collinear PDFs, I refer to the excellent lectures of Marco Stratmann. The most recent and authoritative reference on this issue is the book by John Collins [49].

In very concise and qualitative terms, let me just mention that the inclusion of QCD corrections to the parton model leads to the important results of *factorization* and *evolution*, the second being almost a direct consequence of the first. QCD factorization theorems are central to understanding high energy hadronic scattering cross sections in terms of the fundamentals of perturbative QCD. In addition to providing a practical prescription for order-by-order calculations, derivations of factorization provide a solid theoretical foundation for concepts like PDFs.

The parton-model approach relies on the assumption that we can separate a hard scattering (in DIS, the scattering of an electron off a quark) from a nonperturbative part of the process. When dealing with the hard-scattering side, we can consider the parton as being approximately free and on-shell (the parton is in reality off-shell, but its off-shellness is small compared to the hard scale involved in the scattering, such as the Q^2 of the photon). This situation allows us to compute the hard scattering using purely perturbative QED and QCD. The success of this approach gives a heuristic proof of the validity of the assumptions.

However, using the theoretical framework offered by QCD it is possible to give proofs of the approximate validity of the parton model approach and improve it. Explicit examples are usually given at the so-called "one-loop" level. In DIS, this requires taking into consideration the diagrams shown in Fig. 2.4.

These diagrams contain all sorts of divergences: ultraviolet and infrared (both collinear and soft). Ultraviolet divergences can be taken care of using renormalization. This requires the use of a regularization scheme (e.g. dimensional regularization) and implies the introduction of a

renormalization scale μ_R. Divergences are then "hidden" inside the values of the parameters of the theory, which are fixed by experimental measurements. Physical observables cannot depend on the renormalization scale, leading to renormalization-group equations and, e.g., the running of the coupling constant.

Infrared divergences are of two types: collinear (when the gluon is emitted collinear to the quark) and soft (when the gluon carries vanishing momentum). For DIS, soft divergences cancel in the sum of virtual and real diagrams. Collinear divergences require the use of a regularization scheme (e.g., dimensional regularization or mass regularization) and the introduction of a factorization scale μ_F (often choosen for convenience to be equal to μ_R). Divergences are then hidden inside nonperturbative objects involved in the process (e.g., collinear parton distribution functions). Physical observables cannot depend on the factorization scale, leading to evolution equations of the PDFs.

Factorization theorems show that the above procedure can be explicitly followed and generalized to an arbitrary number of gluon insertions. Eventually, they demonstrate that, order by order, the cross section for, e.g., DIS might be written schematically as

$$d\sigma \sim |\mathcal{H}|^2 \otimes \Phi(x). \tag{2.72}$$

The precise field-theoretic definitions of the correlation function $\Phi(x)$ emerges naturally from factorization. In the hard part $|\mathcal{H}|^2$, all propagators must be off-shell by order the hard scale Q so that asymptotic freedom applies, and small-coupling perturbation theory is valid, with non-factorizing contributions suppressed by powers of Q.

Such theorems have been worked out in detail only for a few processes (DIS, Drell-Yan processes, e^+e^- annihilation). For instance, there exhist no complete factorization proof for hadron-hadron collisions into hadrons (see Sec. 14.7 in the book of Collins [49]).

Finally, already at the level of DIS and collinear PDFs there is the question of the gauge invariance of parton distribution functions.

So far we used the following definition for the correlation function

$$\Phi_{ij}(p, P, S) = \frac{1}{(2\pi)^4} \int \mathrm{d}^4\xi \, \mathrm{e}^{\mathrm{i}p\cdot\xi} \langle P, S \,|\, \bar{\psi}_j(0)\, \psi_i(\xi) \,|\, P, S \rangle \tag{2.73}$$

or alternatively

$$\Phi_{ij}(x, S) = \int \frac{\mathrm{d}\xi^-}{2\pi} \, \mathrm{e}^{-\mathrm{i}p\cdot\xi} \langle P, S \,|\, \bar{\psi}_i^q(\xi)\, \psi_j^q(0) \,|\, P, S \rangle \Big|_{\xi^+ = \boldsymbol{\xi}_T = 0}. \tag{2.74}$$

with $p^+ = xP^+$.

It turns out that something is missing. The reason can be easily understood: the correlator as defined above is not gauge invariant, because the two quark field operators are at two different positions. If we perform a local (Abelian for now) gauge transformation on the fields

$$\psi(\xi) \to \mathrm{e}^{\mathrm{i}\alpha(\xi)}\, \psi(\xi) \tag{2.75}$$

the correlator evidently changes. This is something to worry about because the parton distribution functions composing the correlator can be extracted from experimental measurements and they should be gauge invariant.

To fix the problem, we have to insert a gauge link or Wilson line in between the quark fields, with the following gauge transformation properties

$$\mathcal{L}(\xi_1, \xi_2) \to \mathrm{e}^{\mathrm{i}\alpha(\xi_1)}\, \mathcal{L}(\xi_1, \xi_2)\, \mathrm{e}^{-\mathrm{i}\alpha(\xi_2)}. \tag{2.76}$$

In principle, any gauge link (i.e., running along any path) can make the definition of the correlator gauge-invariant. However, in QCD different gauge links give rise to physically different correlators (because a closed QCD gauge link is not equal to unity). From the appropriate calculations (which are partially covered in Piet Mulders's notes) it turns out that the proper gauge invariant definition of the quark-quark correlator is

$$\Phi_{ij}(x, S) = \int \frac{\mathrm{d}\xi^-}{2\pi}\, \mathrm{e}^{-\mathrm{i}p\cdot\xi} \langle P, S|\bar{\psi}_j(0)\, \mathcal{L}^{n_-}_{(0,+\infty)}\, \mathcal{L}^{n_-}_{(+\infty,\xi)}\, \psi_i(\xi)|P, S\rangle \Big|_{\xi^+=0} \tag{2.77}$$

where the gauge links (Wilson lines) are defined as

$$\mathcal{L}^{n_-}_{(0,+\infty)} = \mathcal{P} \exp\Big[-\mathrm{i}g \int_{\infty^-}^{\xi^-} \mathrm{d}\eta^- A^+(\eta^-, 0, \mathbf{0}_T)\Big] \approx 1 - ig \int_{\infty^-}^{\xi^-} \mathrm{d}\eta^- A^+(\eta^-, 0, \mathbf{0}_T) \tag{2.78}$$

The graphical representation of the gauge link involved in DIS is given in Fig. 2.5

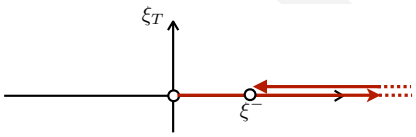

Figure 2.5: The path of the gague link in inclusive DIS. It could be viewed as formed by two infinitely long straight links, which however cancel to give the net result of a finite, straight link along the minus light-cone direction.

If we stop at the single-gluon level, the situation may be understood already at the level of the diagrams in Fig. 2.4. We know that only the sum of all diagrams is gauge invariant. Some diagrams vanish in certain gauges. In light-cone gauges, for instance, only the first diagrams on the left give a nonzero contribution. The gluon polarization sum in that gauge is

$$d^{\mu\nu}(l; n_-) = -g^{\mu\nu} + \frac{l^\mu n_-^\nu + l^\nu n_-^\mu}{l^+}. \tag{2.79}$$

In this gauge, it's easy to operate a kind of separation as the one shown in Fig. 2.7, since the starting diagrams are already of the desired form and the other diagrams do not contribute. In Feynman gauge, the polarization sum includes only the first term on the r.h.s. of Eq. (2.79). However, the contributions corresponding to the second term are recovered in the calculation of the other diagrams in Fig. 2.4.

The gauge link can be derived by calculating the leading-twist contributions of diagrams of the type shown in Fig. 2.6 and their Hermitean conjugates. Let us see roughly how this happens. Let's take a look at the first diagram of Fig. 2.6 . We could write it as

$$2MW^{(a)}_{\mu\nu} \propto \int \mathrm{d}p^-\, \mathrm{d}^2\boldsymbol{p}_T\, \mathrm{d}^4 l\, \mathrm{Tr}\Big(\gamma_\alpha \frac{\not{k} - \not{l} + m}{(k-l)^2 - m^2 + \mathrm{i}\epsilon}\, \gamma_\nu \Phi^\alpha_A(p, p-l) \gamma_\mu\, (\not{k} + m)\Big)\Big|_{k=p+q} \tag{2.80}$$

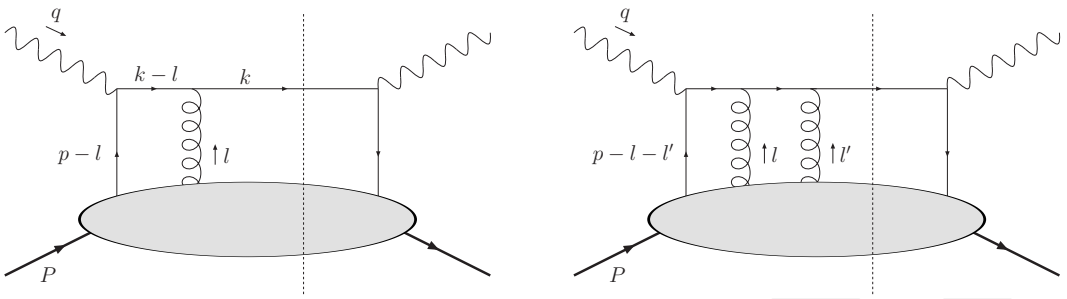

Figure 2.6: Examples of graphs contributing to the gauge link.

where we introduced

$$\Phi^{\alpha}_{Aij}(p, p-l) = \int \frac{\mathrm{d}^4\xi}{(2\pi)^4}\,\frac{\mathrm{d}^4\eta}{(2\pi)^4}\,\mathrm{e}^{\mathrm{i}p\cdot\xi}\,\mathrm{e}^{\mathrm{i}l\cdot(\eta-\xi)}\langle P,S\,|\,\bar{\psi}_i(0)\,gA^{\alpha}(\eta)\,\psi_j(\xi)\,|\,P,S\,\rangle \tag{2.81}$$

so that

$$\begin{aligned} 2MW^{(a)}_{\mu\nu} \propto \int \mathrm{d}p^-\mathrm{d}^2\boldsymbol{p}_T\;\mathrm{d}l^+\,\mathrm{d}^2\boldsymbol{l}_T \int \frac{\mathrm{d}^4\xi}{(2\pi)^4}\,\frac{\mathrm{d}\eta^-\,\mathrm{d}^2\boldsymbol{\eta}_T}{(2\pi)^3}e^{ip\cdot\xi}e^{\,i\,l\cdot(\eta-\xi)} \\ \times\,\langle P,S\,|\overline{\psi}(0)\gamma_\mu\gamma^+\gamma_\alpha\,\frac{\not{k}-\not{l}+m}{(k-l)^2-m^2+i\epsilon}\,\gamma_\nu gA^{\alpha}(\eta)\psi(\xi)|P,S\,\rangle\Big|_{\eta^+=0}\,, \end{aligned} \tag{2.82}$$

where Φ^{α}_{A} is made explicit, the l^- integrations is performed. In the expression after the second equal sign, it is understood that $p^+ = x\,P^+$.

The quark propagator reads explicitly

$$\mathrm{i}\,\frac{\not{k}-\not{l}+m}{(k-l)^2-m^2+i\epsilon} \approx \mathrm{i}\,\frac{(\not{k}+m)-\gamma^-\,l^+-\not{l}_T}{-2\,l^+\,k^- - (\boldsymbol{k}_T-\boldsymbol{l}_T)^2-m^2+i\epsilon}. \tag{2.83}$$

Now, we perform a simplification that goes under the name of "eikonal approximation" and consists simply in taking into account only the leading parts of the momenta of the quark after the photon scattering. As we know, the $-$ components are the leading ones. Therefore, the quark propagator in the upper part of the diagram becomes

$$\frac{\mathrm{i}(\not{p}+\not{q}-\not{l}+m)}{(p+q-l)^2-m^2+\mathrm{i}\epsilon} \approx \mathrm{i}\,\frac{(p+q)^-\gamma^+}{-2l^+(p+q)^-+\mathrm{i}\epsilon} = \frac{\mathrm{i}}{2}\,\frac{\gamma^+}{-l^++\mathrm{i}\epsilon} \tag{2.84}$$

In the last step it is essential that to have $(p+q)^- \geq 0$. This condition is guaranteed by the fact that we want to have an outgoing quark with momentum $p+q$ in the final state. The above expression is often referred to as an *eikonal propagator*.

The crucial observation at this point is that in the spirit of the eikonal approximation, the only possibility to have a nonzero result is if $\gamma^\nu = \gamma^-$

$$\ldots(\not{p}+\not{q}+m)\gamma^\nu\gamma^+\ldots \approx \ldots(p+q)^-\gamma^+\gamma^\nu\gamma^+\ldots = \ldots(p+q)^-\gamma^+\gamma^-\gamma^+\ldots = \ldots 2(p+q)^-\gamma^+\ldots \tag{2.85}$$

We approximate then the propagator with the standard eikonal propagator, see Eq. (2.84)

$$\mathrm{i}\,\frac{\not k - \not l + m}{(k-l)^2 - m^2 + i\epsilon} \approx \frac{\mathrm{i}}{2}\,\frac{\gamma^+}{-l^+ + \mathrm{i}\epsilon}. \tag{2.86}$$

We can use steps similar to what is described in Eq. (2.85) selecting γ_α to be only γ^- and consequently A^α to be A^+

$$\gamma^+\gamma_\alpha\,\frac{\not k - \not l + m}{(k-l)^2 - m^2 + i\epsilon}\,\gamma_\nu g A^\alpha(\eta) \approx \gamma^+\,\frac{1}{2}\,\frac{\gamma^-\gamma^+}{-l^+ + \mathrm{i}\epsilon}\,\gamma_\nu g A^+(\eta) = -\gamma^+\,\frac{gA^+(\eta)}{l^+ - \mathrm{i}\epsilon}\,\gamma_\nu \tag{2.87}$$

Then

$$\int \mathrm{d}l^+\,\mathrm{d}^2\boldsymbol{l}_T\,\frac{\mathrm{d}\eta^-\,\mathrm{d}^2\boldsymbol{\eta}_T}{(2\pi)^3}\,e^{i\,l\cdot(\eta-\xi)}\,\langle P,S\,|\overline{\psi}(0)\gamma_\mu\gamma^+\,\gamma_\nu\,\frac{gA^+(\eta)}{l^+ - i\epsilon}\psi(\xi)|P,S\,\rangle\Big|_{\eta^+=0} \tag{2.88}$$

and using

$$\int \mathrm{d}^2\boldsymbol{l}_T\,\frac{\mathrm{d}^2\boldsymbol{\eta}_T}{(2\pi)^2}\,\mathrm{e}^{\,\mathrm{i}\,\boldsymbol{l}_T(\boldsymbol{\eta}_T-\boldsymbol{\xi}_T)} = \int \frac{\mathrm{d}^2\boldsymbol{\eta}_T}{(2\pi)^2}\,(2\pi)^2\,\delta^2(\boldsymbol{\eta}_T - \boldsymbol{\xi}_T) \tag{2.89}$$

$$\int \mathrm{d}l^+\,\frac{\mathrm{e}^{\,\mathrm{i}\,l^+\,(\eta^- - \xi^-)}}{l^+ - i\epsilon}\,gA^+(\eta) = 2\pi\,\mathrm{i}\,gA^+(\eta)\,\theta(\eta^- - \xi^-) \tag{2.90}$$

we obtain

$$2MW^{(a)}_{\mu\nu} \propto \int \mathrm{d}p^-\,\mathrm{d}^2\boldsymbol{p}_T \int \frac{\mathrm{d}^4\xi}{(2\pi)^4}e^{ip\cdot\xi}\,\langle P,S\,|\overline{\psi}(0)\,\gamma_\mu\gamma^+\,\gamma_\nu\,(-ig)\int_{\infty^-}^{\xi^-}\mathrm{d}\eta^-\,A^+(\eta)\,\psi(\xi)|P,S\,\rangle\Big|_{\eta^+=0;\;\boldsymbol{\eta}_T=\boldsymbol{\xi}_T}. \tag{2.91}$$

By comparing this expression with Eq. (**??**), we can see that it corresponds to the $O(g)$ term in the expansion of the longitudinal part of the Wilson line $\mathcal{L}^-_{[\infty,\xi]}$ multiplying $\psi(\xi)$ in Eq. (3.125). The result of the diagram in Fig. 2.6b with two A^+-gluons gives the $O(g^2)$ term, etc. From the Hermitean conjugate diagram of Fig. 2.6a one obtains the $O(g)$ term in the expansion of the longitudinal part of the Wilson line $\mathcal{L}^-_{[0,\infty]}$ following $\bar{\psi}(0)$. Summing all these contributions we get

$$\Phi_{ij}(x,p_T) = \int \frac{\mathrm{d}\xi^-\,\mathrm{d}^2\xi_T}{(2\pi)^3}\;e^{\mathrm{i}p\cdot\xi}\,\langle P|\bar{\psi}_j(0)\,\mathcal{L}^{n-}(0^-,\infty^-;\mathbf{0}_T)\,\mathcal{L}^{n-}(\infty^-,\xi^-,\boldsymbol{\xi}_T)\,\psi_i(\xi)|P\rangle\Big|_{\xi^+=0} \tag{2.92}$$

If we choose at this point a light-cone gauge, where the A^+ vanish, the Wilson line can be reduced simply to unity.

One final comment at this point: already when considering single-gluon corrections, another class of divergences appear, the so-called light-cone or rapidity divergences. It is beyond the scope of these lectures to give a detailed explanation of these divergences. Let me just say that, when performing the calculation in the light-cone gauge, these divergences arise from the second term on the r.h.s. of Eq. (2.79), containing $1/l^+$. In different gauges, these divergences appear in other diagrams. Similarly to soft infrared divergences, these divergences exist already when one defines collinear PDFs in inclusive DIS. However, they cancel when summing the contributions corresponding to real and virtual diagrams. Graphically, these divergences can be connected to the presence of infinitely long gauge links. However, in the case of collinear PDFs the two gauge links $\mathcal{L}^{n-}_{(0,+\infty)}$ and $\mathcal{L}^{n-}_{(+\infty,\xi)}$ cancel each other, with the net effect of reducing to a finite link $\mathcal{L}^{n-}_{(0,\xi)}$, as depicted in Fig. 2.5.

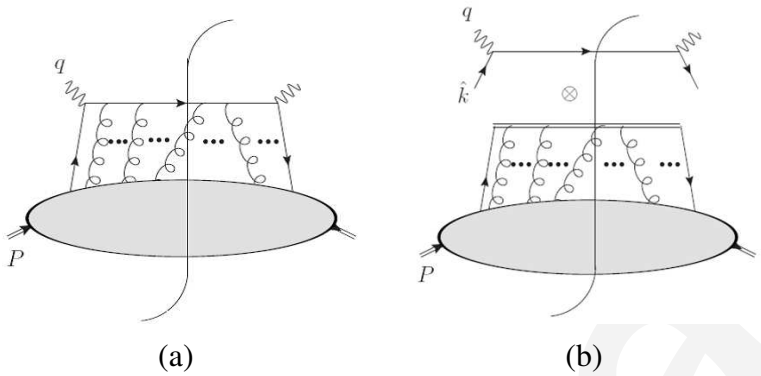

(a) (b)

Figure 2.7: (a) Example of higher-order diagrams that can give rise to the gauge link. (b) Factorization into gauge-link contributions.

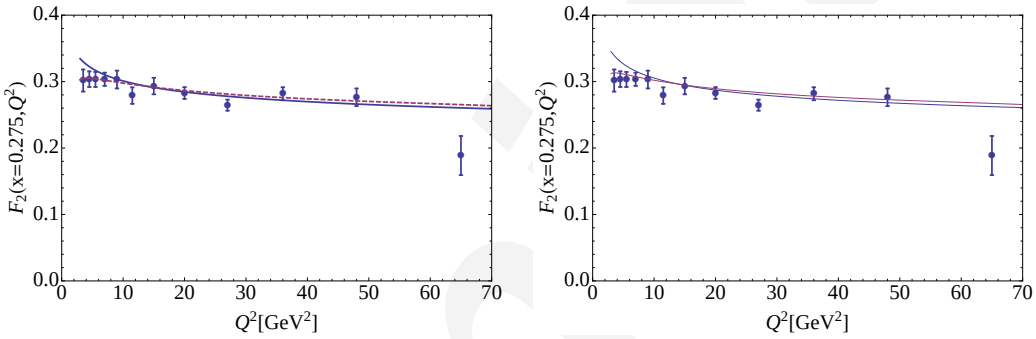

(a) (b)

Figure 2.8: (a) Comparison between experimentally measured F_2 from Ref. [10] and the theoretical LO formula, with (dashed line) or without (solid line) the correction $(1 + R)/(1 + \gamma^2)$. (b) The same but using the LO formula with NLO PDFs.

2.5 Some phenomenology

Let us see if we can reproduce some experimental data using the formulas obtained so far. As an example, we take the DIS data of Ref. [10]. They are relatively old, but still in use in global fits of PDFs.

We can recover the data from the HEPDATA database (http://hepdata.cedar.ac.uk/). We can use the formulas for our structure functions in the parton model, i.e.,

$$F_2(x_B, Q^2) = \frac{1+R}{1+\gamma^2} F_T(x_B, Q^2) \approx F_T(x_B, Q^2) = \sum_q e_q^2 \, f_1^q(x_B, Q^2). \tag{2.93}$$

$$R \equiv \frac{F_L}{F_T} \tag{2.94}$$

For the PDFs, we can use the MSTW08 set [91]. We can choose the LO set to be consistent with our formula. The results obtained from the theoretical formula are depicted in Fig. 2.8.

3

Semi-inclusive DIS

We consider now the process

$$\ell(l) + N(P) \to \ell(l') + h(P_h) + X, \tag{3.1}$$

where ℓ denotes the beam lepton, N the nucleon target, and h the produced hadron, and where four-momenta are given in parentheses. We neglect the lepton mass. We denote by M and M_h respective masses of the nucleon and of the hadron h. As usual we define $q = l - l'$ and $Q^2 = -q^2$ and introduce the variables

$$x_B = \frac{Q^2}{2\,P\cdot q}, \qquad y = \frac{P\cdot q}{P\cdot l}, \qquad z_h = \frac{P\cdot P_h}{P\cdot q}. \tag{3.2}$$

We consider the case where the detected hadron h has spin zero or where its polarization is not measured. $P_{h\perp}$ is the transverse parts P_h with respect to the photon momentum.

The cross section for one-particle inclusive electron-nucleon scattering can be written as

$$\frac{2E_h\,\mathrm{d}^6\sigma}{\mathrm{d}^3\boldsymbol{P}_h\,\mathrm{d}x_B\,\mathrm{d}y\,\mathrm{d}\phi_S} = \frac{\alpha^2}{2sx_BQ^2}\,L_{\mu\nu}(l,l',\lambda_e)\,2MW^{\mu\nu}(q,P,S,P_h), \tag{3.3}$$

or equivalently as

$$\frac{\mathrm{d}^6\sigma}{\mathrm{d}x_B\,\mathrm{d}y\,\mathrm{d}z_h\,\mathrm{d}\phi_S\,\mathrm{d}^2\boldsymbol{P}_{h\perp}} = \frac{\alpha^2}{4z_hsx_BQ^2}\,L_{\mu\nu}(l,l',\lambda_e)\,2MW^{\mu\nu}(q,P,S,P_h). \tag{3.4}$$

To obtain the previous formula, we made use of the relation $\mathrm{d}^3P_h/2E_h \approx \mathrm{d}z_h\,\mathrm{d}^2\boldsymbol{P}_{h\perp}/2z_h$.

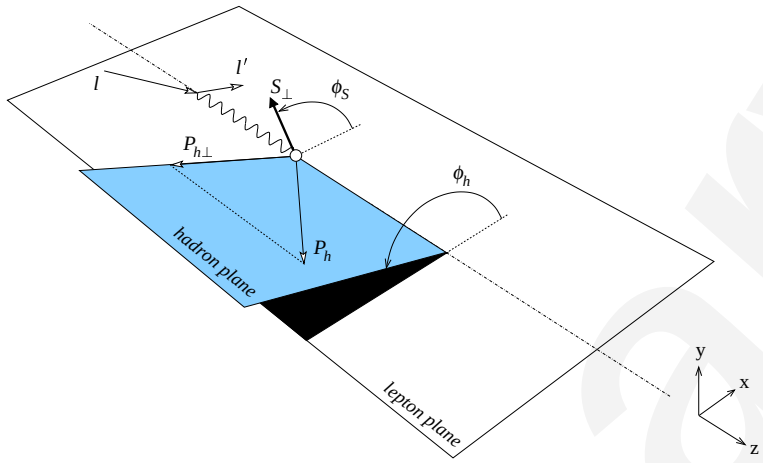

Figure 3.1: Definition of azimuthal angles for semi-inclusive deep inelastic scattering in the target rest frame. $P_{h\perp}$ and $S_\perp$ are the transverse parts of P_h and S with respect to the photon momentum [19].

The hadronic tensor for one-particle inclusive scattering is defined as

$$2MW^{\mu\nu}(q,P,S,P_h) = \frac{1}{(2\pi)^4}\sum_{X'}\int\frac{\mathrm{d}^3\boldsymbol{P}_{X'}}{2P^0_{X'}}\,2\pi\,\delta^{(4)}\big(q+P-P_{X'}-P_h\big)\,H^{\mu\nu}(P,S,P_{X'},P_h), \tag{3.5}$$

$$H^{\mu\nu}(P,S,P_{X'},P_h) = \langle P,S\,|\,J^\mu(0)\,|P_h,X'\rangle\langle P_h,X'\,|\,J^\nu(0)\,|P,S\,\rangle. \tag{3.6}$$

3.1 The unpolarized case

The biggest difference between constructing the decomposition of the hadronic tensor in inclusive and semi-inclusive DIS is that we cannot impose the same condition of time-reversal invariance. To be more precise, time-reversal invariance still holds, but does not correspond to the third transformation below, which we denote now as "naive time-reversal". The origin of the difference is that we are now considering final-states (the outgoing hadron, the state $|P_h,X'\rangle$) and the application of time-reversal requires also the reversal of initial and final states, which is not correctly included in naive time-reversal. Naive time-reversal is time-reversal without the switching of initial and final states. Alternatively, it is the simple change of sign of the time component of all vectors (and pseudovectors).

$$\text{Hermiticity:}\qquad W^*_{\mu\nu}(q,P,S) = W_{\nu\mu}(q,P,S), \tag{3.7a}$$

$$\text{parity:}\qquad L^\rho_\mu L^\sigma_\nu W_{\rho\sigma}(q,P,S) = W_{\mu\nu}(\tilde{q},\tilde{P},-\tilde{S}), \tag{3.7b}$$

$$\text{naive time-reversal:}\qquad L^\rho_\mu L^\sigma_\nu W^*_{\rho\sigma}(q,P,S) = W_{\mu\nu}(\tilde{q},\tilde{P},\tilde{S}) \tag{3.7c}$$

In unpolarized semi-inclusive DIS, the hadronic tensor can be parametrized in terms of 5 struc-

ture functions:

$$
\begin{aligned}
2MW^{\mu\nu}(q,P,S) = \frac{2z_h}{x_B}\Big[& -g_\perp^{\mu\nu} F_{UU,T}(x_B, z_h, P_{h\perp}^2, Q^2) + \hat{t}^\mu \hat{t}^\nu F_{UU,L}(x_B, z_h, P_{h\perp}^2, Q^2) \\
& + \Big(\hat{t}^\mu \hat{h}^\nu + \hat{t}^\nu \hat{h}^\mu\Big) F_{UU}^{\cos\phi_h}(x_B, z_h, P_{h\perp}^2, Q^2) + \Big(\hat{h}^\mu \hat{h}^\nu + g_\perp^{\mu\nu}\Big) F_{UU}^{\cos 2\phi_h}(x_B, z_h, P_{h\perp}^2, Q^2) \\
& - \mathrm{i}\Big(\hat{t}^\mu \hat{h}^\nu - \hat{t}^\nu \hat{h}^\mu\Big) F_{UU}^{\sin\phi_h}(x_B, z_h, P_{h\perp}^2, Q^2)\Big],
\end{aligned}
\tag{3.8}
$$

where we introduced the normalized vector $\hat{h} = P_{h\perp}/|\boldsymbol{P}_{h\perp}|$.

The choice of using the angles as indices for the structure functions is done with hindsight. In fact, the contraction with the leptonic tensor leads to structures such as

$$
\Big(\hat{t}_\mu \hat{l}_\nu + \hat{t}_\nu \hat{l}_\mu\Big)\Big(\hat{t}^\mu \hat{h}^\nu + \hat{t}^\nu \hat{h}^\mu\Big) = -g_\perp^{\mu\nu} \hat{l}_\mu \hat{h}_\nu \equiv \cos\phi_h \tag{3.9}
$$

$$
\Big(\hat{t}_\mu \epsilon_{\perp\nu\rho} \hat{l}^\rho + \hat{t}_\nu \epsilon_{\perp\mu\rho} \hat{l}^\rho\Big)\Big(\hat{t}^\mu \hat{h}^\nu + \hat{t}^\nu \hat{h}^\mu\Big) = -\epsilon_\perp^{\mu\nu} \hat{l}_\mu \hat{h}_\nu \equiv \sin\phi_h \tag{3.10}
$$

The above angles correspond to the definition given in the "Trento conventions" [19] and can be computed in the target rest frame, or in the Breit frame, or in any frame reached from the target rest frame by a boost along $\hat{\boldsymbol{q}}$:

$$
\begin{aligned}
\cos\phi_h &= \frac{(\hat{\boldsymbol{q}} \times \boldsymbol{l})}{|\hat{\boldsymbol{q}} \times \boldsymbol{l}|} \cdot \frac{(\hat{\boldsymbol{q}} \times \boldsymbol{P}_h)}{|\hat{\boldsymbol{q}} \times \boldsymbol{P}_h|}, \\
\sin\phi_h &= \frac{(\boldsymbol{l} \times \boldsymbol{P}_h) \cdot \hat{\boldsymbol{q}}}{|\hat{\boldsymbol{q}} \times \boldsymbol{l}|\,|\hat{\boldsymbol{q}} \times \boldsymbol{P}_h|}.
\end{aligned}
\tag{3.11}
$$

The resulting cross section after contraction with the leptonic tensor is:

$$
\frac{d\sigma}{dx_B\, dy\, dz\, d\phi_h\, dP_{h\perp}^2} = \frac{2\pi\alpha^2}{x_B y\, Q^2} \frac{y^2}{2\,(1-\varepsilon)} \tag{3.12}
$$

$$
\begin{aligned}
\times \Big\{ & F_{UU,T} + \varepsilon F_{UU,L} + \sqrt{2\,\varepsilon(1+\varepsilon)}\, \cos\phi_h\, F_{UU}^{\cos\phi_h} \\
& + \varepsilon \cos(2\phi_h)\, F_{UU}^{\cos 2\phi_h} + \lambda_e\, \sqrt{2\,\varepsilon(1-\varepsilon)}\, \sin\phi_h\, F_{LU}^{\sin\phi_h}
\end{aligned}
\tag{3.13}
$$

The last term requires a polarized letpon beam. If the beam is unpolarized, it drops (but this may not be exactly the case in experiments). The third and fourth terms vanish if we integrate over the angle ϕ_h of the outgoing hadron (but, also in this case, the experimental acceptance may not be perfect).

Integration of Eq. (3.71) over the transverse momentum $\boldsymbol{P}_{h\perp}$ of the outgoing hadron gives the semi-inclusive deep inelastic scattering cross section

$$
\frac{d\sigma}{dx_B\, dy\, dz} = \frac{4\pi\alpha^2}{x_B y Q^2} \frac{y^2}{2\,(1-\varepsilon)} \Big(F_{UU,T} + \varepsilon F_{UU,L}\Big) \tag{3.14}
$$

where now the structure functions on the r.h.s. are integrated versions of the previous ones, i.e.

$$F_{UU,T/L}(x_B, z_h, Q^2) = \int \mathrm{d}^2\boldsymbol{P}_{h\perp}\, F_{UU,T/L}(x_B, z_h, P_{h\perp}^2, Q^2). \tag{3.15}$$

Finally, the connection the result for totally inclusive DIS can be obtained by

$$\frac{d\sigma(\ell p \to \ell X)}{dx_B\, dy} = \sum_h \int \mathrm{d}z_h\, z_h\, \frac{d\sigma(\ell p \to \ell h X)}{dz\, dx_B\, dy} \tag{3.16}$$

where we have summed over all hadrons in the final state. This leads to the result already given in Eq. (2.23) (integrated over ϕ_S), once we identify

$$\sum_h \int \mathrm{d}z_h\, z_h\, F_{UU,T}(x_B, z_h, Q^2) = F_T(x_B, Q^2), \tag{3.17}$$

$$\sum_h \int \mathrm{d}z_h\, z_h\, F_{UU,L}(x_B, z_h, Q^2) = F_L(x_B, Q^2), \tag{3.18}$$

Time-reversal invariance requires (see, e.g., Ref. [61])

$$\sum_h \int \mathrm{d}z_h\, z_h\, F_{UT}^{\sin\phi_S}(x_B, z_h, Q^2) = 0. \tag{3.19}$$

The choice of a convenient frame to deal with semi-inclusive DIS is less straightforward than for inclusive DIS, due to the presence of P_h. We have two choices:

- FRAME 1: Keep the photon and proton to be collinear, give a transverse component to P_h. This means to keep the parametrization of the vectors as given in Eq. (2.29) and simply adding

$$P_h^\mu = \left[\frac{z_h Q}{\sqrt{2}},\ \frac{M_h^2 + |\boldsymbol{P}_{h\perp}|^2}{z_h Q\sqrt{2}},\ \boldsymbol{P}_{h\perp}\right] \tag{3.20}$$

- FRAME 2: Keep the proton and outgoing hadron to be collinear, give a transverse component to q. In terms of light-cone vectors this means choosing

$$P^\mu = P^+ n_+^\mu + \frac{M^2}{2P^+}\, n_-^\mu\,, \tag{3.21}$$

$$P_h^\mu = P_h^- n_-^\mu + \frac{M_h^2}{2P_h^-}\, n_+^\mu\,. \tag{3.22}$$

In this frame, the photon momentum has a transverse component. If we further fix

$$xP^+ = P_h^-/z = Q/\sqrt{2} \tag{3.23}$$

we can explicitly write the vectors involved as follows

$$P^\mu = \left[\frac{x_B M^2}{Q\sqrt{2}},\ \frac{Q}{x_B\sqrt{2}},\ \mathbf{0}\right] \tag{3.24a}$$

$$P_h^\mu = \left[\frac{z_h Q}{\sqrt{2}},\ \frac{M_h^2}{z_h Q\sqrt{2}},\ \mathbf{0}\right] \tag{3.24b}$$

$$q^\mu = \left[\frac{Q}{\sqrt{2}},\ -\frac{\left(Q^2 - |\boldsymbol{q}_T|^2\right)}{Q\sqrt{2}},\ \boldsymbol{q}_T\right] \approx \left[\frac{Q}{\sqrt{2}},\ -\frac{Q}{\sqrt{2}},\ \boldsymbol{q}_T\right] \tag{3.24c}$$

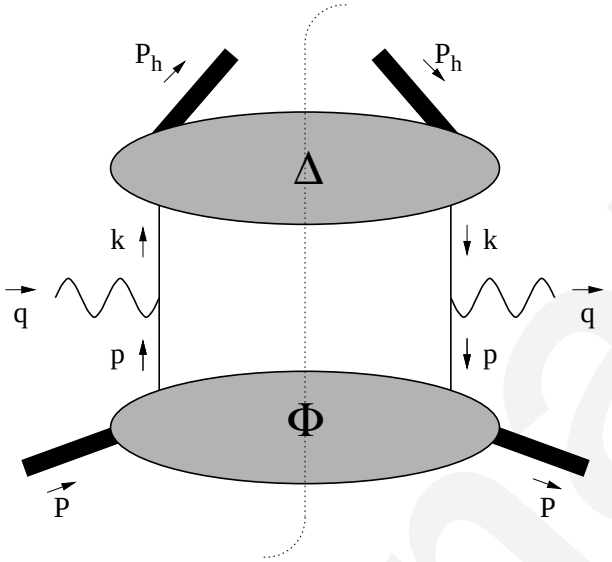

Figure 3.2: The bull diagram, describing the hadronic tensor at tree level.

The first choice seems to be the most simple one, but in reality from the theoretical point of view it is better to stick to the second option, in order to preserve a symmetry between P and P_h.

In any case, it turns out that if we neglect subleading twist corrections, all vectors in the two frames are approximately the same, the only difference is the presence of $\boldsymbol{P}_\perp$ in FRAME 1 and the presence of $\boldsymbol{q}_T$ in FRAME 2, and the two are simply connected by

$$\boldsymbol{q}_T = -z\boldsymbol{P}_{h\perp}. \tag{3.25}$$

Therefore, in this chapter we are not going to care very much about distinguishing the two frames, and every time we have $\boldsymbol{q}_T$ we can replace it with $-z\boldsymbol{P}_{h\perp}$ or vice-versa, at our convenience.

3.2 Unpolarized SIDIS in the parton model

In the spirit of the parton model, the virtual photon strikes a quark inside the nucleon. In the case of current fragmentation, the tagged final state hadron comes from the fragmentation of the struck quark. The scattering process can then be factorized in two soft hadronic parts connected by a hard scattering part, as shown in Fig. 3.2.

Considering only the Born-level contribution to the hard scattering, the hadronic tensor can be written as

$$2MW^{\mu\nu}(q,P,S,P_h) = \sum_q e_q^2 \int \mathrm{d}^4p\,\mathrm{d}^4k\;\delta^{(4)}(p+q-k)\;\mathrm{Tr}\left(\Phi(p,P,S)\,\gamma^\mu\,\Delta(k,P_h)\,\gamma^\nu\right), \tag{3.26}$$

where Φ and Δ are so-called quark-quark correlation functions and are defined as

$$\begin{aligned}\Phi_{ji}(p,P,S) &= \frac{1}{(2\pi)^4}\int \mathrm{d}^4\xi\, \mathrm{e}^{\mathrm{i}p\cdot\xi}\langle P,S\,|\,\bar\psi_i(0)\,\psi_j(\xi)\,|P,S\rangle \\ &= \sum_X \int \frac{\mathrm{d}^3\boldsymbol{P}_X}{(2\pi)^3\,2P_X^0}\,\langle P,S\,|\,\bar\psi_i(0)\,|X\rangle\langle X|\,\psi_j(0)\,|P,S\rangle\,\delta^{(4)}\Big(P-p-P_X\Big),\end{aligned} \tag{3.27}$$

$$\begin{aligned}\Delta_{kl}(k,P_h) &= \frac{1}{(2\pi)^4}\int \mathrm{d}^4\xi\, \mathrm{e}^{\mathrm{i}k\cdot\xi}\,\langle 0|\,\psi_k(\xi)\,|P_h\rangle\langle P_h|\,\bar\psi_l(0)\,|0\rangle \\ &= \sum_Y \int \frac{\mathrm{d}^3\boldsymbol{P}_Y}{(2\pi)^3\,2P_Y^0}\,\langle 0|\,\psi_k(0)\,|P_h,Y\rangle\langle P_h,Y|\,\bar\psi_l(0)\,|0\rangle\,\delta^{(4)}\Big(k-P_h-P_Y\Big).\end{aligned} \tag{3.28}$$

We need to introduce a parametrization for the vectors

$$p^\mu = \left[\frac{p^2+|\boldsymbol{p}_T|^2}{2xP^+},\ xP^+,\ \boldsymbol{p}_T\right], \tag{3.29a}$$

$$k^\mu = \left[\frac{P_h^-}{z},\ \frac{z\left(k^2+|\boldsymbol{k}_T|^2\right)}{2P_h^-},\ \boldsymbol{k}_T\right]. \tag{3.29b}$$

Neglecting terms which are $1/Q$ suppressed, we can write

$$\begin{aligned}\delta^{(4)}(p+q-k) &\approx \delta(p^+ + q^+)\,\delta(q^- - k^-)\,\delta^{(2)}\Big(\boldsymbol{p}_T+\boldsymbol{q}_T-\boldsymbol{k}_T\Big) \\ &\approx \frac{1}{P^+P_h^-}\,\delta(x-x_B)\,\delta(1/z-1/z_h)\,\delta^{(2)}\Big(\boldsymbol{p}_T+\boldsymbol{q}_T-\boldsymbol{k}_T\Big)\end{aligned} \tag{3.30}$$

and replacing

$$\mathrm{d}^4k = \mathrm{d}^2\boldsymbol{k}_T\ \mathrm{d}k^+\ P_h^-\,\frac{\mathrm{d}z}{z^2} \tag{3.31}$$

we obtain the compact expression

$$2MW^{\mu\nu}(q,P,S,P_h) = 2z_h\,\mathcal{I}\Big[\mathrm{Tr}(\Phi(x_B,\boldsymbol{p}_T,S)\,\gamma^\mu\,\Delta(z_h,\boldsymbol{k}_T)\,\gamma^\nu)\Big], \tag{3.32}$$

where, as we shall do very often, we used the shorthand notation

$$\begin{aligned}\mathcal{I}\Big[\cdots\Big] &\equiv \int \mathrm{d}^2\boldsymbol{p}_T\,\mathrm{d}^2\boldsymbol{k}_T\,\delta^{(2)}\Big(\boldsymbol{p}_T+\boldsymbol{q}_T-\boldsymbol{k}_T\Big)\Big[\cdots\Big] \\ &= \int \mathrm{d}^2\boldsymbol{p}_T\,\mathrm{d}^2\boldsymbol{k}_T\,\delta^{(2)}\Big(\boldsymbol{p}_T-\frac{\boldsymbol{P}_{h\perp}}{z}-\boldsymbol{k}_T\Big)\Big[\cdots\Big],\end{aligned} \tag{3.33}$$

and where we introduced the "unintegrated" or "transverse-momentum dependent" correlation functions

$$\Phi(x,\boldsymbol{p}_T,S) \equiv \int \mathrm{d}p^-\Phi(p,P,S)\Big|_{p^+=xP^+}, \tag{3.34a}$$

$$\Delta(z,\boldsymbol{k}_T) \equiv \frac{1}{2z}\int \mathrm{d}k^+\Delta(k,P_h)\Big|_{k^-=P_h^-/z}. \tag{3.34b}$$

While the distribution correlation function Φ describes the *confinement* of partons inside hadrons, the fragmentation correlation function Δ describes the way a virtual parton "decays" into a hadron plus something else, i.e. $q^* \to hY$. This process is referred to as *hadronization*. It is a clear manifestation of color confinement: the asymptotic physical states detected in experiment must be color neutral, so that quarks have to evolve into hadrons.[1]

Integrating the cross section over $\boldsymbol{P}_{h\perp}$ we get

$$\frac{\mathrm{d}^4\sigma}{\mathrm{d}x_B\,\mathrm{d}y\,\mathrm{d}z_h\,\mathrm{d}\phi_S} = \frac{\alpha^2}{4z_h s x_B\,Q^2}\,L_{\mu\nu}(l,l',\lambda_e)\;2MW^{\mu\nu}(q,P,S), \tag{3.35}$$

where

$$2MW^{\mu\nu}(q,P,S) = 2z_h\,\mathrm{Tr}(\Phi(x_B,S)\,\gamma^\mu\,\Delta(z_h)\,\gamma^\nu), \tag{3.36a}$$

$$\Phi(x,S) \equiv \int \mathrm{d}p^-\,\mathrm{d}^2\boldsymbol{p}_T\,\Phi(p,P,S)\Big|_{p^+=xP^+}, \tag{3.36b}$$

$$\Delta(z) \equiv \frac{z}{2}\int \mathrm{d}k^+\,\mathrm{d}^2\boldsymbol{k}_T\,\Delta(k,P_h)\Big|_{k^-=P_h^-/z}. \tag{3.36c}$$

3.3 The unpolarized correlation functions

The big difference from the inclusive DIS calculation is that we now need the transverse-momentum dependent correlation function defined in Eq. (3.34a). Following analogous steps as done for the inclusive DIS case and keeping only the leading-twist terms, we obtain

$$\Phi(x,\boldsymbol{p}_T)_{\mathrm{T}w-2} = \left\{f_1(x,\boldsymbol{p}_T^2) + \mathrm{i}h_1^\perp(x,\boldsymbol{p}_T^2)\frac{\not{p}_T}{M}\right\}\not{n}_+/2. \tag{3.37}$$

Here we introduced the parton distribution functions

$$f_1(x,p_T^2) = 2P^+\int \mathrm{d}p^-\,(A_2 + xA_3)\,, \qquad h_1^\perp(x,p_T^2) = 2P^+\int \mathrm{d}p^-\,(-A_4)\,. \tag{3.38}$$

The function $f_1(x,\boldsymbol{p}_T^2)$ is the unpolarized transverse-momentum-dependent PDF (unpolarized TMD). The function $h_1^\perp(x,\boldsymbol{p}_T^2)$ is the so-called Boer-Mulders TMD [32].

We can do the same exercise also for the fragmentation correlation function defined in Eq. (3.34b), with very few changes. I don't go through all the analysis here, and just quote the final result

$$\Delta(z,\boldsymbol{k}_T)_{\mathrm{T}w-2} = \left(D_1(z,\boldsymbol{k}_T^2) + i\,H_1^\perp(z,\boldsymbol{k}_T^2)\,\frac{\not{k}_T}{M_h}\right)\not{n}_-/2. \tag{3.39}$$

The function $D_1(z,\boldsymbol{k}_T^2)$ is the unpolarized transverse-momentum-dependent fragmentation function (unpolarized TMD FF). The function $H_1^\perp(z,\boldsymbol{k}_T^2)$ is the so-called Collins function [51].

The Boer-Mulders and Collins functions are particularly relevant because they give rise to nontrivial transverse-momentum dependences of cross sections already at the level of unpolarized

[1] Note that on the way to the final state hadrons, the color carried by the initial quark can be neutralized without breaking factorization, for instance via soft gluon contributions.

processes (e.g., SIDIS experiments such as ZEUS and H1 at DESY, e^+e^- annihilation experiments, and in principle even at the LHC).

Another important property of the Boer-Mulders and Collins functions is that they are T-odd (or naive time-reversal odd), according to the definition

$$\Phi^*_{\text{T-even}}(p,P,S) = \mathrm{i}\gamma^1\gamma^3\,\Phi_{\text{T-even}}(\tilde{p},\tilde{P},\tilde{S})\,\mathrm{i}\gamma^1\gamma^3, \tag{3.40a}$$

$$\Phi^*_{\text{T-odd}}(p,P,S) = -\mathrm{i}\gamma^1\gamma^3\,\Phi_{\text{T-odd}}(\tilde{p},\tilde{P},\tilde{S})\,\mathrm{i}\gamma^1\gamma^3. \tag{3.40b}$$

The above definition does not fully correspond to time-reversal invariance and T-odd functions do not violate time-reversal invariance. They give rise to observables to observables that change sign when inverting momenta and angular momenta (e.g., single-spin asymmetries).

As mentioned already for inclusive DIS, the correlation function is a 4×4 Dirac matrix. However, its leading-twist part spans only a 2×2 Dirac subspace. Using the chiral or Weyl representation, the correlation function reads

$$\left(\mathcal{P}_+\,\Phi(x,\boldsymbol{p}_T)\gamma^+\right)_{ji} = \begin{pmatrix} f_1 & 0 & 0 & \mathrm{i}\mathrm{e}^{\mathrm{i}\phi_p}\,\dfrac{|\boldsymbol{p}_T|}{M}\,h_1^\perp \\ 0 & 0 & 0 & 0 \\ 0 & 0 & 0 & 0 \\ -\mathrm{i}\mathrm{e}^{-\mathrm{i}\phi_p}\,\dfrac{|\boldsymbol{p}_T|}{M}\,h_1^\perp & 0 & 0 & f_1 \end{pmatrix}. \tag{3.41}$$

As shown by this explicit form, the four-dimensional Dirac space can be reduced to a two-dimensional space, retaining only the nonzero part of the correlation function. The relevant part of the Dirac space is the one corresponding to good quark fields. The correlation matrix in the good quark chirality space is then simply

$$\left(\mathcal{P}_+\,\Phi\gamma^+\right)_{\chi_1'\chi_1} = \begin{pmatrix} f_1 & \mathrm{i}\mathrm{e}^{\mathrm{i}\phi_p}\,\dfrac{|\boldsymbol{p}_T|}{M}\,h_1^\perp \\ -\mathrm{i}\mathrm{e}^{-\mathrm{i}\phi_p}\,\dfrac{|\boldsymbol{p}_T|}{M}\,h_1^\perp & f_1 \end{pmatrix}. \tag{3.42}$$

From the matrix representation in the chirality space it should be clear why the function $h_1^\perp$ is defined to be *chiral odd*.

The distribution matrix is clearly Hermitean. When an exponential $\mathrm{e}^{\mathrm{i}l'\phi_p}$ appears in the matrix, we have to take into account l' units of angular momentum in the final state. The condition of angular momentum conservation then requires $\chi_1' + l' = \chi_1$. The condition parity conservation is

$$F(x,\boldsymbol{p}_T)_{\chi_1\chi_1'} = (-1)^{l'}\,F(x,\boldsymbol{p}_T)_{-\chi_1\,-\chi_1'}\Big|_{l'\to-l'}. \tag{3.43}$$

The fact that the matrix has to be positive definite allows us to derive the positivity bound

$$\frac{|\boldsymbol{p}_T|}{M}\,|h_1^\perp(x,\boldsymbol{p}_T^2)| \le f_1(x,\boldsymbol{p}_T^2). \tag{3.44}$$

3.4 Some phenomenology: unpolarized cross sections

In this section, I briefly outline the steps that are necessary to interpret unpolarized cross-section data in terms of TMDs.

The unpolarized cross sections for SIDIS integrated over the azimuthal angle, but not on the absolute value of $P_{h\perp}$ read

$$\frac{d\sigma}{dx\,dy\,dz\,dP_{h\perp}^2} = \frac{4\pi^2\alpha^2}{xQ^2}\,\frac{y}{2\,(1-\varepsilon)}\Big(F_{UU,T}(x,z,P_{h\perp}^2,Q^2) + \varepsilon F_{UU,L}(x,z,P_{h\perp}^2,Q^2)\Big). \tag{3.45}$$

To have a compact notation for the results, we introduce the notation

$$f\otimes D = x_B\int d^2\boldsymbol{p}_T\,d^2\boldsymbol{k}_T\,\delta^{(2)}(\boldsymbol{p}_T-\boldsymbol{k}_T-\boldsymbol{P}_{h\perp}/z)\,f^a(x_B,p_T^2)\,D^a(z,k_T^2). \tag{3.46}$$

We obtain

$$F_{UU,T} = \sum_a e_a^2 f_1^a\otimes D_1^a, \qquad\qquad F_{UU,L} = O\Big(\frac{M^2}{Q^2},\frac{P_{h\perp}^2}{Q^2}\Big), \tag{3.47}$$

Since the longitudinal structure function is suppressed as $1/Q^2$ in the low transverse momentum region, we will neglect it.

To introduce some simplification, we resort to tsospin and charge-conjugation relations, which imply for "favored" functions

$$D_1^{u\to\pi^+} = D_1^{\bar d\to\pi^+} = D_1^{d\to\pi^-} = D_1^{\bar u\to\pi^-}, \equiv D_1^{\rm f} \tag{3.48}$$
$$D_1^{u\to K^+} = D_1^{\bar u\to K^-}, \equiv D_1^{\rm fd} \tag{3.49}$$
$$D_1^{\bar s\to K^+} = D_1^{s\to K^-} \equiv D_1^{\rm f'} \tag{3.50}$$

for the "unfavored" functions

$$D_1^{\bar u\to\pi^+} = D_1^{d\to\pi^+} = D_1^{\bar d\to\pi^-} = D_1^{u\to\pi^-} \equiv D_1^{\rm d}, \tag{3.51}$$
$$D_1^{s\to\pi^+} = D_1^{\bar s\to\pi^+} = D_1^{s\to\pi^-} = D_1^{\bar s\to\pi^-} \equiv D_1^{\rm df}, \tag{3.52}$$
$$D_1^{\bar u\to K^+} = D_1^{\bar d\to K^+} = D_1^{d\to K^+} = D_1^{\bar d\to K^-} = D_1^{d\to K^-} = D_1^{u\to K^-} \equiv D_1^{\rm dd}, \tag{3.53}$$
$$D_1^{s\to K^+} = D_1^{\bar s\to K^-} \equiv D_1^{\rm d'}. \tag{3.54}$$

There are in principle seven independent functions. If needed, a further assumption could be to set $D_1^{\rm f'} = D_1^{\rm f}$ and $D_1^{\rm d'} = D_1^{\rm d}$, leaving five independent functions.

In general, the convolution cannot be disentangled. Only if the functions have a specific functional form we can obtain a simple expression.

To study the flavor structure of TMDs, it is necessary to use different targets and detect different final-state hadrons. The structure functions for the different combinations of target and outgoing

hadron read then

$$9F_{UU,T}^{p/\pi^+}(x,z,P_{h\perp}^2) = \left(4\,f_1^u + f_1^{\bar{d}}\right)\otimes D_1^{\mathrm{f}} + \left(4\,f_1^{\bar{u}} + f_1^{d}\right)\otimes D_1^{\mathrm{d}} + \left(f_1^{s} + f_1^{\bar{s}}\right)\otimes D_1^{\mathrm{df}}, \tag{3.55}$$

$$9F_{UU,T}^{p/\pi^-}(x,z,P_{h\perp}^2) = \left(4\,f_1^{\bar{u}} + f_1^{d}\right)\otimes D_1^{\mathrm{f}} + \left(4\,f_1^{u} + f_1^{\bar{d}}\right)\otimes D_1^{\mathrm{d}} + \left(f_1^{s} + f_1^{\bar{s}}\right)\otimes D_1^{\mathrm{df}}, \tag{3.56}$$

$$9F_{UU,T}^{n/\pi^+}(x,z,P_{h\perp}^2) = \left(4\,f_1^{d} + f_1^{\bar{u}}\right)\otimes D_1^{\mathrm{f}} + \left(4\,f_1^{\bar{d}} + f_1^{u}\right)\otimes D_1^{\mathrm{d}} + \left(f_1^{s} + f_1^{\bar{s}}\right)\otimes D_1^{\mathrm{df}} \tag{3.57}$$

$$9F_{UU,T}^{n/\pi^-}(x,z,P_{h\perp}^2) = \left(4\,f_1^{\bar{d}} + f_1^{u}\right)\otimes D_1^{\mathrm{f}} + \left(4\,f_1^{d} + f_1^{\bar{u}}\right)\otimes D_1^{\mathrm{d}} + \left(f_1^{s} + f_1^{\bar{s}}\right)\otimes D_1^{\mathrm{df}}, \tag{3.58}$$

$$9F_{UU,T}^{p/K^+}(x,z,P_{h\perp}^2) = 4\,f_1^{u}\otimes D_1^{\mathrm{fd}} + \left(4\,f_1^{\bar{u}} + f_1^{d} + f_1^{\bar{d}}\right)\otimes D_1^{\mathrm{dd}} + f_1^{\bar{s}}\otimes D_1^{\mathrm{f}'} + f_1^{s}\otimes D_1^{\mathrm{d}'}, \tag{3.59}$$

$$9F_{UU,T}^{p/K^-}(x,z,P_{h\perp}^2) = 4\,f_1^{\bar{u}}\otimes D_1^{\mathrm{fd}} + \left(4\,f_1^{u} + f_1^{d} + f_1^{\bar{d}}\right)\otimes D_1^{\mathrm{dd}} + f_1^{s}\otimes D_1^{\mathrm{f}'} + f_1^{\bar{s}}\otimes D_1^{\mathrm{d}'}, \tag{3.60}$$

$$9F_{UU,T}^{n/K^+}(x,z,P_{h\perp}^2) = 4\,f_1^{d}\otimes D_1^{\mathrm{fd}} + \left(4\,f_1^{\bar{d}} + f_1^{u} + f_1^{\bar{u}}\right)\otimes D_1^{\mathrm{dd}} + f_1^{\bar{s}}\otimes D_1^{\mathrm{f}'} + f_1^{s}\otimes D_1^{\mathrm{d}'}, \tag{3.61}$$

$$9F_{UU,T}^{n/K^-}(x,z,P_{h\perp}^2) = 4\,f_1^{\bar{d}}\otimes D_1^{\mathrm{fd}} + \left(4\,f_1^{d} + f_1^{u} + f_1^{\bar{u}}\right)\otimes D_1^{\mathrm{dd}} + f_1^{s}\otimes D_1^{\mathrm{f}'} + f_1^{\bar{s}}\otimes D_1^{\mathrm{d}'} \tag{3.62}$$

Were there no difference in the transverse momentum distribution for different flavors and/or for different fragmentation functions, all the above structure functions would display the same $P_{h\perp}$ behavior. Therefore, a non-flat $P_{h\perp}$ dependence of any ratio of them would expose these differences.

For illustration purposes, let us neglect the sea-quark contributions and focus only on the pions. We obtain

$$9F_{UU,T}^{p/\pi^+}(x,z,P_{h\perp}^2) = 4\,f_1^{u}\otimes D_1^{\mathrm{f}} + f_1^{d}\otimes D_1^{\mathrm{d}}, \tag{3.63}$$

$$9F_{UU,T}^{p/\pi^-}(x,z,P_{h\perp}^2) = f_1^{d}\otimes D_1^{\mathrm{f}} + 4\,f_1^{u}\otimes D_1^{\mathrm{d}}, \tag{3.64}$$

$$9F_{UU,T}^{n/\pi^+}(x,z,P_{h\perp}^2) = 4\,f_1^{d}\otimes D_1^{\mathrm{f}} + f_1^{u}\otimes D_1^{\mathrm{d}}, \tag{3.65}$$

$$9F_{UU,T}^{n/\pi^-}(x,z,P_{h\perp}^2) = f_1^{u}\otimes D_1^{\mathrm{f}} + 4\,f_1^{d}\otimes D_1^{\mathrm{d}} \tag{3.66}$$

Let us assume Gaussians distribution of transverse momentum, both for the distribution and fragmentation function, i.e.,

$$f_1^a(x,p_T^2) = \frac{f_1^a(x)}{\pi\rho_a^2}e^{-p_T^2/\rho_a^2}, \qquad D_1^a(z,k_T^2) = \frac{D_1^a(z)}{\pi\sigma_a^2}e^{-z^2\boldsymbol{k}_T^2/\sigma_a^2}. \tag{3.67}$$

The convolution turns out to be in this case

$$f_1^a\otimes D_1^a = f_1^a(x)D_1^a(z)\frac{1}{\pi(z^2\rho_a^2+\sigma_a^2)}\,e^{-\boldsymbol{P}_{h\perp}^2/(z^2\rho_a^2+\sigma_a^2)} \tag{3.68}$$

The transverse-momentum dependence of the partonic functions is usually assumed to be a flavor-independent Gaussian [59, 110]. The tree-level approximation and the Gaussian assumption are known to be inadequate at $P_{h\perp}^2 \gg M^2$, but they could effectively describe the physics at $P_{h\perp}^2 \approx M^2$. Especially for low-energy experiments, this is where the bulk of the data is.

Let us see an example: a multiplicity measurement as a function of $P_{h\perp}$ from COMPASS. Data are not published yet, but there are already some preliminary plots where we can at least

qualitatively check the behavior of our computation [105, 106]. The quantity that is plotted should be

$$\frac{\frac{d\sigma}{dxdydzdP_{h\perp}}}{\frac{d\sigma}{dxdydz}} = \frac{1}{\pi(z^2\rho_a^2 + \sigma_a^2)}\, e^{-\boldsymbol{P}_{h\perp}^2/(z^2\rho_a^2+\sigma_a^2)}. \tag{3.69}$$

Let us use the values... [not finished]

There is an extensive literature where the analysis is carried out to a higher level of complication, but only for the specific case of unpolarized observables integrated over the azimuthal angle of the measured transverse momentum. The analysis is usually performed in the space of the Fourier-conjugate to $P_{h\perp}$ (b-space) in the Collins–Soper–Sterman (CSS) framework [57]. The relation with the TMD formalism has been explicitly shown in Ref. [12]. The most recent study along these lines is presented in Ref. [40]. The region of $P_{h\perp}^2 \gg M^2$, or $b^2 \ll 1/M^2$, can be calculated perturbatively, but when $P_{h\perp}^2 \approx M^2$ a nonperturbative component has to be introduced and its parameters must be fitted to experimental data. This component is usually assumed to be a flavor-independent Gaussian. The most advanced extraction of the nonperturbative contributions is presented in Ref. [87]. A slightly different approach for the extraction has been followed in Ref. [104].

At present, we can make the conservative statement that unpolarized quark TMDs seems to be well described by flavor-independent Gaussians with $\sqrt{\langle p_T^2 \rangle} \approx 0.4 - 0.8$ GeV, depending on the kinematics.

The knowledge of the details of the unpolarized TMDs has an impact also on high-energy physics. In Fig. 3.3b, the cross section for Z boson production at the Tevatron is plotted [99]. The difference between the curves originates from different models and fits of the nonperturbative component of the TMDs. Apart from the details, the plot shows that the knowledge of TMDs is essential for precision studies at the Tevatron. Even the determination of a fundamental parameter of the Standard Model, the mass of the W boson, is affected by the uncertainties of the knowledge of unpolarized TMDs. In Ref. [1], the CDF collaboration discussed several ways to fit the W mass. According to the analysis, TMDs uncertainties generate an error of 3.9 MeV on the W mass determination (the total systematic error is about 34 MeV).

More information is needed to study in detail the flavor structure of TMDs. Interesting are coming out from JLab, COMPASS and HERMES and it is an exciting time for this kind of studies [80, 96, 105, 106].

3.5 Polarized SIDIS

In this case, the hadronic tensor can be parametrized in terms of 18 structure functions [20].

We do not give here the explicit formula of the hadronic tensor but only give the resulting cross

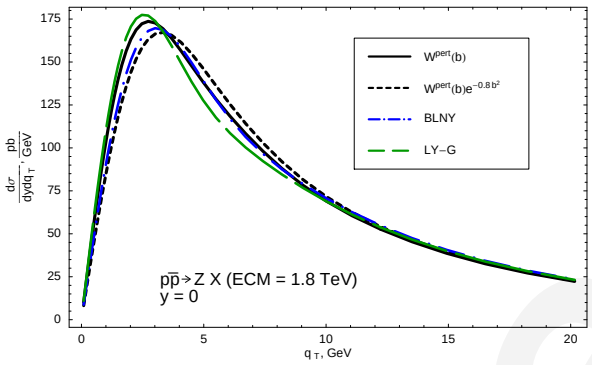

Figure 3.3: The cross sections of Z boson production at the Tevatron, computed in the CSS formalism. The difference between the curves shows the impact of choosing different nonperturbative components for the TMDs. See Ref. [99] for details.

section after contraction with the leptonic tensor:

$$\frac{d\sigma}{dx_B\,dy\,d\phi_S\,dz\,d\phi_h\,dP_{h\perp}^2} = \frac{\alpha^2}{x_B y\,Q^2}\,\frac{y^2}{2\,(1-\varepsilon)} \tag{3.70}$$

$$\begin{aligned}
&\times\Big\{F_{UU,T} + \varepsilon F_{UU,L} + \sqrt{2\,\varepsilon(1+\varepsilon)}\,\cos\phi_h\,F_{UU}^{\cos\phi_h} \\
&\quad + \varepsilon\cos(2\phi_h)\,F_{UU}^{\cos 2\phi_h} + \lambda_e\,\sqrt{2\,\varepsilon(1-\varepsilon)}\,\sin\phi_h\,F_{LU}^{\sin\phi_h} \\
&\quad + S_\parallel\Big[\sqrt{2\,\varepsilon(1+\varepsilon)}\,\sin\phi_h\,F_{UL}^{\sin\phi_h} + \varepsilon\sin(2\phi_h)\,F_{UL}^{\sin 2\phi_h}\Big] \\
&\quad + S_\parallel\,\lambda_e\Big[\sqrt{1-\varepsilon^2}\,F_{LL} + \sqrt{2\,\varepsilon(1-\varepsilon)}\,\cos\phi_h\,F_{LL}^{\cos\phi_h}\Big] \\
&\quad + |\boldsymbol{S}_\perp|\Big[\sin(\phi_h-\phi_S)\Big(F_{UT,T}^{\sin(\phi_h-\phi_S)} + \varepsilon\,F_{UT,L}^{\sin(\phi_h-\phi_S)}\Big) \\
&\qquad + \varepsilon\,\sin(\phi_h+\phi_S)\,F_{UT}^{\sin(\phi_h+\phi_S)} + \varepsilon\,\sin(3\phi_h-\phi_S)\,F_{UT}^{\sin(3\phi_h-\phi_S)} \\
&\qquad + \sqrt{2\,\varepsilon(1+\varepsilon)}\,\sin\phi_S\,F_{UT}^{\sin\phi_S} + \sqrt{2\,\varepsilon(1+\varepsilon)}\,\sin(2\phi_h-\phi_S)\,F_{UT}^{\sin(2\phi_h-\phi_S)}\Big] \\
&\quad + |\boldsymbol{S}_\perp|\lambda_e\Big[\sqrt{1-\varepsilon^2}\,\cos(\phi_h-\phi_S)\,F_{LT}^{\cos(\phi_h-\phi_S)} + \sqrt{2\,\varepsilon(1-\varepsilon)}\,\cos\phi_S\,F_{LT}^{\cos\phi_S} \\
&\qquad + \sqrt{2\,\varepsilon(1-\varepsilon)}\,\cos(2\phi_h-\phi_S)\,F_{LT}^{\cos(2\phi_h-\phi_S)}\Big]\Big\}.
\end{aligned} \tag{3.71}$$

The first and second subscript of the above structure functions indicate the respective polarization of beam and target, whereas the third subscript in $F_{UU,T}$ and $F_{UU,L}$ specifies the polarization of the virtual photon. Using the definition (2.24), the depolarization factors can be written in terms of the

y variable as

$$\frac{y^2}{2\,(1-\varepsilon)} = \left(1 - y + y^2/2\right) \tag{3.72}$$

$$\frac{y^2}{2\,(1-\varepsilon)}\,\varepsilon = (1-y) \tag{3.73}$$

$$\frac{y^2}{2\,(1-\varepsilon)}\,\sqrt{1-\varepsilon^2} = y\,(1-y/2) \tag{3.74}$$

$$\frac{y^2}{2\,(1-\varepsilon)}\,\sqrt{2\,\varepsilon(1+\varepsilon)} = (2-y)\,\sqrt{1-y} \tag{3.75}$$

$$\frac{y^2}{2\,(1-\varepsilon)}\,\sqrt{2\,\varepsilon(1-\varepsilon)} = y\,\sqrt{1-y} \tag{3.76}$$

Integration of Eq. (3.71) over the transverse momentum $\boldsymbol{P}_{h\perp}$ of the outgoing hadron gives the semi-inclusive deep inelastic scattering cross section

$$\begin{aligned}\frac{d\sigma}{dx_B\,dy\,d\phi_S\,dz} = \frac{2\alpha^2}{x_B y Q^2}\,\frac{y^2}{2\,(1-\varepsilon)}\Big\{&F_{UU,T} + \varepsilon F_{UU,L} + S_\parallel \lambda_e\,\sqrt{1-\varepsilon^2}\,F_{LL} \\ &+ |\boldsymbol{S}_\perp|\,\sqrt{2\,\varepsilon(1+\varepsilon)}\,\sin\phi_S\,F_{UT}^{\sin\phi_S} + |\boldsymbol{S}_\perp|\lambda_e\,\sqrt{2\,\varepsilon(1-\varepsilon)}\,\cos\phi_S\,F_{LT}^{\cos\phi_S}\Big\},\end{aligned} \tag{3.77}$$

where now the structure functions on the r.h.s. are integrated versions of the previous ones, i.e.

$$F_{UU,T}(x_B, z_h, Q^2) = \int \mathrm{d}^2\boldsymbol{P}_{h\perp}\,F_{UU,T}(x_B, z_h, P_{h\perp}^2, Q^2) \tag{3.78}$$

and similarly for the other functions.

Finally, the connection the result for totally inclusive DIS can be obtained by

$$\frac{d\sigma(\ell p \to \ell X)}{dx_B\,dy\,d\phi_S} = \sum_h \int \mathrm{d}z_h\,z_h\,\frac{d\sigma(\ell p \to \ell h X)}{dz\,dx_B\,dy\,d\phi_S} \tag{3.79}$$

where we have summed over all hadrons in the final state. This leads to the result already given in Eq. (2.23), once we identify

$$\sum_h \int \mathrm{d}z_h\,z_h\,F_{UU,T}(x_B, z_h, Q^2) = F_T(x_B, Q^2), \tag{3.80}$$

$$\sum_h \int \mathrm{d}z_h\,z_h\,F_{UU,L}(x_B, z_h, Q^2) = F_L(x_B, Q^2), \tag{3.81}$$

$$\sum_h \int \mathrm{d}z_h\,z_h\,F_{LL}(x_B, z_h, Q^2) = 2x_B\,(g_1(x_B, Q^2) - \gamma^2 g_2(x_B, Q^2)), \tag{3.82}$$

$$\sum_h \int \mathrm{d}z_h\,z_h\,F_{LT}^{\cos\phi_S}(x_B, z_h, Q^2) = -2x_B\gamma\,(g_1(x_B, Q^2) + g_2(x_B, Q^2)). \tag{3.83}$$

Time-reversal invariance requires (see, e.g., Ref. [61])

$$\sum_h \int \mathrm{d}z_h\,z_h\,F_{UT}^{\sin\phi_S}(x_B, z_h, Q^2) = 0. \tag{3.84}$$

3.6 Semi-inclusive DIS in the parton model

When including also target polarization, starting from the general decomposition presented in Eq. (2.50), the leading order part of the transverse-momentum dependent correlation function becomes

$$\Phi(x, p_T) = \frac{1}{2}\left\{ f_1 \not{n}_+ + f_{1T}^{\perp} \frac{\epsilon_T^{\rho\sigma} S_{T\rho} p_{T\sigma}}{M} \not{n}_+ + g_{1s}\gamma_5 \not{n}_+ \right. \\ \left. + h_{1T} \frac{[\not{S}_T, \not{n}_+]\gamma_5}{2} + h_{1s}^{\perp} \frac{[\not{p}_T, \not{n}_+]\gamma_5}{2M} + \mathrm{i}\, h_1^{\perp} \frac{[\not{p}_T, \not{n}_+]}{2M} \right\}$$

Here we introduced

$$\epsilon_T^{\alpha\beta} = \epsilon^{\alpha\beta\rho\sigma} n_{+\rho} n_{-\sigma}. \tag{3.85}$$

The distribution functions on the r.h.s. depend on x and p_T^2, except for the functions with subscript s, where we use the shorthand notation [97]

$$g_{1s}(x, p_T) = S_L\, g_{1L}(x, p_T^2) - \frac{S_T \cdot p_T}{M}\, g_{1T}(x, p_T^2) \tag{3.86}$$

and so forth for the other functions. It is also useful to introduce the function

$$h_1(x, \boldsymbol{p}_T^2) \equiv h_{1T}(x, \boldsymbol{p}_T^2) + h_{1T}^{\perp(1)}(x, \boldsymbol{p}_T^2). \tag{3.87}$$

The definition of the parton distribution functions in terms of the amplitudes A_i, introduced in Eq. (2.50), can be found elsewhere [73, 88, 115].

The two functions $f_{1T}^{\perp}$ (Sivers function) and $h_1^{\perp}$ (Boer-Mulders function) are T-odd [32, 66]. The notation for the distribution functions follows closely that of Ref. [97], sometimes referred to as "Amsterdam notation." We remark that a number of other notations exist for some of the distribution functions, see e.g. Refs. [24, 70, 107]. In particular, transverse-momentum-dependent functions at leading twist have been widely discussed by Anselmino et al. [5, 7, 8]. The connection between the notation in these papers and the one used here is discussed in App. C of Ref. [7]. The following names are in common use for the TMDs:

- f_1: unpolarized TMD;
- g_{1L}: helicity TMD;
- h_1: transversity TMD;
- $f_{1T}^{\perp}$: Sivers TMD;
- $h_1^{\perp}$: Boer-Mulders TMD;
- $g_{1T}^{\perp}$: worm-gear TMD, or transversal helicity TMD;
- $h_{1L}^{\perp}$: worm-gear TMD, or Kotzinian-Mulders TMD, or longitudinal transversity TMD;

nucleon pol. \ quark pol.	U	L	T	
U	$\boldsymbol{f_1}$		$h_1^\perp$	
L		$\boldsymbol{g_1}$	$h_{1L}^\perp$	
T	$f_{1T}^\perp$	g_{1T}	$\boldsymbol{h_1}$	$h_{1T}^\perp$

Figure 3.4: Twist-2 transverse-momentum-dependent distribution functions. The U,L,T correspond to unpolarized, longitudinally polarized and transversely polarized nucleons (rows) and quarks (columns). Functions in boldface survive transverse momentum integration. Functions in gray cells are T-odd.

- $h_{1T}^\perp$: pretzelosity TMD or quadrupole TMD.

The table in Fig. 3.4 lists the TMDs with their connection to quark and target polarizations. Useful relations are

$$\Phi^{[\gamma^+]} = f_1(x, p_T^2) - \frac{\epsilon_T^{\rho\sigma} p_{T\rho} S_{T\sigma}}{M} f_{1T}^\perp(x, p_T^2)\,, \tag{3.88}$$

$$\Phi^{[\gamma^+\gamma_5]} = S_L\, g_{1L}(x, p_T^2) - \frac{p_T \cdot S_T}{M} g_{1T}(x, p_T^2)\,, \tag{3.89}$$

$$\begin{aligned}\Phi^{[i\sigma^{\alpha+}\gamma_5]} &= S_T^\alpha\, h_1(x, p_T^2) + S_L \frac{p_T^\alpha}{M} h_{1L}^\perp(x, p_T^2) \\ &\quad - S_{T\rho} \frac{p_T^\alpha p_T^\rho - \frac{1}{2} p_T^2 g_T^{\alpha\rho}}{M^2} h_{1T}^\perp(x, p_T^2) - \frac{\epsilon_T^{\alpha\rho} p_{T\rho}}{M} h_1^\perp(x, p_T^2)\,.\end{aligned} \tag{3.90}$$

Transverse-momentum dependent parton distributions of leading twist can be interpreted as number densities (see e.g. Refs. [6,9,24]). To connect with this interpretation, we take the example of the distribution of unpolarized quarks in a polarized proton. , which is given by [19]

$$\begin{aligned} f_{q/p^\uparrow}(x, p_T) &= \Phi^{[\not{n}_-]} \\ &= f_1^q(x, p_T^2) - f_{1T}^{\perp q}(x, p_T^2) \frac{\epsilon^{\mu\nu\rho\sigma} P_\mu p_\nu S_\rho (n_-)_\sigma}{M\,(P \cdot n_-)} \\ &= f_1^q(x, p_T^2) - f_{1T}^{\perp q}(x, p_T^2) \frac{(\hat{\boldsymbol{P}} \times \boldsymbol{p}_T) \cdot \boldsymbol{S}}{M}, \end{aligned} \tag{3.91}$$

The second expression in (3.91) holds in any frame where $\boldsymbol{n}$ and the direction $\hat{\boldsymbol{P}}$ of the proton momentum point in opposite directions. Therefore $f_{1T}^{\perp q} > 0$ corresponds to a preference of the quark to move to the left if the proton is moving towards the observer and the proton spin is pointing upwards.

Let us give the corresponding relation for the Boer-Mulders function. The distribution of trans-

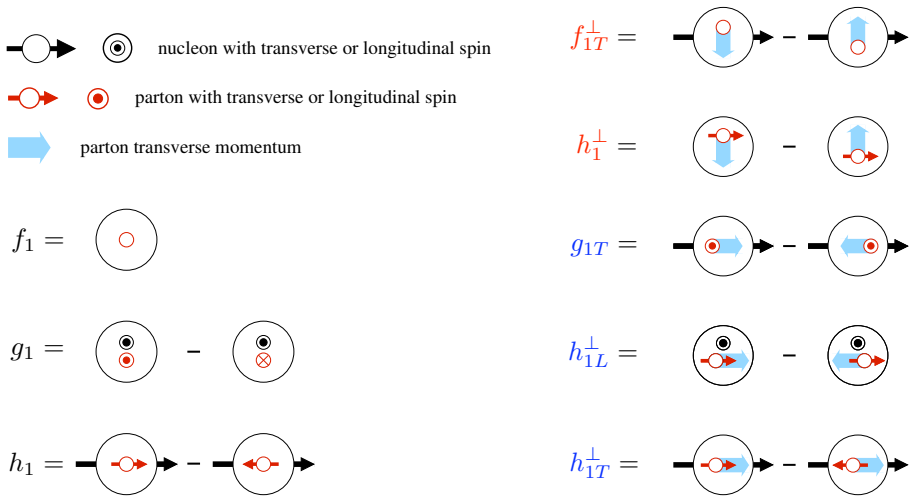

Figure 3.5: Probabilistic interpretation of twist-2 transverse-momentum-dependent distribution functions. To avoid ambiguities, it is necessary to indicate the directions of quark's transverse momemtum, target spin and quark spin, and specify that the proton is moving out of the page, or alternatively the photon is moving into the page.

versely polarized quarks in an unpolarized proton is (see Eq. (11) and (12) of [37])

$$\begin{aligned} f_{q^\uparrow/p}(x,p_T) &= \Phi(S=0)^{[/n_-]} + \Phi(S=0)^{[i\sigma_{\mu\nu}\gamma_5 n_-^\mu S_q^\nu]} \\ &= \frac{1}{2}\left(f_1^q(x,p_T^2) - h_1^{\perp q}(x,p_T^2)\,\frac{\epsilon^{\mu\nu\rho\sigma}P_\mu p_\nu S_{q\rho}(n_-)_\sigma}{M\,(P\cdot n_-)}\right) \\ &= \frac{1}{2}\left(f_1^q(x,p_T^2) - h_1^{\perp q}(x,p_T^2)\,\frac{(\hat{\boldsymbol{P}}\times\boldsymbol{p}_T)\cdot\boldsymbol{S}_q}{M}\right), \end{aligned} \tag{3.92}$$

where S_q is the covariant spin vector of the quark. Therefore, $h_1^{\perp q} > 0$ corresponds to a preference of the quark to move to the left if the proton is moving towards the observer and the quark spin is pointing upwards.

The probabilistic interpretation of TMDs is summarized in Fig. 3.5.

For any transverse-momentum dependent distribution function, it will turn out to be convenient to define the notation

$$f^{(1/2)}(x,\boldsymbol{p}_T^2) \equiv \frac{|\boldsymbol{p}_T|}{2M}\,f(x,\boldsymbol{p}_T^2), \tag{3.93a}$$

$$f^{(n)}(x,\boldsymbol{p}_T^2) \equiv \left(\frac{\boldsymbol{p}_T^2}{2M^2}\right)^n f(x,\boldsymbol{p}_T^2), \tag{3.93b}$$

for n integer.

As done previously, we can express the transverse momentum dependent correlation function as a matrix in the parton chirality space $\otimes$ target helicity space. The steps for the chirality space are analogous to the previous case, but the treatment of the target spin is obviously new.

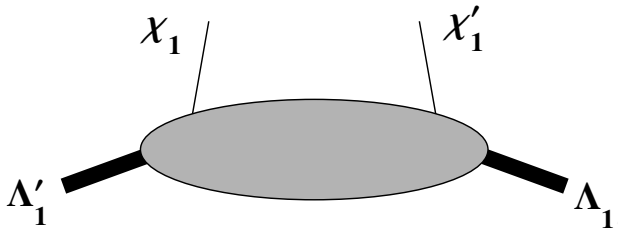

Figure 3.6: Illustration of the position of the indices of the correlation matrix.

Using the Weyl representation, the correlation function reads

$$\left(\mathcal{P}_+\,\Phi(x,S)\gamma^+\right)_{ji} = \begin{pmatrix} f_1(x)+S_L\,g_1(x) & 0 & 0 & (S_x-\mathrm{i}S_y)\,h_1(x) \\ 0 & 0 & 0 & 0 \\ 0 & 0 & 0 & 0 \\ (S_x+\mathrm{i}S_y)\,h_1(x) & 0 & 0 & f_1(x)-S_L\,g_1(x) \end{pmatrix}. \tag{3.94}$$

The four-dimensional Dirac space can be reduced to a two-dimensional space, retaining only the nonzero part of the correlation function, i.e.

$$\left(\mathcal{P}_+\,\Phi(x,S)\gamma^+\right)_{\chi_1'\chi_1} = \rho(S)_{\Lambda_1\Lambda_1'}\left(\mathcal{P}_+\,\Phi(x)\gamma^+\right)^{\Lambda_1'\Lambda_1}_{\chi_1'\chi_1}. \tag{3.95}$$

We will refer to the last term of this relation as the matrix representation of the correlation function or, more simply, as the correlation matrix. Fig. 3.6 shows pictorially the position of the spin indices.

Starting from Eq. (2.51) and using the relation

$$\Psi_U + S_L\Psi_L + S_x\Psi_x + S_y\Psi_y = \rho(S)_{\Lambda_1\Lambda_1'}\begin{pmatrix}\Psi_U+\Psi_L & \Psi_x-\mathrm{i}\Psi_y \\ \Psi_x+\mathrm{i}\Psi_y & \Psi_U-\Psi_L\end{pmatrix}^{\Lambda_1'\Lambda_1} \tag{3.96}$$

we can cast the correlation function in the matrix form

$$\left(\mathcal{P}_+\,\Phi(x)\gamma^+\right)^{\Lambda_1'\Lambda_1} = \begin{pmatrix}(f_1(x)+g_1(x)\,\gamma_5)\,\mathcal{P}_+ & h_1(x)\,(\gamma_x-\mathrm{i}\gamma_y)\,\gamma_5\mathcal{P}_+ \\ h_1(x)\,(\gamma_x+\mathrm{i}\gamma_y)\,\gamma_5\mathcal{P}_+ & (f_1(x)-g_1(x)\,\gamma_5)\,\mathcal{P}_+\end{pmatrix}. \tag{3.97}$$

Finally, by expressing the Dirac structures in Weyl representation and reducing the Dirac space as done before, we obtain the matrix representation of the correlation function

$$\left(\mathcal{P}_+\,\Phi(x)\gamma^+\right)^{\Lambda_1'\Lambda_1}_{\chi_1'\chi_1} = \left(\begin{array}{cc|cc} f_1(x)+g_1(x) & 0 & 0 & 0 \\ 0 & f_1(x)-g_1(x) & 2h_1(x) & 0 \\ \hline 0 & 2h_1(x) & f_1(x)-g_1(x) & 0 \\ 0 & 0 & 0 & f_1(x)+g_1(x) \end{array}\right), \tag{3.98}$$

where the inner blocks are in the hadron helicity space (indices $\Lambda_1'\Lambda_1$), while the outer matrix is in the quark chirality space (indices $\chi_1'\chi_1$).

The form of the correlation matrix can also be established directly from angular momentum conservation (requiring $\Lambda_1' + \chi_1' = \Lambda_1 + \chi_1$) and the conditions of Hermiticity and parity invariance. In matrix language, the condition of parity invariance consists in [72]

$$\left(\mathcal{P}_+ \,\Phi(x)\gamma^+\right)^{\Lambda_1'\Lambda_1}_{\chi_1'\chi_1} = \left(\mathcal{P}_+ \,\Phi(x)\gamma^+\right)^{-\Lambda_1'\,-\Lambda_1}_{-\chi_1'\,-\chi_1}. \tag{3.99}$$

The most general form of the correlation matrix complying with the previous conditions corresponds to Eq. (3.98).

As mentioned at the end of Sec. **??** on page ??, with transposing the quark chirality indices of the correlation matrix

To simplify the formulae, it is useful to identify the T-odd functions as imaginary parts of some of the T-even functions, which become then complex scalar functions. The following redefinitions are required:[2]

$$g_{1T} + \mathrm{i} f_{1T}^{\perp} \to g_{1T}, \qquad\qquad h_{1L}^{\perp} + \mathrm{i} h_1^{\perp} \to h_{1L}^{\perp}. \tag{3.100}$$

The resulting correlation matrix is [13, 14]

$$F(x,\boldsymbol{p}_T)^{\Lambda_1'\Lambda_1}_{\chi_1\chi_1'} = \left(\begin{array}{cc|cc} f_1 + g_{1L} & \dfrac{|\boldsymbol{p}_T|}{M}\,\mathrm{e}^{-\mathrm{i}\phi_p}\, g_{1T} & \dfrac{|\boldsymbol{p}_T|}{M}\,\mathrm{e}^{\mathrm{i}\phi_p}\, h_{1L}^{\perp *} & 2\,h_1 \\ \dfrac{|\boldsymbol{p}_T|}{M}\,\mathrm{e}^{\mathrm{i}\phi_p}\, g_{1T}^{*} & f_1 - g_{1L} & \dfrac{|\boldsymbol{p}_T|^2}{M^2}\mathrm{e}^{2\mathrm{i}\phi_p}\, h_{1T}^{\perp} & -\dfrac{|\boldsymbol{p}_T|}{M}\,\mathrm{e}^{\mathrm{i}\phi_p}\, h_{1L}^{\perp} \\ \hline \dfrac{|\boldsymbol{p}_T|}{M}\,\mathrm{e}^{-\mathrm{i}\phi_p}\, h_{1L}^{\perp} & \dfrac{|\boldsymbol{p}_T|^2}{M^2}\mathrm{e}^{-2\mathrm{i}\phi_p}\, h_{1T}^{\perp} & f_1 - g_{1L} & -\dfrac{|\boldsymbol{p}_T|}{M}\,\mathrm{e}^{-\mathrm{i}\phi_p}\, g_{1T}^{*} \\ 2\,h_1 & -\dfrac{|\boldsymbol{p}_T|}{M}\,\mathrm{e}^{-\mathrm{i}\phi_p}\, h_{1L}^{\perp *} & -\dfrac{|\boldsymbol{p}_T|}{M}\,\mathrm{e}^{\mathrm{i}\phi_p}\, g_{1T} & f_1 + g_{1L} \end{array}\right), \tag{3.101}$$

where for sake of brevity we did not explicitly indicate the x and $\boldsymbol{p}_T^2$ dependence of the distribution functions and where ϕ_p is the azimuthal angle of the transverse momentum vector.

The distribution matrix is clearly Hermitean. The condition of angular momentum conservation becomes $\Lambda_1' + \chi_1' + l' = \Lambda_1 + \chi_1$. The condition of parity invariance becomes

$$F(x,\boldsymbol{p}_T)^{\Lambda_1'\Lambda_1}_{\chi_1\chi_1'} = (-1)^{l'}\, F(x,\boldsymbol{p}_T)^{-\Lambda_1'\,-\Lambda_1}_{-\chi_1\,-\chi_1'}\Big|_{l'\to -l'}. \tag{3.102}$$

Bounds to insure positivity of any matrix element can be obtained by looking at the one-dimensional and two-dimensional subspaces and at the eigenvalues of the full matrix. The one-dimensional subspaces give the trivial bounds

$$f_1(x,\boldsymbol{p}_T^2) \geq 0\,, \qquad\qquad \left|g_{1L}(x,\boldsymbol{p}_T^2)\right| \leq f_1(x,\boldsymbol{p}_T^2)\,. \tag{3.103}$$

[2] From a rigorous point of view, it would be better to introduce new functions, e.g. $\tilde{g}_{1T}$ and $\tilde{h}_{1L}^{\perp}$, but this would overload the notation.

From the two-dimensional subspaces we get

$$|h_1| \leq \frac{1}{2}(f_1 + g_{1L}) \leq f_1, \tag{3.104a}$$

$$\left|h_{1T}^{\perp(1)}\right| \leq \frac{1}{2}(f_1 - g_{1L}) \leq f_1, \tag{3.104b}$$

$$\left|g_{1T}^{(1)}\right|^2 + \left|f_{1T}^{\perp(1)}\right|^2 \leq \frac{\boldsymbol{p}_T^2}{4M^2}(f_1 + g_{1L})(f_1 - g_{1L}) \leq \left(f_1^{(1/2)}\right)^2, \tag{3.104c}$$

$$\left|h_{1L}^{\perp(1)}\right|^2 + \left|h_1^{\perp(1)}\right|^2 \leq \frac{\boldsymbol{p}_T^2}{4M^2}(f_1 + g_{1L})(f_1 - g_{1L}) \leq \left(f_1^{(1/2)}\right)^2, \tag{3.104d}$$

where, once again, we did not explicitly indicate the x and $\boldsymbol{p}_T^2$ dependence to avoid too heavy a notation. Besides the Soffer bound of Eq. (3.104a), now extended to include the transverse momentum dependence, new bounds for the distribution functions are found. These bounds can be very useful for phenomenological applications.

The positivity bounds can be sharpened even further by imposing the positivity of the eigenvalues of the correlation matrix. The complete analysis has been accomplished in Ref. 13 (see also Ref. 14).

The connection with the integrated distribution functions defined in Eq. (2.52) is

$$f_1(x) = \int \mathrm{d}^2\boldsymbol{p}_T \; f_1(x, \boldsymbol{p}_T^2), \tag{3.105a}$$

$$g_{1L}(x) = \int \mathrm{d}^2\boldsymbol{p}_T \; g_{1L}(x, \boldsymbol{p}_T^2), \tag{3.105b}$$

$$h_1(x) = \int \mathrm{d}^2\boldsymbol{p}_T \; h_1(x, \boldsymbol{p}_T^2). \tag{3.105c}$$

The above identification is however a dangerous step. At parton-model level, it is not a big problem if we assume that TMDs fall-off sufficently fast (i.e., they are integrable and their total integral is approximately equal to their integral in the region $\boldsymbol{p}_T^2 \ll Q^2$). We may have in mind that partons have some "intrinsic" transverse momentum of order $\boldsymbol{p}_T^2 \sim M^2$ or $\boldsymbol{p}_T^2 \sim \Lambda_{QCD}^2$. This is however *not* the case when we take into consideration QCD corrections. In this case, partons acquire transverse momentum also through gluon radiation. First of all, this has the consequence that TMDs in QCD are *not* integrable, so we must give up the above relations in general. Secondly, it becomes impossible–or a matter of conventions–to distinguish an intrinsic part of transverse momentum from a perturbative part. TMDs contain both.

Another way to state the problem is the following: the steps we took to analyze SIDIS were based on the assumption that $\boldsymbol{P}_{h\perp}^2 \ll Q^2$. We never needed this approximation for inclusive DIS, where we introduced collinear PDFs. Collinear PDFs are obtained from an integration over $\boldsymbol{P}_{h\perp}^2$ up to a limit of the order of Q^2. They contain therefore also contributions that are outside the reach of the TMD formalism. Therefore, we should not expect in general that the integral of TMDs gives back collinear PDFs: something must be missing.

Is there then no relation between TMDs and collinear PDFs? The full QCD formalism tells us that there is a relation, but it's between PDFs and the high-transverse-momentum tail of TMDs.

3.7 Structure functions in the parton model

Inserting the parameterizations of the different correlators in the expression (3.32) of the hadronic tensor and contracting it with the leptonic tensor, one can calculate the leptoproduction cross section for semi-inclusive DIS and project out the different structure functions appearing in Eq. 3.71. To have a compact notation for the results, we introduce the notation

$$C[wfD] = x_B \sum_q e_q^2 \int d^2\boldsymbol{p}_T\, d^2\boldsymbol{k}_T\, \delta^{(2)}(\boldsymbol{p}_T - \boldsymbol{k}_T - \boldsymbol{P}_{h\perp}/z)\, w(\boldsymbol{p}_T, \boldsymbol{k}_T)\, f^q(x_B, p_T^2)\, D^q(z, k_T^2), \quad (3.106)$$

with the unit vector $\hat{\boldsymbol{h}} = \boldsymbol{P}_{h\perp}/|\boldsymbol{P}_{h\perp}|$, where $w(\boldsymbol{p}_T, \boldsymbol{k}_T)$ is an arbitrary function.

These are the expressions for the structure functions appearing in Eq. (3.71)

$$F_{UU,T} = C[f_1 D_1], \quad (3.107)$$

$$F_{UU,L} = 0, \quad (3.108)$$

$$F_{UU}^{\cos\phi_h} = 0 \quad (3.109)$$

$$F_{UU}^{\cos 2\phi_h} = C\left[-\frac{2\,(\hat{\boldsymbol{h}}\cdot\boldsymbol{k}_T)\,(\hat{\boldsymbol{h}}\cdot\boldsymbol{p}_T) - \boldsymbol{k}_T\cdot\boldsymbol{p}_T}{MM_h} h_1^\perp H_1^\perp\right], \quad (3.110)$$

$$F_{LU}^{\sin\phi_h} = 0, \quad (3.111)$$

$$F_{UL}^{\sin\phi_h} = 0, \quad (3.112)$$

$$F_{UL}^{\sin 2\phi_h} = C\left[-\frac{2\,(\hat{\boldsymbol{h}}\cdot\boldsymbol{k}_T)\,(\hat{\boldsymbol{h}}\cdot\boldsymbol{p}_T) - \boldsymbol{k}_T\cdot\boldsymbol{p}_T}{MM_h} h_{1L}^\perp H_1^\perp\right], \quad (3.113)$$

$$F_{LL} = C[g_{1L} D_1], \quad (3.114)$$

$$F_{LL}^{\cos\phi_h} = 0, \quad (3.115)$$

$$F_{UT,T}^{\sin(\phi_h-\phi_S)} = C\left[-\frac{\hat{\boldsymbol{P}}_{h\perp}\cdot\boldsymbol{p}_T}{M} f_{1T}^\perp D_1\right], \quad (3.116)$$

$$F_{UT,L}^{\sin(\phi_h-\phi_S)} = 0, \quad (3.117)$$

$$F_{UT}^{\sin(\phi_h+\phi_S)} = C\left[-\frac{\hat{\boldsymbol{P}}_{h\perp}\cdot\boldsymbol{k}_T}{M_h} h_1 H_1^\perp\right], \quad (3.118)$$

$$F_{UT}^{\sin(3\phi_h-\phi_S)} = C\left[\frac{2\,(\hat{\boldsymbol{P}}_{h\perp}\cdot\boldsymbol{p}_T)\,(\boldsymbol{p}_T\cdot\boldsymbol{k}_T) + \boldsymbol{p}_T^2\,(\hat{\boldsymbol{P}}_{h\perp}\cdot\boldsymbol{k}_T) - 4\,(\hat{\boldsymbol{P}}_{h\perp}\cdot\boldsymbol{p}_T)^2\,(\hat{\boldsymbol{P}}_{h\perp}\cdot\boldsymbol{k}_T)}{2M^2 M_h} h_{1T}^\perp H_1^\perp\right], \quad (3.119)$$

$$F_{UT}^{\sin\phi_S} = 0, \quad (3.120)$$

$$F_{UT}^{\sin(2\phi_h-\phi_S)} = 0, \quad (3.121)$$

$$F_{LT}^{\cos(\phi_h-\phi_S)} = C\left[\frac{\hat{\boldsymbol{P}}_{h\perp}\cdot\boldsymbol{p}_T}{M} g_{1T} D_1\right], \quad (3.122)$$

$$F_{LT}^{\cos\phi_S} = 0, \quad (3.123)$$

$$F_{LT}^{\cos(2\phi_h-\phi_S)} = 0, \tag{3.124}$$

It has to be stressed that in much of the past literature a different definition of the azimuthal angles has been used, whereas in the present work we adhere to the Trento conventions [19].

Ex. 1
Compute some of the structure functions above using Mathematica and Feyncalc. For convenince, you can use the following definitions

```
eta= {{0, 1, 0, 0}, {1, 0, 0, 0}, {0, 0, -1, 0}, {0, 0, 0, -1}}

GAp = GS[Momentum[nm]];
GAm = GS[Momentum[np]];
GA5 = DiracGamma[5];
```

And you have to introduce the following scalar products (the first two instructions are just a convenient way to write all scalar products of light-cone vectors)

```
Unit = {nm, np, ni, nj};
Table[ScalarProduct[Unit[[i]], Unit[[j]]] = eta[[i, j]], {i, 1,
   4}, {j, 1, 4}];

ScalarProduct[pt, np] = 0;
ScalarProduct[pt, nm] = 0;
ScalarProduct[kt, np] = 0;
ScalarProduct[kt, nm] = 0;

ScalarProduct[St, nm] = 0;
ScalarProduct[St, np] = 0;
```

Now you can introduce the decompositions of the correlation functions. In this first example, we take into consideration only three of the eight terms in Eq. (3.85)

```
Phi = (f1 - g1T Pair[Momentum[pt], Momentum[St]]/M GA5 -
    f1Tperp Pair[Momentum[pt], Momentum[epsT[St]]]/M).(GAm/2)

Delta = ( D1 + I H1perp 1/Mh GS[Momentum[kt]]).(GAp/2)
```

Build a first version of the hadronic tensor, according to Eq. (3.32). Note that for convenience we can avoid introducing explicitly the convolution in Eq. (3.33). We need to remember to include it in the final result.

```
MW0 = 1/2 2 z (Tr[Phi.GA[\[Mu]].Delta .GA[\[Nu]]]) //
  Collect[#, {f1 D1, f1Tperp D1, D1 g1T}, Simplify] &
```

Apply the following crucial replacements and cast the tensor in a convenient form

```
HadTensSimpl = {Pair[Momentum[pt], Momentum[St]] ->
   SSt Cos[-\[Phi] + \[Phi]St] Pair[Momentum[pt], Momentum[h]],
  Pair[Momentum[pt], Momentum[epsT[St]]] ->
   SSt Sin[-\[Phi] + \[Phi]St] Pair[Momentum[pt], Momentum[h]]}

MW = MW0 /. HadTensSimpl // Simplify
```

Finally, contract with the leptonic tensor (obtained in Ex. 1)

```
crosssection1 = (\[Alpha]^2 y)/(2 z Q^4)
     Contract[Lept 2 MW]// Expand //
  Collect[#, {f1 D1, f1Tperp D1, h1 H1perp, D1 g1T}, Simplify] &
```

By comparing the result with Eq. (3.71) and after fixing all small mistakes in the above, you should be able to identify the structure functions corresponding to Eqs. (3.107), (3.116), and (3.122).

3.8 Beyond the parton model

A first important difference between TMDs and PDFs when we also start taking gluons into account is in the shape of the gauge link. The proper gauge invariant definition of the quark-quark correlator is

$$\Phi_{ij}(x, p_T) = \int \frac{\mathrm{d}\xi^- \,\mathrm{d}^2\xi_T}{(2\pi)^3}\, e^{\mathrm{i}p\cdot\xi}\, \langle P|\bar{\psi}_j(0)\, \mathcal{L}^{n_-}_{(0,+\infty)}\, \mathcal{L}^{n_-}_{(+\infty,\xi)}\, \psi_i(\xi)|P\rangle\Big|_{\xi^+=0} \tag{3.125}$$

where the gauge links (Wilson lines) are defined as

$$\mathcal{L}^{n_-}_{(0,+\infty)} = \mathcal{L}^{n_-}(0^-, \infty^-; \mathbf{0}_T)\, \mathcal{L}^{T}(\mathbf{0}_T, \boldsymbol{\infty}_T; \infty^-), \tag{3.126}$$

$$\mathcal{L}^{n_-}_{(+\infty,\xi)} = \mathcal{L}^{T}(\boldsymbol{\infty}_T, \boldsymbol{\xi}_T; \infty^-)\, \mathcal{L}^{n_-}(\infty^-, \xi^-, \boldsymbol{\xi}_T). \tag{3.127}$$

Here $\mathcal{L}^{n_-}(a^-, b^-; \boldsymbol{c}_T)$ indicates a Wilson line running along the minus direction from $[a^-, 0, \boldsymbol{c}_T]$ to $[b^-, 0, \boldsymbol{c}_T]$, while $\mathcal{L}^{T}(\boldsymbol{a}_T, \boldsymbol{b}_T; c^-)$ indicates a Wilson line running in the transverse direction from $[c^-, 0, \boldsymbol{a}_T]$ to $[c^-, 0, \boldsymbol{b}_T]$, i.e.

$$\mathcal{L}^{n_-}(a^-, b^-; \boldsymbol{c}_T) = \mathcal{P}\exp\Big[-\mathrm{i}g \int_{a^-}^{b^-} \mathrm{d}\eta^- A^+(\eta^-, 0, \boldsymbol{c}_T)\Big], \tag{3.128}$$

$$\mathcal{L}^{T}(\boldsymbol{a}_T, \boldsymbol{b}_T; c^-) = \mathcal{P}\exp\Big[-\mathrm{i}g \int_{\boldsymbol{a}_T}^{\boldsymbol{b}_T} \mathrm{d}\boldsymbol{\eta}_T \cdot A_T(c^-, 0, \boldsymbol{\eta}_T)\Big]. \tag{3.129}$$

In particular

$$\mathcal{L}^{n^-}(\infty^-,\xi^-,\boldsymbol{\xi}_T) = \mathcal{P}\exp\Big[-ig\int_{\infty^-}^{\xi^-} d\eta^- A^+(\eta^-,0,\boldsymbol{\xi}_T)\Big]$$
$$\approx 1 - ig\int_{\infty^-}^{\xi^-} d\eta^- A^+(\eta^-,0,\boldsymbol{\xi}_T) \tag{3.130}$$
$$\mathcal{L}^{T}(\infty_T,\boldsymbol{\xi}_T;\infty^-) = \mathcal{P}\exp\Big[-ig\int_{\infty_T}^{\boldsymbol{\xi}_T} d\boldsymbol{\eta}_T\cdot A_T(\infty^-,0,\boldsymbol{\eta}_T)\Big]$$
$$\approx 1 - ig\int_{\infty_T}^{\boldsymbol{\xi}_T} d\boldsymbol{\eta}_T\cdot A_T(\infty^-,0,\boldsymbol{\eta}_T) \tag{3.131}$$

The correlator in Eq. (3.125) is the one appearing in semi-inclusive DIS. Its path is pictorially shown in Fig. 3.7.

A remarkable property of TMDs is that the detailed shape of the Wilson line is process-dependent. This immediately leads to the conclusion that TMDs are not universal. However, for transverse-momentum-dependent fragmentation functions, the shape of the Wilson line appears to have no influence on physical observables [54, 64, 92, 117]. In SIDIS and Drell–Yan, the difference between the Wilson line consists in a simple direction reversal and leads to calculable effects, namely a simple sign reversal of all T-odd TMDs [52].

In more complex processes, such as proton-proton collisions into hadrons, it was initially proposed to introduce more intricate gauge links [15, 38, 39], but it seems now that it becomes even impossible to disentangle them [108].

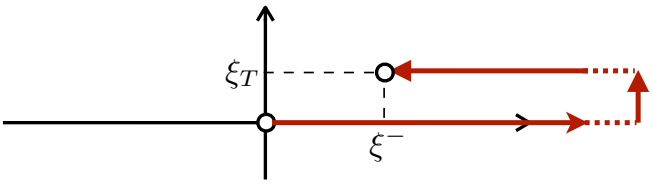

Figure 3.7: Path of the gauge link for semi-inclusive DIS.

Similarly to standard collinear PDFs, it is essential to define TMDs in a formally clear way, through the proof of factorization theorems. TMDs appear when factorizing semi-inclusive processes. For instance, while totally inclusive DIS can be described introducing collinear PDFs, TMDs appear in semi-inclusive DIS if the transverse momentum of one outgoing hadron, $P_{h\perp}$, is measured.

Dealing with semi-inclusive processes pushes the difficulty of proving factorization theorems to a higher level of complications. TMD factorization is in fact a challenging arena where many of the simplifications used in collinear factorization cannot be applied. Nevertheless, factorization for semi-inclusive DIS has been worked out explicitly at leading twist (twist 2) and one-loop order [12, 49, 56, 77]. For instance, the structure function $F_{UU,T}$ in the region $P_{h\perp}^2 \ll Q^2$ can be

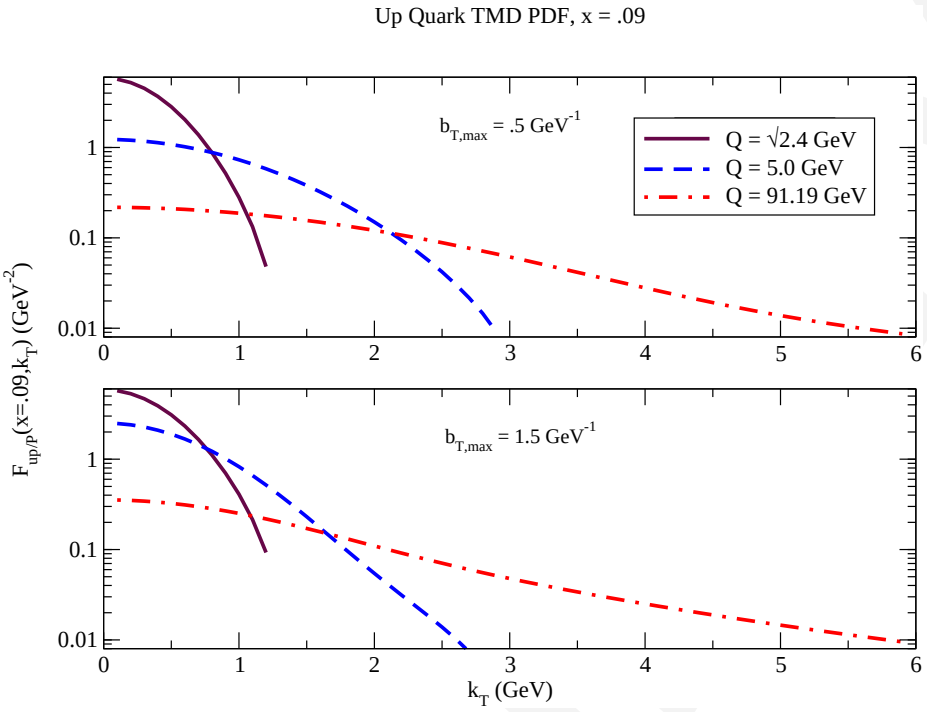

Figure 3.8: The up quark TMD for $Q = \sqrt{2.4}, 5.0$ and 91.19 GeV and $x = 0.09$ from Ref. [12]. The upper and lower plot refer to two different choices for the parameter b_{max} needed in the full TMD formula.

expressed as

$$F_{UU,T} = \left|H(x\zeta^{1/2}, z^{-1}\zeta_h^{1/2}, \mu_F)\right|^2 \sum_a x\, e_a^2 \int \mathrm{d}^2\boldsymbol{p}_T\ \mathrm{d}^2\boldsymbol{k}_T \\ \times \delta^{(2)}(\boldsymbol{p}_T - \boldsymbol{k}_T - \boldsymbol{P}_{h\perp}/z)\, f_1^a(x, p_T^2; \zeta, \mu_F)\, D_1^a(z, k_T^2; \zeta_h, \mu_F). \tag{3.132}$$

The formula contains the (calculable) hard scattering factor H and the transverse-momentum-dependent PDFs and fragmentation functions. Following Refs. [12, 49], there is no "soft factor" in the above formula. The soft factor can be introduced to absorb infrared soft divergences. In this alternative definition, these divergences are absorbed already in the TMDs.

According to TMD factorization, TMDs depend also on a cutoff ζ. This cutoff is used to regulate light-cone or rapidity divergences. As we mentioned in the DIS discussion, these divergences cancel in inclusive DIS thanks to the summation of virtual and real diagrams and the integration over transverse momentum, similarly to soft divergences. In semi-inclusive DIS, they do not cancel. Various ways to deal with these divergences have been proposed [46, 53, 56, 77].

TMD evolution is different from that of standard PDFs and takes into account how TMD shape is influenced by the radiation of infinitely many gluons (transverse-momentum resummation) [57]. What needs to be obtained from data is the nonperturbative part of the functions (i.e., what cannot be computed with perturbative QCD). Fig. 3.8 (from [12]) shows the effect of TMD evolution on the distribution of up quarks (the nonperturbative part is taken from [87] and [110]). The effect of gluon radiation is a broadening of the TMD.

In general and in simplified terms, the study of TMD factorization requires a deeper under-

standing of what happens when a quark is hit inside a nucleon, with a particular attention to the infinitely many gluons that surround the quark, beyond the simple case when its transverse momentum is integrated over.

3.9 Beyond the parton model: high transverse momentum

Three scales are involved in semi-inclusive DIS: the scale of nonperturbative QCD dynamics, which we represent by the nucleon mass M, the transverse momentum $P_{h\perp}$, and the photon virtuality Q, which we require to be large compared with M. For the considerations of this section, it is convenient to consider the transverse momentum $q_T^2 \approx P_{h\perp}^2/z^2$.

At high q_T ($q_T \gg M$) the structure functions can be described using collinear factorization, i.e., in terms of collinear distribution and fragmentation functions together with perturbative radiation. At low-q_T ($q_T \ll Q$) the structure functions can be described using TMD factorization [56,77], i.e., in terms transverse-momentum-dependent (TMD) parton distribution and fragmentation functions. The low- and high-q_T domains overlap for $M \ll q_T \ll Q$ (intermediate transverse momentum), where both descriptions can hence be applied. This important property is what allows us to establish a connection between collinear PDFs and the tail of TMDs.

Ideally, we would like to have an expression for the polarized SIDIS cross section that describes in a smooth way the physics from low to high transverse momentum. This issue becomes crucial at collider experiments, where the possibility to reach high values of Q leaves room to meaningfully distinguish between high, intermediate, and low transverse momentum.

In order to address the problem two steps are needed: (i) identify the structure functions for which a matching is possible, (ii) work out a formula that describes the structure function at any transverse momentum. In the following I will briefly discuss some crucial results.

To study the power behavior of the structure functions, it is important to realize that the power expansions are done in two different ways in the two descriptions. At low q_T, first we expand in $(q_T/Q)^{n-2}$ and neglect terms with n bigger than a certain value (so far, analyses have been carried out only up to $n = 3$, i.e., twist-3). To study the behavior at intermediate q_T we further expand in $(M/q_T)^k$. Vice versa, at high q_T we first expand in $(M/q_T)^n$ (also in this case, analyses are available up to $n = 3$, i.e., twist-3). To study the intermediate-q_T region, we further expand in $(q_T/Q)^{k-2}$. We can encounter two different situations:

- Type-I observables, where the leading terms at high and low transverse momentum have the same behavior. For instance,

$$F(q_T, Q) = A\left[\frac{q_T}{Q}\right]^0\left[\frac{M}{q_T}\right]^2 + B\left[\frac{q_T}{Q}\right]^2\left[\frac{M}{q_T}\right]^2 + \dots, \tag{3.133}$$

  where the term A is leading in both the low- and high-q_T calculations. In this case, the calculations at high and low transverse momentum must yield exactly the same result at intermediate transverse momentum [57, 79]. If a mismatch occurs, it means that one of the calculations is incorrect or incomplete.

- Type-II observables, where the leading terms at high and low transverse momentum have different behavior. For instance,

$$F(q_T, Q) = A' \left[\frac{q_T}{Q}\right]^0 \left[\frac{M}{q_T}\right]^4 + B' \left[\frac{q_T}{Q}\right]^2 \left[\frac{M}{q_T}\right]^2 + \dots . \tag{3.134}$$

  where the first term is leading and the second term subleading in the low-q_T calculation, whereas the reverse holds in the high-q_T calculation. In this case, if the calculations at high and low transverse momentum are performed at their respective leading order, they describe two different mechanisms and will not lead to the same result at intermediate transverse momentum. In order to "match", the calculations should be carried out in both regimes up to the sub-subleading order. We could call this situation an "expected mismatch", since it is simply due to the difference between the two expansions.

In Tab. 3.1 we list the power behavior of the structure functions at intermediate transverse momentum, as obtained from the limits of the low-q_T and high-q_T calculation. For details of the calculation, we refer to [16].

In the last column of the table we identify type-II structure functions, fow which the low-q_T and high-q_T calculations at leading order pick up two different components of the full structure function. They therefore describe two different mechanisms and do not match.

For type-II observables, if one aims at studying the leading-twist contribution from transverse momentum distributions, some considerations have to be kept in mind:

- the leading contribution from the high-q_T calculation (often referred to as a pQCD or radiative correction) is a competing effect that has to be taken into account [25, 26, 100];
- q_T-weighted asymmetries enhance the high-q_T mechanism and thus are not appropriate to extract TMDs;
- it is at present impossible to construct an expression that extends the high-q_T calculation to $q_T \approx M$, since this requires a smooth merging into unknown twist-4 contributions, which most probably cannot be factorized (see also Ref. [29]);
- it may be useful to build observables that are least sensitive to the effect of radiative corrections.

We stress that the above considerations apply not only to semi-inclusive DIS, but also to Drell-Yan and e^+e^- annihilation [34], which have been already used to extract the Boer–Mulders and Collins functions [25, 90].

The structure functions with a "yes" or "no" in the last column of Tab. 3.1 are type-I observables, where on the basis of power counting we know that two calculations describe the same physics and should therefore exactly match. In these cases, the high-q_T calculation describes the perturbative tail of the low-q_T effect. The two mechanisms need not be distinguished. Using resummation it should be possible to construct expressions for these observables that are valid at any q_T.

Six of these structure functions have been calculated explicitly. The following structure functions all involve twist-2 TMDs and indeed present an exact matching: $F_{UU,T}$, F_{LL} [82], $F_{UT,T}^{\sin(\phi_h-\phi_S)}$ (Sivers structure function) [78] (see also the additions in Ref. [83]) and $F_{UT}^{\sin(\phi_h+\phi_S)}$ (Collins structure function) [118]. We expect also $F_{LT}^{\cos(\phi_h-\phi_S)}$ to match exactly, since it has been shown explicitly for a similar structure function in the Drell–Yan case [119].

The structure functions $F_{UU}^{\cos\phi_h}$ and $F_{LL}^{\cos\phi_h}$ do not match [16]. In analogy to these results, we expect that also all the others will not match, since they are twist-3 in the low-q_T regime, and the TMD factorization formalism is probably complete only at twist 2.

In summary, at the moment there is the hope to build descriptions of the structure functions that go from low to high transverse momentum for the five structure functions with a "yes" in the last column of Tab. 3.1.

3.10 Weighted asymmetries

In the structure functions we have expressions such as

$$C\Big[-\frac{\hat{\boldsymbol{P}}_{h\perp}\cdot\boldsymbol{p}_T}{M}f_{1T}^{\perp}D_1\Big] \tag{3.135}$$

where the two functions appear in a convolution. The general way to split the convolution is to use transverse-momentum-weighted asymmetries. For instance

$$W = \int d^2\boldsymbol{P}_{h\perp}\,\frac{|\boldsymbol{P}_{h\perp}|}{M}\,C\Big[-\frac{\hat{\boldsymbol{P}}_{h\perp}\cdot\boldsymbol{p}_T}{M}f_{1T}^{\perp}D_1\Big] \tag{3.136}$$

in fact

$$\begin{aligned}
W &= -x_B\sum_q e_q^2\int d^2\boldsymbol{P}_{h\perp}\,d^2\boldsymbol{p}_T\,d^2\boldsymbol{k}_T\,\delta^{(2)}(\boldsymbol{p}_T-\boldsymbol{k}_T-\boldsymbol{P}_{h\perp}/z_h)\,\frac{\boldsymbol{P}_{h\perp}\cdot\boldsymbol{p}_T}{M}f_{1T}^{\perp q}D_1^q,\\
&= -x_B\,z_h^2\sum_q e_q^2\int d^2\boldsymbol{p}_T\,d^2\boldsymbol{k}_T\,\frac{(\boldsymbol{p}_T-\boldsymbol{k}_T)\cdot\boldsymbol{p}_T}{M^2}f_{1T}^{\perp q}D_1^q,\\
&= -x_B\sum_q e_q^2\int d^2\boldsymbol{p}_T\,\frac{|\boldsymbol{p}_T|^2}{M^2}\,f_{1T}^{\perp q}\,z_h^2\int d^2\boldsymbol{k}_T\,D_1^q\\
&= -x_B\sum_q e_q^2\,2f_{1T}^{\perp(1)q}(x_B)\,D_1(z_h).
\end{aligned} \tag{3.137}$$

Why weighted asymmetries are important? From a phenomenological side, they allow us to separately study transverse moments of TMDs and fragmentation functions, as simple products instead of convolutions. From the theoretical point of view, after the weighted integral is performed we can deal with collinear objects again and some of the complications entailed in TMD factorization may drop.

The above expression is again a parton-model level expression. If we want a QCD expression, the minimal requirement is that the involved transverse-momentum integrals could be treated in a

similar way as the functions f_1 and D_1. To this purpose, Tab. 3.1 can be useful. You can see that the structure function containing the Sivers function, (3.116), in Tab. 3.1 is indicated as a type-I observable with exact matching. Moreover, the structure function falls as $1/q_T^3$, which means that if we weigh it with a power of q_T it acquires the same power behavior as the "standard" unpolarized structure function. This may indicate that we can analyze weighted asymmetries with similar techniques as collinear structure functions.

struct. function	low-q_T power	high-q_T power	exact match
$F_{UU,T}$	$1/q_T^2$	$1/q_T^2$	yes
$F_{UU,L}$		$1/Q^2$	
$F_{UU}^{\cos\phi_h}$	$1/(Qq_T)$	$1/(Qq_T)$	no
$F_{UU}^{\cos 2\phi_h}$	$1/q_T^4$	$1/Q^2$	typeII
$F_{LU}^{\sin\phi_h}$	$1/(Qq_T)$	$1/(Qq_T)$	(no)
$F_{UL}^{\sin\phi_h}$	$1/(Qq_T)$		(no)
$F_{UL}^{\sin 2\phi_h}$	$1/q_T^4$		(typeII)
F_{LL}	$1/q_T^2$	$1/q_T^2$	yes
$F_{LL}^{\cos\phi_h}$	$1/(Qq_T)$	$1/(Qq_T)$	no
$F_{UT,T}^{\sin(\phi_h-\phi_S)}$	$1/q_T^3$	$1/q_T^3$	yes
$F_{UT,L}^{\sin(\phi_h-\phi_S)}$		$1/(Q^2q_T)$	
$F_{UT}^{\sin(\phi_h+\phi_S)}$	$1/q_T^3$	$1/q_T^3$	yes
$F_{UT}^{\sin(3\phi_h-\phi_S)}$	$1/q_T^3$	$1/(Q^2q_T)$	typeII
$F_{UT}^{\sin\phi_S}$	$1/(Qq_T^2)$	$1/(Qq_T^2)$	(no)
$F_{UT}^{\sin(2\phi_h-\phi_S)}$	$1/(Qq_T^2)$	$1/(Qq_T^2)$	(no)
$F_{LT}^{\cos(\phi_h-\phi_S)}$	$1/q_T^3$		(yes)
$F_{LT}^{\cos\phi_S}$	$1/(Qq_T^2)$		(no)
$F_{LT}^{\cos(2\phi_h-\phi_S)}$	$1/(Qq_T^2)$		(no)

Table 3.1: Behavior of SIDIS structure functions in the region $M \ll q_T \ll Q$, as deduced from the low-q_T calculation based on TMD factorization and the high-q_T calculation based on collinear factorization. Empty fields indicate that no calculation is available. The last column indicate whether the expressions match exactly, do not match exactly, or should not be expected to match. In parentheses: expected answers based on analogy, rather than actual calculation.

4

Drell-Yan

4.1 Unpolarized Drell–Yan processes

The most complete analysis of Drell–Yan with the formalism of TMDs and with polarization has been carried out in Ref. [11], but we should also mention Refs. [33, 116].

To be now specific we consider the dilepton production

$$H_a(P_a, S_a) + H_b(P_b, S_b) \to l^-(l, \lambda) + l^+(l', \lambda') + X\,, \tag{4.1}$$

with (P_a, S_a) and (P_b, S_b) denoting the 4-momenta and the spin vectors of the incoming hadrons. One has $P_a^2 = M_a^2$, $P_a \cdot S_a = 0$, $S_a^2 = -1$, and corresponding relations for the second hadron. Throughout this work the mass of the leptons in the final state is neglected. We will sum over the helicities λ, λ' of the leptons.

In the one-photon exchange approximation the (frame-independent) cross section of the Drell-Yan process is given by

$$\frac{l^0 l'^0\, d\sigma}{d^3\boldsymbol{l}\, d^3\boldsymbol{l'}} = \frac{\alpha_{em}^2}{F\, q^4}\, L_{\mu\nu} W^{\mu\nu}\,, \tag{4.2}$$

where

$$F = 4\sqrt{(P_a \cdot P_b)^2 - M_a^2 M_b^2} \tag{4.3}$$

represents the flux of the incoming hadrons. If hadron masses are neglected one can write $F = 2s = 2(P_a + P_b)^2$. In Eq. (4.2) the quantity $L^{\mu\nu}$ denotes the spin-averaged leptonic tensor,

$$L^{\mu\nu} = \sum_{\lambda,\lambda'} (\bar{u}(l,\lambda)\gamma^\mu v(l',\lambda'))(\bar{u}(l,\lambda)\gamma^\nu v(l',\lambda'))^* = 4\Big(l^\mu l'^\nu + l^\nu l'^\mu - \frac{q^2}{2} g^{\mu\nu}\Big), \tag{4.4}$$

while

$$W^{\mu\nu}(P_a, S_a; P_b, S_b; q) = \frac{1}{(2\pi)^4} \int d^4x\, e^{iq\cdot x} \langle P_a, S_a; P_b, S_b \,|\, J^\mu_{em}(0) J^\nu_{em}(x) \,|\, P_a, S_a; P_b, S_b \rangle \tag{4.5}$$

is the hadronic tensor

The angular distribution of the Drell-Yan cross section is most conveniently be considered in a dilepton rest frame like the Collins-Soper frame [55] or the Gottfried-Jackson frame [67]. In any dilepton rest frame, one can rewrite Eq. (4.2) according to

$$\frac{d\sigma}{d^4q\, d\Omega} = \frac{\alpha^2_{em}}{2\, F\, q^4} L_{\mu\nu} W^{\mu\nu}\,, \tag{4.6}$$

where the solid angle Ω specifies the orientation of the leptons.

the unpolarized hadronic tensor:

$$W^{\mu\nu}_u = \sum_{i=1}^{4} t^{\mu\nu}_{u,i} V_{u,i}\,, \tag{4.7}$$

with the four structure functions $V_{u,i}$, and the tensor basis

$$\begin{aligned} t^{\mu\nu}_{u,1} &= g^{\mu\nu} - \frac{q^\mu q^\nu}{q^2}\,, \\ t^{\mu\nu}_{u,2} &= \tilde{P}^\mu_a \tilde{P}^\nu_a\,, \\ t^{\mu\nu}_{u,3} &= \tilde{P}^\mu_b \tilde{P}^\nu_b\,, \\ t^{\mu\nu}_{u,4} &= \tilde{P}^\mu_a \tilde{P}^\nu_b + \tilde{P}^\nu_a \tilde{P}^\mu_b\,. \end{aligned} \tag{4.8}$$

In Eq. (4.8) we make use of the vectors

$$\tilde{P}^\mu_a = P^\mu_a - \frac{P_a \cdot q\, q^\mu}{q^2}\,, \qquad \tilde{P}^\mu_b = P^\mu_b - \frac{P_b \cdot q\, q^\mu}{q^2}\,, \tag{4.9}$$

which vanish upon contraction with q.

Expressing the orientation of the leptons through the CS-angles θ_{CS} and ϕ_{CS} and contracting the leptonic tensor in (4.4) with the hadronic tensor one finds the following general form of the cross section in Eq. (4.6):

$$\begin{aligned} \frac{d\sigma}{d^4q\, d\Omega} &= \frac{\alpha^2_{em}}{F\, q^2} \times \\ &\Big[(1+\cos^2\theta)\, F^1_{UU} + (1-\cos^2\theta)\, F^2_{UU} + \sin 2\theta \cos\phi\, F^{\cos\phi}_{UU} + \sin^2\theta \cos 2\phi\, F^{\cos 2\phi}_{UU}\Big] \end{aligned} \tag{4.10}$$

The structure functions again depend on the three variables $P_a \cdot q$, $P_b \cdot q$, and q^2.

In particular for the angular distribution of the unpolarized cross section different notations can be found in the literature (see, e.g., [36] and references therein). Here we just quote the frequently used formula

$$\frac{dN}{d\Omega} \equiv \frac{d\sigma}{d^4q\, d\Omega} \Big/ \frac{d\sigma}{d^4q} = \frac{3}{4\pi} \frac{1}{\lambda+3} \Big(1 + \lambda \cos^2\theta + \mu \sin 2\theta \cos\phi + \frac{\nu}{2} \sin^2\theta \cos 2\phi\Big). \tag{4.11}$$

One readily finds

$$\lambda = \frac{F_{UU}^1 - F_{UU}^2}{F_{UU}^1 + F_{UU}^2}\,, \qquad \mu = \frac{F_{UU}^{\cos\phi}}{F_{UU}^1 + F_{UU}^2}\,, \qquad \nu = \frac{2\,F_{UU}^{\cos 2\phi}}{F_{UU}^1 + F_{UU}^2}\,. \tag{4.12}$$

The so-called Lam-Tung relation [50, 84, 85]

$$\lambda + 2\nu = 1\,, \tag{4.13}$$

which in terms of the structure functions defined in (4.10) reads

$$F_{UU}^2 = 2\,F_{UU}^{\cos 2\phi}\,, \tag{4.14}$$

has attracted considerable attention in the past. This relation is exact if one computes the DY process to $O(\alpha_s)$ in the standard collinear perturbative QCD framework. Even at $O(\alpha_s^2)$ the numerical violation of (4.13) is small [95]. On the other hand data for $\pi^- N \to \mu^-\mu^+ X$ taken at CERN [62,68] and at Fermilab [58] are in disagreement with the Lam-Tung relation. In particular, an unexpectedly large $\cos 2\phi$ modulation of the cross section was observed, and in the meantime different explanations for this phenomenon have been put forward in the literature [23, 28, 31, 41–43, 69]. In Ref. [33] it was pointed out that intrinsic transverse motion of initial state partons might be responsible for the observed violation of the Lam-Tung relation. In the following section we will briefly return to this point in connection with the parton model calculation. It is also worthwhile to mention that more recent Fermilab data on proton-deuteron Drell-Yan do agree with the Lam-Tung relation [120].

4.2 Drell–Yan in the parton model

The hadronic tensor

$$W^{\mu\nu} = \frac{1}{N_c}\sum_q e_q^2 \int d^4k_a\, d^4k_b\, \delta^{(4)}(q-k_a-k_b)\,\mathrm{Tr}[\gamma^\mu\,\Phi^q(k_a,P_a,S_a|n_a)\,\gamma^\nu\,\bar\Phi^q(k_b,P_b,S_b|n_b)] + \{\Phi\leftrightarrow\bar\Phi\}\,, \tag{4.15}$$

The hadronic tensor then reduces to

$$W^{\mu\nu} = \frac{1}{N_c}\sum_q e_q^2 \int d^2\boldsymbol{k}_{aT}\, d^2\boldsymbol{k}_{bT}\, \delta^{(2)}(\boldsymbol{q}_T - \boldsymbol{k}_{aT} - \boldsymbol{k}_{bT})\,\mathrm{Tr}[\gamma^\mu\,\Phi^q(x_a,\boldsymbol{k}_{aT},S_a|n_a)\,\gamma^\nu\,\bar\Phi^q(x_b,\boldsymbol{k}_{bT},S_b|n_b)] + \{\Phi\leftrightarrow\bar\Phi\}\,, \tag{4.16}$$

where we used the common DY variables

$$x_a = \frac{q^2}{2P_a\cdot q} \approx \frac{k_a^+}{P_a^+}\,, \qquad x_b = \frac{q^2}{2P_b\cdot q} \approx \frac{k_b^-}{P_b^-}\,. \tag{4.17}$$

Using the unit vector $\boldsymbol{h} \equiv \boldsymbol{q}_T/q_T$ one eventually finds the following leading order structure functions in the CS-frame:

$$F_{UU}^{1} = C\left[f_1\,\bar{f}_1\right], \tag{4.18}$$

$$F_{UU}^{\cos 2\phi} = C\left[\frac{2(\boldsymbol{h}\cdot\boldsymbol{k}_{aT})(\boldsymbol{h}\cdot\boldsymbol{k}_{bT}) - \boldsymbol{k}_{aT}\cdot\boldsymbol{k}_{bT}}{M_a M_b}\, h_1^{\perp}\,\bar{h}_1^{\perp}\right] \tag{4.19}$$

where we made use of the following notation for the convolution of TMDs in the transverse momentum space:

$$C\left[w(\boldsymbol{k}_{aT},\boldsymbol{k}_{bT}) f_1 \bar{f}_2\right] \equiv \frac{1}{N_c}\sum_q e_q^2 \int d^2\boldsymbol{k}_{aT}\, d^2\boldsymbol{k}_{bT}\, \delta^{(2)}(\boldsymbol{q}_T - \boldsymbol{k}_{aT} - \boldsymbol{k}_{bT})\, w(\boldsymbol{k}_{aT},\boldsymbol{k}_{bT}) \times \left[f_1^q(x_a,\boldsymbol{k}_{aT}^2)\, f_2^{\bar{q}}(x_b,\boldsymbol{k}_{bT}^2) + f_1^{\bar{q}}(x_a,\boldsymbol{k}_{aT}^2)\, f_2^q(x_b,\boldsymbol{k}_{bT}^2)\right]. \tag{4.20}$$

Bibliography

[1] CDF Collaboration, T. Aaltonen *et al.*, "First Run II Measurement of the W Boson Mass," Phys. Rev. **D77** (2008) 112001, [0708.3642].

[2] HERMES Collaboration, A. Airapetian *et al.*, "Single-spin asymmetries in semi-inclusive deep-inelastic scattering on a transversely polarized hydrogen target," Phys. Rev. Lett. **94** (2005) 012002, [hep-ex/0408013].

[3] I. Akushevich, N. Shumeiko, and A. Soroko, "Radiative effects in the processes of hadron electroproduction," Eur.Phys.J. **C10** (1999) 681–687, [hep-ph/9903325].

[4] COMPASS Collaboration, M. Alekseev *et al.*, "Measurement of the Collins and Sivers asymmetries on transversely polarised protons," Phys. Lett. **B692** (2010) 240–246, [1005.5609].

[5] M. Anselmino, M. Boglione, J. Hansson, and F. Murgia, "Polarized inclusive leptoproduction, $\ell N \to hX$, and the hadron helicity density matrix, $\rho(h)$: possible measurements and predictions," Phys. Rev. **D54** (1996) 828–837, [hep-ph/9512379].

[6] M. Anselmino, M. Boglione, and F. Murgia, "Single spin asymmetry for $p^{\uparrow}p \to \pi X$ in perturbative QCD," Phys. Lett. **B362** (1995) 164–172, [hep-ph/9503290].

[7] M. Anselmino *et al.*, "The general partonic structure for hadronic spin asymmetries," Phys. Rev. **D73** (2006) 014020, [hep-ph/0509035].

[8] M. Anselmino, E. Leader, and F. Murgia, "Single spin asymmetries in DIS," Phys. Rev. **D56** (1997) 6021–6024, [hep-ph/9610407].

[9] M. Anselmino, M. Boglione, and F. Murgia, "Phenomenology of single spin asymmetries in $p^{\uparrow}p \to \pi X$," Phys. Rev. **D60** (1999) 054027, [hep-ph/9901442].

[10] New Muon Collaboration Collaboration, M. Arneodo *et al.*, "Measurement of the proton and deuteron structure functions, F2(p) and F2(d), and of the ratio sigma-L / sigma-T," Nucl.Phys. **B483** (1997) 3–43, [hep-ph/9610231].

[11] S. Arnold, A. Metz, and M. Schlegel, "Dilepton production from polarized hadron hadron collisions," Phys. Rev. **D79** (2009) 034005, [0809.2262].

[12] S. Aybat and T. C. Rogers, "TMD Parton Distribution and Fragmentation Functions with QCD Evolution," Phys. Rev. **D83** (2011) 114042, [1101.5057].

[13] A. Bacchetta, M. Boglione, A. Henneman, and P. J. Mulders, "Bounds on transverse momentum dependent distribution and fragmentation functions," Phys. Rev. Lett. **85** (2000) 712–715, [hep-ph/9912490].

[14] A. Bacchetta, M. Boglione, A. Henneman, and P. J. Mulders, "The full spin structure of quarks in the nucleon," [hep-ph/0005140]. Proceedings of the Workshop on Nucleon Structure in the High x-Bjorken Region (HiX 2000), Philadelphia, PA, USA, 30 Mar - 1 Apr 2000.

[15] A. Bacchetta, C. J. Bomhof, P. J. Mulders, and F. Pijlman, "Single spin asymmetries in hadron hadron collisions," Phys. Rev. **D72** (2005) 034030, [hep-ph/0505268].

[16] A. Bacchetta, D. Boer, M. Diehl, and P. J. Mulders, "Matches and mismatches in the descriptions of semi- inclusive processes at low and high transverse momentum," JHEP **08** (2008) 023, [0803.0227].

[17] A. Bacchetta and M. Contalbrigo, "The proton in 3D," Il Nuovo Saggiatore **28** (2012) 16–27.

[18] A. Bacchetta, F. Conti, and M. Radici, "Transverse-momentum distributions in a diquark spectator model," Phys. Rev. **D78** (2008) 074010, [0807.0323].

[19] A. Bacchetta, U. D'Alesio, M. Diehl, and C. A. Miller, "Single-spin asymmetries: The Trento conventions," Phys. Rev. **D70** (2004) 117504, [hep-ph/0410050].

[20] A. Bacchetta, M. Diehl, K. Goeke, A. Metz, P. J. Mulders, and M. Schlegel, "Semi-inclusive deep inelastic scattering at small transverse momentum," JHEP **02** (2007) 093, [hep-ph/0611265].

[21] A. Bacchetta, P. J. Mulders, and F. Pijlman, "New observables in longitudinal single-spin asymmetries in semi-inclusive DIS," Phys. Lett. **B595** (2004) 309–317, [hep-ph/0405154].

[22] A. Bacchetta and M. Radici, "Constraining quark angular momentum through semi-inclusive measurements," Phys.Rev.Lett. **107** (2011) 212001, [1107.5755].

[23] A. Bakulev, N. Stefanis, and O. Teryaev, "Polarized and unpolarized mu-pair meson-induced Drell-Yan production and the pion distribution amplitude," Phys.Rev. **D76** (2007) 074032, [0706.4222].

[24] V. Barone, A. Drago, and P. G. Ratcliffe, "Transverse polarisation of quarks in hadrons," Phys. Rept. **359** (2002) 1–168, [hep-ph/0104283].

[25] V. Barone, S. Melis, and A. Prokudin, "The Boer-Mulders effect in unpolarized SIDIS: an analysis of the COMPASS and HERMES data on the $\cos 2\phi$ asymmetry," Phys. Rev. **D81** (2010) 114026, [0912.5194].

[26] V. Barone, A. Prokudin, and B.-Q. Ma, "A systematic phenomenological study of the $\cos 2\phi$ asymmetry in unpolarized semi–inclusive DIS," [0804.3024].

[27] A. V. Belitsky, X. Ji, and F. Yuan, "Quark imaging in the proton via quantum phase-space distributions," Phys. Rev. **D69** (2004) 074014, [hep-ph/0307383].

[28] E. L. Berger and S. J. Brodsky, "Quark structure functions of mesons and the Drell-Yan process," Phys.Rev.Lett. **42** (1979) 940–944.

[29] E. L. Berger, J.-W. Qiu, and R. A. Rodriguez-Pedraza, "Transverse momentum dependence of the angular distribution of the Drell-Yan process," Phys. Rev. **D76** (2007) 074006, [arXiv:0708.0578 [hep-ph]].

[30] J. D. Bjorken and E. A. Paschos, "Inelastic electron-proton and γ-proton scattering and the structure of the nucleon," Phys. Rev. **185** (1969) 1975–1982.

[31] D. Boer, A. Brandenburg, O. Nachtmann, and A. Utermann, "Factorisation, parton entanglement and the Drell-Yan process," Eur.Phys.J. **C40** (2005) 55–61, [hep-ph/0411068].

[32] D. Boer and P. J. Mulders, "Time-reversal odd distribution functions in leptoproduction," Phys. Rev. **D57** (1998) 5780–5786, [hep-ph/9711485].

[33] D. Boer, "Investigating the origins of transverse spin asymmetries at RHIC," Phys. Rev. **D60** (1999) 014012, [hep-ph/9902255].

[34] D. Boer, "Angular dependences in inclusive two-hadron production at BELLE," Nucl. Phys. **B806** (2009) 23–67, [0804.2408].

[35] D. Boer, M. Diehl, R. Milner, R. Venugopalan, W. Vogelsang, *et al.*, "Gluons and the quark sea at high energies: Distributions, polarization, tomography," [1108.1713].

[36] D. Boer and W. Vogelsang, "Drell-Yan lepton angular distribution at small transverse momentum," Phys. Rev. **D74** (2006) 014004, [hep-ph/0604177].

[37] M. Boglione and P. J. Mulders, "Time-reversal odd fragmentation and distribution functions in $p\,p$ and $e\,p$ single spin asymmetries," Phys. Rev. **D60** (1999) 054007, [hep-ph/9903354].

[38] C. J. Bomhof, P. J. Mulders, and F. Pijlman, "Gauge link structure in quark quark correlators in hard processes," Phys. Lett. **B596** (2004) 277–286, [hep-ph/0406099].

[39] C. J. Bomhof, P. J. Mulders, and F. Pijlman, "The construction of gauge-links in arbitrary hard processes," Eur. Phys. J. **C47** (2006) 147–162, [hep-ph/0601171].

[40] G. Bozzi, S. Catani, G. Ferrera, D. de Florian, and M. Grazzini, "Production of Drell-Yan lepton pairs in hadron collisions: Transverse-momentum resummation at next-to-next-to-leading logarithmic accuracy," Phys.Lett. **B696** (2011) 207–213, [1007.2351].

[41] A. Brandenburg, S. Brodsky, V. V. Khoze, and D. Mueller, "Angular distributions in the Drell-Yan process: A Closer look at higher twist effects," Phys.Rev.Lett. **73** (1994) 939–942, [hep-ph/9403361].

[42] A. Brandenburg, O. Nachtmann, and E. Mirkes, "Spin effects and factorization in the Drell-Yan process," Z.Phys. **C60** (1993) 697–710.

[43] A. Brandenburg, A. Ringwald, and A. Utermann, "Instantons in Lepton Pair Production," Nucl.Phys. **B754** (2006) 107–126, [hep-ph/0605234].

[44] S. J. Brodsky, D. S. Hwang, and I. Schmidt, "Final-state interactions and single-spin asymmetries in semi-inclusive deep inelastic scattering," Phys. Lett. **B530** (2002) 99–107, [hep-ph/0201296].

[45] M. Burkardt, "Impact parameter dependent parton distributions and off- forward parton distributions for zeta –¿ 0," Phys. Rev. **D62** (2000) 071503, [hep-ph/0005108].

[46] I. O. Cherednikov and N. G. Stefanis, "Renormalization-group properties of transverse-momentum dependent parton distribution functions in the light-cone gauge with the Mandelstam-Leibbrandt prescription," Phys. Rev. **D80** (2009) 054008, [0904.2727].

[47] F. Close, F. Halzen, and D. Scott, "What Is the Transverse Momentum of Partons?," Phys.Lett. **B68** (1977) 447.

[48] J. C. Collins, T. C. Rogers, and A. M. Stasto, "Fully Unintegrated Parton Correlation Functions and Factorization in Lowest Order Hard Scattering," Phys. Rev. **D77** (2008) 085009, [0708.2833].

[49] J. Collins, *Foundations of Perturbative QCD*. Cambridge Monographs on Particle Physics, Nuclear Physics and Cosmology. Cambridge University Press, 2011.

[50] J. C. Collins, "Simple prediction of QCD for angular distribution of dilepton in hadron collisions," Phys.Rev.Lett. **42** (1979) 291.

[51] J. C. Collins, "Fragmentation of transversely polarized quarks probed in transverse momentum distributions," Nucl. Phys. **B396** (1993) 161–182, [hep-ph/9208213].

[52] J. C. Collins, "Leading twist single transverse-spin asymmetries: Drell-Yan and deep inelastic scattering," Phys.Lett. **B536** (2002) 43–48, [hep-ph/0204004].

[53] J. C. Collins, "What exactly is a parton density?," Acta Phys. Polon. **B34** (2003) 3103, [hep-ph/0304122].

[54] J. C. Collins and A. Metz, "Universality of soft and collinear factors in hard- scattering factorization," Phys. Rev. Lett. **93** (2004) 252001, [hep-ph/0408249].

[55] J. C. Collins and D. E. Soper, "Angular Distribution of Dileptons in High-Energy Hadron Collisions," Phys.Rev. **D16** (1977) 2219.

[56] J. C. Collins and D. E. Soper, "Back-to-back jets in QCD," Nucl. Phys. **B193** (1981) 381.

[57] J. C. Collins, D. E. Soper, and G. Sterman, "Transverse momentum distribution in Drell-Yan pair and W and Z boson production," Nucl. Phys. **B250** (1985) 199.

[58] J. Conway, C. Adolphsen, J. Alexander, K. Anderson, J. Heinrich, *et al.*, "Experimental study of muon pairs produced by 252-GeV pions on tungsten," Phys.Rev. **D39** (1989) 92–122.

[59] U. D'Alesio and F. Murgia, "Parton intrinsic motion in inclusive particle production: Unpolarized cross sections, single spin asymmetries and the Sivers effect," Phys. Rev. **D70** (2004) 074009, [hep-ph/0408092].

[60] M. Diehl, "Generalized parton distributions," Phys. Rept. **388** (2003) 41–277, [hep-ph/0307382].

[61] M. Diehl and S. Sapeta, "On the analysis of lepton scattering on longitudinally or transversely polarized protons," Eur. Phys. J. **C41** (2005) 515–533, [hep-ph/0503023].

[62] NA10 Collaboration Collaboration, S. Falciano *et al.*, "Angular distributions of muon pairs produced by 194 GeV/c negative pions," Z.Phys. **C31** (1986) 513.

[63] R. P. Feynman, "Very high-energy collisions of hadrons," Phys. Rev. Lett. **23** (1969) 1415–1417.

[64] L. P. Gamberg, A. Mukherjee, and P. J. Mulders, "Spectral analysis of gluonic pole matrix elements for fragmentation," Phys. Rev. **D77** (2008) 114026, [0803.2632].

[65] K. Goeke, A. Metz, P. V. Pobylitsa, and M. V. Polyakov, "Lorentz invariance relations among parton distributions revisited," Phys. Lett. **B567** (2003) 27–30, [hep-ph/0302028].

[66] K. Goeke, A. Metz, and M. Schlegel, "Parameterization of the quark-quark correlator of a spin-1/2 hadron," Phys. Lett. **B618** (2005) 90–96, [hep-ph/0504130].

[67] K. Gottfried and J. D. Jackson, "On the Connection between production mechanism and decay of resonances at high-energies," Nuovo Cim. **33** (1964) 309–330.

[68] NA10 Collaboration Collaboration, M. Guanziroli *et al.*, "Angular distributions of muon pairs produced by negative pions on deuterium and tungsten," Z.Phys. **C37** (1988) 545.

[69] P. Hoyer, M. Jarvinen, and S. Kurki, "Factorization at fixed Q**2(1-x)," JHEP **0810** (2008) 086, [0808.0626].

[70] A. Idilbi, X. Ji, J.-P. Ma, and F. Yuan, "Collins-Soper equation for the energy evolution of transverse-momentum and spin dependent parton distributions," Phys. Rev. **D70** (2004) 074021, [hep-ph/0406302].

[71] R. L. Jaffe, "Can transversity be measured?," [hep-ph/9710465].

[72] R. L. Jaffe, "Spin, twist and hadron structure in deep inelastic processes," [hep-ph/9602236].

[73] R. Jakob, P. J. Mulders, and J. Rodrigues, "Modelling quark distribution and fragmentation functions," Nucl. Phys. **A626** (1997) 937–965, [hep-ph/9704335].

[74] X. Ji, "Generalized parton distributions," Ann.Rev.Nucl.Part.Sci. **54** (2004) 413–450.

[75] X. Ji, "Gauge invariant decomposition of nucleon spin," Phys. Rev. Lett. **78** (1997) 610–613, [hep-ph/9603249].

[76] X. Ji, "Viewing the proton through 'color'-filters," Phys. Rev. Lett. **91** (2003) 062001, [hep-ph/0304037].

[77] X. Ji, J.-P. Ma, and F. Yuan, "QCD factorization for semi-inclusive deep-inelastic scattering at low transverse momentum," Phys. Rev. **D71** (2005) 034005, [hep-ph/0404183].

[78] X. Ji, J.-W. Qiu, W. Vogelsang, and F. Yuan, "Single-transverse spin asymmetry in semi-inclusive deep inelastic scattering," Phys. Lett. **B638** (2006) 178–186, [hep-ph/0604128].

[79] X. Ji, J.-W. Qiu, W. Vogelsang, and F. Yuan, "A unified picture for single transverse-spin asymmetries in hard processes," Phys. Rev. Lett. **97** (2006) 082002, [hep-ph/0602239].

[80] S. Joosten, "Effects of intrinsic parton motion in SIDIS,". to appear in proceedings of the 19th International Workshop on Deep Inelastic Scattering (DIS 2008), Newport News, VA, USA, 11-15 April 2011.

[81] H. Jung, "Un-integrated uPDFs in CCFM," [hep-ph/0411287].

[82] Y. Koike, J. Nagashima, and W. Vogelsang, "Resummation for polarized semi-inclusive deep-inelastic scattering at small transverse momentum," Nucl. Phys. **B744** (2006) 59–79, [hep-ph/0602188].

[83] Y. Koike, W. Vogelsang, and F. Yuan, "On the Relation Between Mechanisms for Single-Transverse- Spin Asymmetries," Phys. Lett. **B659** (2008) 878–884, [0711.0636].

[84] C. Lam and W.-K. Tung, "A systematic approach to inclusive lepton pair production in hadronic collisions," Phys.Rev. **D18** (1978) 2447.

[85] C. Lam and W.-K. Tung, "A parton model relation sans QCD modifications in lepton pair productions," Phys.Rev. **D21** (1980) 2712.

[86] B. Lampe and E. Reya, "Spin physics and polarized structure functions," Phys. Rept. **332** (2000) 1–163, [hep-ph/9810270].

[87] F. Landry, R. Brock, P. M. Nadolsky, and C. P. Yuan, "Tevatron Run-1 Z boson data and Collins-Soper-Sterman resummation formalism," Phys. Rev. **D67** (2003) 073016, [hep-ph/0212159].

[88] J. Levelt, *Deep inelastic semi-inclusive processes*. PhD thesis, Vrije Universiteit Amsterdam, 1993.

[89] C. Lorce, B. Pasquini, and M. Vanderhaeghen, "Unified framework for generalized and transverse-momentum dependent parton distributions within a 3Q light-cone picture of the nucleon," JHEP **1105** (2011) 041, [1102.4704].

[90] Z. Lu and I. Schmidt, "Updating Boer-Mulders functions from unpolarized pd and pp Drell-Yan data," Phys. Rev. **D81** (2010) 034023, [0912.2031].

[91] A. D. Martin, W. J. Stirling, R. S. Thorne, and G. Watt, "Parton distributions for the LHC," Eur. Phys. J. **C63** (2009) 189–285, [0901.0002].

[92] S. Meissner and A. Metz, "Partonic pole matrix elements for fragmentation," Phys. Rev. Lett. **102** (2009) 172003, [0812.3783].

[93] S. Meissner, A. Metz, and M. Schlegel, "Generalized parton correlation functions for a spin-1/2 hadron," JHEP **0908** (2009) 056, [0906.5323].

[94] G. A. Miller, "Charge Density of the Neutron," Phys. Rev. Lett. **99** (2007) 112001, [0705.2409].

[95] E. Mirkes and J. Ohnemus, "Angular distributions of Drell-Yan lepton pairs at the Tevatron: Order $\alpha - s^2$ corrections and Monte Carlo studies," Phys.Rev. **D51** (1995) 4891–4904, [hep-ph/9412289].

[96] H. Mkrtchyan *et al.*, "Transverse momentum dependence of semi-inclusive pion production," Phys. Lett. **B665** (2008) 20–25, [0709.3020].

[97] P. J. Mulders and R. D. Tangerman, "The complete tree-level result up to order $1/Q$ for polarized deep-inelastic leptoproduction," Nucl. Phys. **B461** (1996) 197–237, [hep-ph/9510301]. Erratum-ibid. **B484** (1996) 538.

[98] B. U. Musch, P. Hagler, J. W. Negele, and A. Schafer, "Exploring quark transverse momentum distributions with lattice QCD," Phys.Rev. **D83** (2011) 094507, [1011.1213].

[99] P. M. Nadolsky, "Theory of W and Z boson production," AIP Conf. Proc. **753** (2005) 158–170, [hep-ph/0412146].

[100] K. Oganesian, H. Avakian, N. Bianchi, and P. Di Nezza, "Investigations of azimuthal asymmetry in semiinclusive leptoproduction," Eur. Phys. J. **C5** (1998) 681–685, [hep-ph/9709342].

[101] G. Parisi and R. Petronzio, "Small Transverse Momentum Distributions in Hard Processes," Nucl.Phys. **B154** (1979) 427.

[102] M. E. Peskin and D. V. Schroeder, *An introduction to quantum field theory*. Addison-Wesley, Reading, MA, USA, 1995.

[103] R. Pohl, A. Antognini, F. Nez, F. D. Amaro, F. Biraben, *et al.*, "The size of the proton," Nature **466** (2010) 213–216.

[104] J.-w. Qiu and X.-f. Zhang, "Role of the nonperturbative input in QCD resummed Drell- Yan Q_T distributions," Phys. Rev. **D63** (2001) 114011, [hep-ph/0012348].

[105] J.-F. Rajotte. PhD thesis, München U., 2010.

[106] COMPASS Collaboration Collaboration, J.-F. Rajotte, "Hadron transverse momentum distributions and TMD studies," [1008.5125].

[107] J. P. Ralston and D. E. Soper, "Production of dimuons from high-energy polarized proton-proton collisions," Nucl. Phys. **B152** (1979) 109.

[108] T. C. Rogers and P. J. Mulders, "No Generalized TMD-Factorization in the Hadro-Production of High Transverse Momentum Hadrons," Phys. Rev. **D81** (2010) 094006, [1001.2977].

[109] M. Schlegel and A. Metz, "Two-Photon Exchange in (Semi-)Inclusive DIS," AIP Conf.Proc. **1149** (2009) 543–546, [0902.0781].

[110] P. Schweitzer, T. Teckentrup, and A. Metz, "Intrinsic transverse parton momenta in deeply inelastic reactions," Phys. Rev. **D81** (2010) 094019, [1003.2190].

[111] D. Sivers, "The Adventure and the Prize," [1109.2521].

[112] D. W. Sivers, "Single spin production asymmetries from the hard scattering of pointlike constituents," Phys. Rev. **D41** (1990) 83.

[113] J. Soffer, "Positivity constraints for spin dependent parton distributions," Phys. Rev. Lett. **74** (1995) 1292–1294, [hep-ph/9409254].

[114] D. E. Soper, "Large Transverse Momentum Partons and Massive mu Pair Production," Phys. Rev. Lett. **38** (1977) 461.

[115] R. D. Tangerman, *Higher-twist correlations in polarized hadrons*. PhD thesis, Vrije Universiteit Amsterdam, 1996.

[116] R. D. Tangerman and P. J. Mulders, "Intrinsic transverse momentum and the polarized Drell-Yan process," Phys. Rev. **D51** (1995) 3357–3372, [hep-ph/9403227].

[117] F. Yuan, "Collins Asymmetry at Hadron Colliders," Phys. Rev. **D77** (2008) 074019, [0801.3441].

[118] F. Yuan and J. Zhou, "Collins Fragmentation and the Single Transverse Spin Asymmetry," Phys. Rev. Lett. **103** (2009) 052001, [0903.4680].

[119] J. Zhou, F. Yuan, and Z.-T. Liang, "Transverse momentum dependent quark distributions and polarized Drell-Yan processes," Phys. Rev. **D81** (2010) 054008, [0909.2238].

[120] FNAL-E866/NuSea Collaboration Collaboration, L. Zhu *et al.*, "Measurement of Angular Distributions of Drell-Yan Dimuons in p + d Interaction at 800-GeV/c," Phys.Rev.Lett. **99** (2007) 082301, [hep-ex/0609005].